Modélisation mathématique de la contagion de défaut

Andreea Minca

UNIVERSITÉ PIERRE ET MARIE CURIE
ÉCOLE DOCTORALE DE PARIS CENTRE

THÈSE

pour obtenir le titre de

Docteur en Mathématiques Appliquées

de l'Université Pierre et Marie Curie

Présentée par

Andreea Catalina MINCA

Modélisation mathématique de la contagion de défaut

Mathematical modeling of financial contagion

Préparée sous la direction de

Rama CONT

Soutenue publiquement le 5 Septembre 2011

devant le jury composé de :

M. Marco AVELLANEDA (Rapporteur)
M. Rama CONT
M. Stéphane CREPEY (Rapporteur)
M. Michel CROUHY
M. Gilles PAGES
Mme Agnès SULEM
Mlle Emily TANIMURA

To my family

Résumé

Cette thèse porte sur la modélisation mathématique de la contagion de défaut. Un choc économique induit des pertes initiales, de là le défaut de quelques institutions est amplifié par des liens financiers complexes ce qui engendre alors des défauts à large échelle. Une première approche est donnée par les modèles à forme réduite. Les défauts ont lieu en fonction des instants d'arrivée d'un processus ponctuel marqué. On propose une approche rigoureuse de la calibration des modes "top down" pour les dérivés de crédit multi noms, en utilisant des méthodes de projection Markovienne et de contrôle d'intensité. Une deuxième approche est celle des modèles structurels de risque de défaut. On modélise spécifiquement les liens économiques qui mènent à la contagion, en représentant le système financier par un réseaux de contreparties. Les principaux types de contagion sont l'illiquidité et l'insolvabilité. En modélisant le réseau financier par un graphe aléatoire pondéré et orienté on obtient des résultats asymptotiques pour la magnitude de la contagion dans un grand réseau financier. On aboutit à une expression analytique pour la fraction finale de défauts en fonction des caractéristiques du réseau. Ces résultats donnent un critère de robustesse d'un grand réseau financier et peuvent s'appliquer dans le cadre des stress tests effectués par les régulateurs. Enfin, on étudie la taille et la dynamique des cascades d'illiquidité dans les marchés OTC et l'impact, en terme de risque systémique, dû à l'introduction d'une chambre de compensation pour les CDS.

Mots clés : Risque systémique, contrôle d'intensité, réseaux financiers, graphes aléatoires, contagion de défaut, chambres de compensation.

Abstract

The subject of this thesis is the mathematical modeling of episodes of default contagion, by which an economic shock causing initial losses and defaults of a few institutions is amplified due to complex financial linkages, leading to large scale defaults. A first approach is represented by reduced form modeling by which defaults occur according to the arrival times of a marked point process. We propose a rigorous approach to the calibration of "top down" models for portfolio credit derivatives, using Markovian projection methods and intensity control. A second, more ambitious approach is that of structural models of default risk. Here, one models specifically the economical linkages leading to contagion, building on the representation of the financial system as a network of counterparties with interlinked balance sheets. The main types of financial distress that cause financial failure are illiquidity and insolvency. Using as underlying model for a financial network a random directed graph with prescribed degrees and weights, we derive asymptotic results for the magnitude of balance-sheet contagion in a large financial network. We give an analytical expression for the asymptotic fraction of defaults, in terms of network characteristics. These results, yielding a criterion for the resilience of a large financial network to the default of a small group of financial institutions may be applied in a stress testing framework by regulator who can efficiently contain contagion. Last, we study the magnitude and dynamics of illiquidity cascades in over-the-counter markets and assess the much-debated impact, in terms of systemic risk, of introducing a CDS clearinghouse.

Keywords:Systemic risk, intensity control, financial networks, random graphs, default contagion, clearing house.

Remerciements

J'ai une profonde gratitude envers mon directeur de thèse Rama Cont, qui durant les dernières quatre années, a complètement changé la trajectoire de ma carrière. Je le remercie pour m'avoir suggéré un sujet nouveau et passionnant, pour m'avoir appris à veiller continûment à la fois au réalisme mais aussi à la rigueur mathématique. Merci de m'avoir fait confiance!

Je remercie également Agnès Sulem pour m'avoir accueillie dans son équipe à l'INRIA. J'ai bénéficié de son soutien et de ses judicieux conseils. Une jeune femme en début de carrière ne pourrait pas avoir meilleur modèle que vous!

Je suis très reconnaissante envers Marco Avellaneda et Stéphane Crepey qui m'ont fait l'honneur d'être rapporteurs de ma thèse. Leurs remarques precieuses m'ont permis d'améliorer la présentation finale de mon manuscrit. Je les remercie pour leur gentillesse et la rapidité, malgré leur programme chargé, dont ils ont fait preuve pour envoyer leurs rapports. Je remercie chaleureusement Agnès Sulem, Michel Crouhy, Gilles Pagès et Emily Tanimura pour avoir accepté de faire partie de mon jury et pour l'intérêt qu'ils ont porté à mon travail.

Je tiens à remercier Michel Crouhy, qui m'a toujours appuyée dans mes démarches ainsi que la Fondation Natixis pour la Recherche Quantitative pour avoir sélectionné mon projet de thèse et avoir soutenu mon travail. A l'INRIA, j'ai eu la chance de bénéficier des échanges scientifiques avec Agnès Sulem et Jean Philippe Chancelier lors de notre groupe de travail sur le contrôle du risque systémique.

Merci aux collègues de LPMA grâce à qui mon travail s'est déroulé dans une belle ambiance. Merci à Sophie, Cyril, Reda et Karim, à la "famille Rama", Amel, Lakshithe, Adrien et Amal pour leur amitié et les beaux moments qu'on a pu partager!

Une pensée à Jacques Portès, Corentin, Isabelle et Josette.

Je suis reconnaissante envers mes professeurs de Paris 6, et tout particulièrement Nicole El Karoui et Gilles Pagès, qui ont encadré ma formation en finance pendant le DEA.

Les dernières lignes de ces remerciements vont à ma famille : ma mère Angela, mon père Marian et ma soeur Anca. C'est grâce à leur sacrifices et leur encouragements que j'en suis arrivée là. Enfin, je remercie infiniment Hamed, c'est grace à toi et à ton soutien dans les moments difficiles que j'ai pu parcourir ce bout de chemin que represente la thèse. Merci de m'avoir donné le courage!

Contents

Chapter I
Overview

Since the onset of the financial crisis in 2007, more than 370 of the almost 8000 US banks insured by the Federal Deposit Insurance Corporation have failed. By comparison, between 2000 and 2004 there were around 30 failures and no failures occurred between 2005 and the beginning of 2007.

The subject of this thesis is the mathematical modeling of such episodes of default contagion, by which an economic shock causing initial losses and defaults of a few institutions is amplified due to complex financial linkages, leading to large scale defaults.

Drawing a parallel with single name credit risk models we can distinguish between two classes of default contagion models.

An approach, commonly used in credit risk management, is represented by *reduced form models*. Here one regards firms as an ensemble of names in a portfolio and models the probability of defaults in this portfolio. Defaults occur according to the arrival times of a marked point process, where the mark determines the loss in the portfolio upon default. Clearly, capturing contagion effects depends in reduced form models on the ability of the underlying point process to exhibit clusters. In this sense, more recently, self exciting processes like time-changed birth processes and Hawkes processes have been proposed as a way to model default contagion [71, 60].

A second, more ambitious approach is that of *structural models* of default risk. Here, one models specifically the economical linkages leading to contagion, building on the representation of the financial system as *a network* of counterparties with interlinked balance sheets. The main types of financial distress that cause financial failure are illiquidity and insolvency. Illiquidity occurs when the liquidity reserves at a certain time cannot cover the payment obligations at that time, whereas insolvency means that the total value of the banks' liabilities exceeds the total value of assets. Propagation of financial distress is modeled via domino effects: a shock (which may be a liquidity shock or a loss in assets' value) affecting balance sheets of a few institutions will propagate due to interconnectedness to neighboring institutions and may possibly affect an important fraction of the financial system. The acknowledgement of bank's interconnectedness and the associated contagion mechanisms has led to an increased advocacy to account for network effects when discussing regulatory requirements [84, 85, 47, 37], be it for liquidity or capital.

The *difference between these classes of models* lies primarily in the information set available to the modeler. Structural models of contagion rely on a large set of information on balance sheets and the interrelations between those balance sheets. On the other hand, reduced form models rely on a much smaller information set, for example the market information. Therefore,

the scope of these two classes of models is different. First, as argued in [97], for pricing and hedging of derivatives, the relevant set of information is the market information, since this set of information is used by market participants to determine prices. In this case, the reduced form modeling is appropriate. On the other hand, the relevant set of information available to a regulator is much more detailed, containing information on the composition of balance sheets, the degree of interconnectedness of each bank, etc. As such, for regulatory purposes - for example identifying sets of banks which pose the highest systemic risk, setting regulatory minimal ratios of liquidity and capital, rendering a network resilient to contagion - the network approach is natural.

This introductory chapter is organized as follows. In Section 1, we summarize the main elements of our framework of Chapter II for reconstructing the default intensity in a portfolio from market prices of credit derivatives referencing the respective portfolio. The calibration problem can be formalized in terms of minimization of relative entropy with respect to a given prior under calibration constraints. The dual problem is shown to be an intensity control problem, characterized in terms of a HJB system of differential equations, for which an analytical solution can be found.

Then, passing to the structural approach, Section 2 describes the economical mechanisms that can lead to a system level contagion like the financial crisis we have witnessed. We identify different types of linkages that transmit financial distress across institutions. In Section 2.2 we introduce a detailed model of balance sheets, that allows for joint modeling of insolvency and illiquidity cascades on the financial network. In Section 2.3, we introduce two classes of weighted random graphs that will serve us as models of financial networks throughout this thesis. Last, Section 3 summarizes the original contributions of this thesis.

1 Reduced form modeling of portfolio credit risk

A model of portfolio credit risk is specified by a filtration that represents the set of observable pieces of information, a default process counting the credit events in the portfolio and the distribution of losses at these credit events [78]. When the model is intended for pricing and hedging, the set of observable pieces of information is the market information and in most cases default time is inaccessible [97]. This is the assumption made in reduced form models, where defaults arrive according to a point process with a continuous compensator. The literature of reduced form modeling for portfolio credit risk can be traced back to Kusuoka [102], Davis and Lo [57] and Jarrow and Yu [98]. One approach is the so-called bottom up approach, where one models the default intensity for each name in the portfolio while specifying a dependence structure between these processes. Besides the previously cited papers, other examples include [39, 62, 56, 125]. The other approach, is the so-called top-down approach, where one models directly the intensity of the aggregate loss process [32, 124, 77, 71, 10, 108, 60]. While top down models lose the information on the identity of the defaulted names, they have an important gain in analytical tractability, in particular regarding calibration to market prices. We contribute to this literature by introducing a non-parametric algorithm for calibration of top-down models. We begin this section by giving some background on credit derivatives. Then, we briefly discuss pricing of portfolio credit derivatives, and finally precise our contributions to this literature.

1.1 Credit derivatives: CDSs and CDOs

The simplest credit derivative is a credit default swap (CDS). A CDS is a contract between two parties, a protection buyer and a protection seller, having a third party a as reference entity. Upon the default of the reference entity, the protection buyer receives a payment equal to the notional $N^{(a)}$ of the swap, times the loss given default $1 - R(a)$ of the reference entity. The quantity $R(a)$ is known as the recovery rate of the entity a: how much will this entity be able to repay its creditors for one dollar of debt. In return, the protection buyer pays a premium, equal to an annual percentage X of the notional, to the protection seller. The premium X is called the CDS spread. This spread is paid until either maturity is reached or default occurs.

Consider now a portfolio of N reference entities and let us denote by $\tau(1) < \tau(2) < \cdots < \tau(N)$ the ordered default times of these entities. The underlying process of this portfolio is the piecewise constant loss process

$$L_t = \sum_{\tau_k \leq t} N^{(k)}(1 - R(k)), \tag{I.1}$$

where $N^{(k)}$ and $R(k)$ denote here the notional and respectively the recovery rate of the k-th entity to default.

Investors, depending on their risk appetite, seek exposure to a certain *tranche* or interval. The CDO is decomposed in a set of I tranches: $\{[K_i, K_{i+1}]\}_{i=0}^{I-1}$ with $K_0 = 0$ and $K_I = 1$. An investor in the i-th tranche sells protection only on losses within the interval $[K_i, K_{i+1}]$, in return for a periodic spread $S(K_i, K_{i+1}, T)$ paid at dates $(t_j, j = 1, \ldots, J)$ on the notional remaining in the tranche after losses have been accounted for. Therefore an investor in the tranche i is exposed only to the loss process

$$L_t^i := (L_t - K_i)_+ - (L_t - K_{i+1})_+. \tag{I.2}$$

We say a tranche i is more senior than a tranche j if $K_i > K_j$. The tranches absorb losses in order of seniority.

1.2 Pricing of portfolio credit derivatives

By the Fundamental Theorem of Asset Pricing, absence of arbitrage in the market is equivalent to the existence of a probability measure $\mathbb{Q}$ called the risk-neutral measure under which the process of discounted prices of financial assets are martingales. The concept of arbitrage is that it is not possible, by starting from nothing and betting on the asset to create at the end positive value without bearing any risk. Otherwise said, there is no trading strategy, such that the final payoff represented by the stochastic integral of this strategy with respect to the price process is nonnegative and strictly positive with positive probability [58]. Thus, in absence of arbitrage, the problem of pricing contingent claims is reduced to taking expectations under the risk neutral measure.

We denote by $B(0, t)$ the discount factor, i.e. the value at time 0 of one dollar paid at time t. According to risk neutral pricing, the 'fair value', or the mark-to-market value of the tranche i is equal to the expectation under the risk neutral measure of the discounted cash inflows minus the cash outflows.

From the point of view of a seller of protection, the mark-to-market value of tranche i can be written as $E^{\mathbb{Q}}(H_i \mid \mathcal{F}_0)$, with

$$H_i = S_0(K_i, K_{i+1}, T) \sum_{t_j \leq T} B(0,t_j)(t_j - t_{j-1})[K_{i+1} - K_i - L^i_{t_j}] - \sum_{t_j \leq T_k} B(0,t_j)[L^i_{t_j} - L^i_{t_{j-1}}] \quad \text{(I.3)}$$

From the point of view of the buyer, the mark-to-market value has the opposite value, since at any time on party's cash inflows are the other party's outflows. At the inception date of the contract, time 0, the buyer and the seller agree on a spread value $S_0(K_i, K_{i+1}, T)$ such that this contract has zero value for both parties, i.e.

$$E^{\mathbb{Q}}[H_i|\mathcal{F}_0] = 0.$$

Clearly, the values of CDO tranches, as opposed to the value of the basket of CDS, depend on the joint distribution of default risk across the reference entities. Moreover, prices of senior tranches depend on the right tail of the portfolio loss distribution [108]. Understating contagion effects seriously overvalues these senior tranches.

1.3 The inverse problem of reconstructing the portfolio default intensity

Top-down models for credit derivatives have been introduced as an alternative to the class of factor based models, which before the crisis was a banking industry standard. Factor based models like the Gaussian copula model, which specify directly a distribution of credit events, have well known shortcomings, among which the most important are the inability to provide a dynamics for the risk factors, preventing any model-based assessment of hedging strategies and the instability of their calibrated parameters [106, 124, 126].

The class of top-down models solves the first part of the problem while allowing for a parsimonious parametrization of the model, and consequently tractable pricing methods. Calibration methods have been proposed in the literature, but relied on suitable parameterizations of the transition probabilities of the underlying jump process [126, 10]. Nonetheless, efficient and stable non-parametric calibration methods for top-down models were lacking and Chapter II, published as [46], was aimed at filling in this gap.

Chapter II is dedicated to reconstructing the intensity of the loss process from market prices. To this end, we first assess the information contained in market data. We show a "mimicking theorem", (Proposition 3.1) for point processes which states that the marginal distributions of a loss process L with arbitrary stochastic intensity λ can be matched using a *Markovian* point process $\tilde{L}$. This process is called the Markovian projection of L and has the (effective) intensity

$$\lambda_{\text{eff}}(t,l) = E^{\mathbb{Q}}[\lambda_t | L_{t-} = l, \mathcal{F}_0]. \quad \text{(I.4)}$$

The relation between λ and λ_{eff} is analogous to the relation between instantaneous and local volatility in diffusion models (see Győngy [83], Dupire [64]).

This implies that values of any derivative whose payoff depends continuously on the aggregate loss L_T of the portfolio on a fixed grid of dates, depends in any top down model on the intensity λ only through the effective default intensity $\lambda_{\text{eff}}(.,.)$. Being able to mimick the marginal distribution of the loss processes using a Markovian model allows for considerable simplification of pricing and calibration algorithms. We exemplify with the case of Collateralized Debt Obligations (CDOs)

Having stated the Mimicking theorem 3.1, we proceed to solving the problem of calibrating to the market spreads the effective default intensity associated to the loss process. This is an ill-posed inverse problem where one attempts to recover a risk-neutral probability measure from a finite set of expectations. We formalize this problem in terms of the minimization of relative entropy with respect to the law of a prior loss process under calibration constraints, following similar approaches to model calibration in Avellaneda at al. [16] and Cont and Tankov [50]. We are given the spreads for the I tranches of the portfolio. The payment dates are denoted $(t_j, j = 1, \ldots, J)$. At $t = 0$ we observe the tranche spreads $(S_0(K_i, K_{i+1}, T_k), i = 1, \ldots, I-1)$.

(**Problem 4.4** - Calibration via relative entropy minimization)**.** *Given a prior loss process with law $\mathbb{Q}_0$, find a loss process with law $\mathbb{Q}^\lambda$ and default intensity $(\lambda_t)_{t\in[0,T^*]}$ which minimizes*

$$\inf_{\mathbb{Q}^\lambda\in\mathbb{M}} E^{\mathbb{Q}_0}[\frac{d\mathbb{Q}^\lambda}{d\mathbb{Q}_0}\ln\frac{d\mathbb{Q}^\lambda}{d\mathbb{Q}_0}] \quad \text{under} \quad E^{\mathbb{Q}^\lambda}[H_i|\mathcal{F}_0] = 0, \quad i = 0, \ldots, I-1. \tag{I.5}$$

This problem is an infinite-dimensional constrained optimization problem whose solution does not seem obvious. A key advantage of using the relative entropy as a calibration criterion is that it can be computed explicitly in the case of point processes. The constrained optimization problem can then be simplified by introducing Lagrange multipliers and using convex duality methods [54, 67].

(**Proposition 4.7** - Duality)**.** *Given a prior measure $\mathbb{Q}_0$ in which the canonical loss process has the prior intensity γ_s, the primal problem (II.21) is equivalent to*

$$\sup_{\mu\in\mathbb{R}^I}\inf_{\lambda\in\Lambda} E^{\mathbb{Q}^\lambda}[\int_0^T(\lambda_s\ln\frac{\lambda_s}{\gamma_s}+\gamma_s-\lambda_s)ds-\sum_{i=0}^{I-1}\mu_i H_i. \tag{I.6}$$

The inner optimization problem

$$J(\mu) = \mathcal{L}(\lambda^*(\mu), \mu) = \inf_{\lambda\in\Lambda}\mathcal{L}(\lambda, \mu)$$

is an example of an *intensity control* problem studied by Brémaud [29] and Bismut [23]: the optimal choice of the intensity of a jump process in order to minimize a criterion of the type

$$\mathcal{L}(\lambda, \mu) = E^{\mathbb{Q}^\lambda}[\int_0^T \varphi(t, \lambda_t, N_t)dt + \sum_{j=1}^{J}\Phi_j(L_{t_j})], \tag{I.7}$$

where $t_j,\ j = 1, \ldots, J$ are the spread payment dates, $\varphi(t, \lambda_t, N_t)$ is a *running cost* and $\Phi_j(L)$ represents a "terminal" cost.

In our case, letting $g(t, k)$ be the prior intensity function (i.e. $\gamma_t = g(t, N_t)$) we obtain

$$\varphi(t, x, k) = x\ln\frac{x}{g(t,k)} + g(t, k) - x \text{ and } \Phi_j(L) = \sum_{i=1}^{I-1} M_{ij}(K_i - L)^+, \tag{I.8}$$

with

$$\begin{aligned} M_{ij} = {} & B(0, t_{j+1})(\mu_{ik} - \mu_{i-1,k})+ \\ & B(0, t_j)[\mu_i(-1 - \Delta S(K_i, K_{i+1}, T)) - \mu_{i-1}(1 - \Delta S(K_{i-1}, K_i, T)], \end{aligned} \tag{I.9}$$

with $\Delta = t_j - t_{j-1}$ is the interval between payments.

The solution of this intensity control problem is characterized in terms of a system of Hamilton-Jacobi equations [29, Ch. VII] which can be solved explicitly in our setting through a logarithmic change of variable. Once the inner optimization/ intensity control problem has been solved we have to solve the outer problem by optimizing $J(\mu)$ over the Lagrange multipliers $\mu \in \mathbb{R}^I$: the corresponding optimal control λ^* then yields precisely the default intensity which calibrates the observations.

The calibrated default intensity $\lambda^*(.,.)$ can then be used for pricing of portfolio credit derivatives in an efficient way. First, thanks to the Mimicking theorem, the transition probabilities for the loss process solve a Fokker-Planck equation. Then, it is easy to show that the term structure of expected tranche losses can be obtained by solving a (single) forward equation [49]. Numerical results in Chapter II reveal strong evidence for the dependence of loss transitions rates on the previous number of defaults, and offer quantitative evidence for contagion effects in the (risk–neutral) loss process.

2 Structural modeling of default contagion: the network approach

The previous section presented one point view on the modeling of default dependence. We now give to this problem a much more structural view, aiming to first understand the underlying economical mechanisms that perpetrate default contagion.

The economics literature on domino effects in an economy of interlinked firms goes back to Kiyotaki and Moore [99], Hellwig [86] and Allen and Gale [5]. In [99], the authors investigate how liquidity shocks propagate across small entrepreneurial firms that lend and borrow from one another. They do not model the precise linkages of this network, but rather the behavior of a typical agent. Hellwig [86] points out the overall maturity mismatch of the financial system as a whole: while at an individual level the mismatch might be quite small - take the example of a firm i that funds a fixed-interest instrument with maturity $i+1$ by issuing an instrument with maturity i - the overall maturity mismatch can be very large: place now firm i in a chain of n firms, where firm i borrows from firm $i-1$ with maturity $i-1$ and lends firm $i+1$ with maturity $i+1$. The overall mismatch scales linearly with the size of the system in this simple example. Allen and Gale [5] model specifically a network of banks. Based on equilibrium models on stylized networks like the complete network and circular networks, this study points out the crucial role played by the network structure in the trade off between risk sharing and contagion. In the same sense, Stiglitz et al. [19] investigate the impact of connectivity on the spread of financial insolvency on a regular graph.

Building on economics literature [1, 33, 61] that described the mechanisms of contagion in the recent crisis, our first contribution is to propose a stylized network model which accounts for different types of linkages and in which one can model illiquidity cascades, insolvency cascades and price feedback effects. Indeed, insolvency cascades have been extensively investigated in the literature and Subsection 2.2.2 reviews the different contagion models and the assumptions of the respective approaches. Meanwhile, models that place the two types of cascades in relation have been lacking. Subsections 2.2.3 and 2.2.4 attempt to feel in this gap.

A crucial question in this thesis regards the impact of the network features on the magnitude of contagion: is the underlying topology of the financial network and the local properties of

the nodes (i.e., balance sheets, positions in their trading book, reliance on short term funding etc.) such that the initial distress of several institutions can propagate to a large fraction of the system, or on the contrary, is the network resilient, and the propagation of distress will die out quickly? When the network is large, such questions can be answered by limit theorems that hold on a random network that has the same features as the observed financial network. The purpose of Subsection 2.3 is to review the related random graph literature and to introduce our extensions to existing random graphs models.

2.1 Financial linkages and domino effects

The financial system acted during the recent financial crisis as an amplificator of initial losses in one asset class, mortgage backed securities, to losses that threatened the functioning of the system as a whole and spilled out into the global economy. These may be understood as modern counterparts of bank runs.

In the classical version of a bank run, depositors, worried about the solvency of a bank, rush to withdraw their funds. The bank, unable to satisfy the liquidity withdrawals, fails and, in turn, due to interconnectedness in the financial system, brings down other financial institutions with it, and also companies, which in absence of credit are unable to function. Bank runs have the following ingredients: an institution that holds debt with short maturity (like deposits that can be withdrawn at any moment) and assets with long maturity (like long term loans) and depositors that are uninsured. Whereas classical bank runs have no longer occurred in the US since the introduction of federal insurance after the Great Depression (which eliminated the last ingredient above), the recent crisis can be deemed as a "modern bank run".

Modern "bank runs" are complex and several mechanisms are at work. First, as explained in [1, 33, 61], modern financial institutions, depending more and more on short term financing via money markets, face a run from short-term lenders. These may decide to withdraw their funding, for example in anticipation of their own future needs of liquidity or because of counterparty risk. Even if a bank can still obtain funding of its less liquid assets, such funding bears the risk of increasing haircuts - the difference between the book value of the asset and the funding obtained when using it as collateral. Second, banks may face large liquidity demands, for example in the form of margin payments on outstanding derivatives. Such cases may be deemed as "margin runs" and arise from large jumps in the mark-to-market values of the derivatives. Credit default swaps are particularly prone to large jumps, even in absence of default of the reference entity. One can cite the example of leverage buyouts, i.e. the acquisition of a company using a significant amount of borrowed money, when the spreads of the acquiring company suffer large jumps. Third, when an illiquid portfolio of a defaulted bank is sold on the market, there is a price feedback effect on the portfolios of other banks holding similar assets. This can be seen as a shock that fragilizes the capitalization of the whole financial system. When the capital position of a bank no longer can withstand losses, it becomes insolvent. Its counterparties, with their already fragile capital positions, write off their exposures to the defaulted bank and in turn they may become insolvent, leading to a potential insolvency cascade.

The channels of contagion described above create **systemic risk**, defined as the risk that an initial shock is amplified by the way institutions respond and further transmit it to other institutions, such that the overall effect on the system goes largely beyond the initial shock. These contagion mechanisms rely on intricate network effects: financial institutions are interlinked by their mutual claims, be it on their balance sheets or not. Distress may propagate to

neighboring institutions in a way depending solely on the local properties of the network.

The first kind of links are represented by cash flows between institutions, including margin calls and short term funding that is withdrawn. A node A is a out-neighbor of a node B if B has an immediate payment obligation to A (conversely we say that B is an in-neighbor of A). Depending on the set of out-neighbors that cannot meet their payment obligations, node A may become illiquid. But then, node A cannot meet its own payment obligations to its out-neighbors and so on. So the state of 'illiquidity' can spread in the network.

The second kind of links are balance sheet exposures of financial institutions to one another. By exposure we understand the expected loss on outstanding claims in case of counterparty default. A node B is a out-neighbor of a node A if A has a positive exposure to B. Depending on the set out-neighbors in default, node A may in turn become insolvent if its capital buffer cannot withstand the losses due to direct exposures to these out-neighbors, and in this case the state of 'insolvency' may spread.

We identify a third kind of links, that do not represent direct claims, but relations of similarity between portfolios of banks. A node B is said to be a neighbor of node A if they hold in the portfolio similar assets. When node B becomes illiquid, its illiquid assets that were funded in the interbank market are sold at fire sale prices. When the liquidated portfolio is large, there are important price effects on the assets comprising that portfolio. Therefore, the value of the portfolio of any neighbor A will be negatively impacted. This last kind of linkages produce losses have similar economic effects as direct claims, while the size of the losses they induce can even be much larger.

2.2 Distress propagation in a financial network

2.2.1 Financial networks

At a given point in time, a cross section of the financial system reveals a set of n financial institutions ("banks") that are interlinked by their mutual claims. This cross section may thus be modeled by a weighted directed graph $\mathbf{g} = (\mathbf{v}, \mathbf{e})$, on the vertex set $\mathbf{v} = [1, \ldots, n]$, where for any two institutions i and j, $e(i, j)$ represents the maximum loss related to direct claims incurred by i upon the default of j. We will call $e(i, j)$ the exposure of i to j, and this may include any kind of interbank loans of short or long maturities, or derivatives contracts, but also deposits held in custody by a dealer bank. If $e(i, j) < 0$, we also say that j has a liability or negative exposure to i.

In some cases, interbank contracts are placed under a netting agreement. Such an agreement specifies that, in case of default of one counterparty, the claims will net out. For example, if party j owes party i $\$100M$ and party i owes party j $\$50M$, then if those claims are placed under a netting agreement, the exposure of i to j is equal to $\$50M$. From now on, we will understand exposures as exposures after netting if they are placed under such an agreement.

Another issue is the fact that some interbank exposures are collateralized with cash of cash equivalents, in the sense that the party with negative exposure posts collateral to its counterparty. When this collateral is deposited in a margin account, it is available to the party receiving it for its own purposes, so we will consider that the exposure $e(i, j)$ is net of collateral.

In addition to these interbank assets and liabilities, a bank holds a portfolio of non-interbank assets $\tilde{x}(i)$ and liabilities, such as deposits $D(i)$. Since we considered exposures net of collateral, we consider then that collateral received by bank i and placed in a margin account is included

Interbank assets $A(i) = \sum_j e(i,j)$	Net worth $\tilde{c}(i)$
	Deposits $D(i)$
Other assets $\tilde{x}(i)$	Interbank liabilities $L(i) = \sum_j e(j,i)$
Assets	Liabilities

(a) Stylized balance sheet of a bank.

	$\varepsilon(i)$ - loss on capital
Interbank assets $A(i) = \sum_j e(i,j)$	Net worth $c(i) = (\tilde{c}(i) - \varepsilon(i))_+$
	Deposits $D(i)$
$\varepsilon(i)$ - loss on assets	
Other assets $x(i) = \tilde{x} - \varepsilon(i)$	Interbank liabilities $L(i) = \sum_j e(j,i)$
Assets	Liabilities

(b) Balance sheet after shock.

Table I.1

in $\tilde{x}(i)$. The reason for this is that, from a modeling point of view, receiving collateral against an exposure is equivalent to having already received partial payment against that exposure.

The total interbank assets of i are given by $A(i) = \sum_j e(i,j)$, whereas $L(i) = \sum_j e(j,i)$ represents the total interbank liabilities of i.

We denote by $\tilde{c}(i)$ the Tier I + Tier II capital of bank i which is the institution's buffer that absorbs losses.

Table I.1a displays a stylized "balance sheet" of a financial institution i.

Now consider that a shock $\varepsilon(i)$ affects the non-interbank assets $\tilde{x}(i)$.

As shown in Table I.1b the shock $\varepsilon(i)$ is first absorbed by the capital $\tilde{c}(i)$. By the limited liability rule, the capital becomes

$$c(i) := (\tilde{c}(i) - \varepsilon(i))_+ = \max(\tilde{c}(i) - \varepsilon(i), 0) \tag{I.10}$$

after the shock. A bank is solvent while its (Tier I and Tier II) capital is positive, i.e. $c(i) > 0$. An insolvent bank defaults.

From now on, we refer as time 1 to the time immediately after the shock. Our reference balance sheet is given then given by Table I.1b.

2.2.2 Insolvency cascades

A defaulted bank i is liquidated, and depending on how much of the bank's own assets are recovered, its creditors lose a fraction $1 - R(i)$, which may equal their total exposure to the defaulted bank. If this loss is greater than their capital, than, in turn, the creditors may become insolvent and so on. It is clear that the impact of defaults on the other institutions is highly dependent on the recovery rates.

We now describe several cases treated in the literature and, for each case, we discuss its assumptions.

Case 1) Orderly liquidation.

The model introduced by Eisenberg and Noe for payment systems [66] endogenizes recovery rates. When applying this model to a network of interbank exposures, the following assumptions are implicitly made.

Assumption 2.1 (Orderly liquidation)**.**

(i) All assets are liquid and the price elasticity of the demand for them is perfectly inelastic, i.e. during the liquidation of the portfolio there is no effect on its price.

(ii) There exists a clearing mechanism that redistributes the proceeds of defaulted banks among their creditors proportionally to their outstanding debt.

Let us denote by $(L^*(i))_{i\in\mathbf{v}}$ the effective payable liability after all insolvent banks have been liquidated and the proceeds redistributed among creditors. Under assumptions of orderly liquidation, [66] show that $\mathbf{L}^*$ can be obtained as a solution of fixed point equation $\mathbf{y} = H(\mathbf{y})$, with the mapping H given by:

$$(y(i))_{i=1}^n \overset{H}{\to} (\max\{L(i), x(i) + \sum_j y(j)\frac{e(i,j)}{L(j)} - D(i) - y(i)\})_{i=1}^n. \tag{I.11}$$

If a fixed point $\mathbf{L}^*$ to the mapping H given by Equation (I.11) exists, then it defines the set of insolvent banks by

$$\{i \mid L^*(i) < L(i)\}.$$

Eisenberg and Noe [66] proved that there exists a fixed point of the mapping above. They also show the uniqueness under some supplementary conditions. Let $C^-(i)$ denote the set of nodes reaching i by a directed path in the graph $(\mathbf{v}, \mathbf{e})$, i.e. $C^-(i) := \{j \mid j \to i\}$. Then uniqueness holds if, and only if, for every node i,

(i) no node in $C^-(i)$ has a liability to a node outside this set, and,

(ii) $C^-(i)$ has positive net external assets, i.e., $\sum_{j\in C^-(i)} x(j) > \sum_{j\in C^-(i)} D(j)$.

One example where these conditions hold is where the financial network is strongly connected: there is a directed path between any pair of two nodes. In this case, for all i $C^-(i) = \mathbf{v}$. The first condition above is trivially satisfied, while the second condition is equivalent to

$$\sum_j x(j) - D(i) > 0,$$

which can be interpreted as the positivity of the total equity in the system.

The recovery rate $R(i) := \frac{L^*(i)}{L(i)}$ can be understood as the recovery rate under orderly liquidation: all external assets have been liquidated at their book value $x(i)$ and interbank assets of a defaulted bank have been redistributed at face value among the holders of the bank's liabilities according to the proportionality rule.

A crucial observation related to this model is the fact that, while initial losses are redistributed in the system, potentially causing subsequent defaults, there exists no mechanism that amplifies them. This is a probable cause while many simulation studies conducted by central banks and based on this model dismiss the danger of contagion.

Case 2) The long term horizon.

As Cifuentes et al. [38] point out, liquidation generally has feedback effects on the mark-to-market value of external assets. The fixed point of the mapping H given by Eq. (I.11) (assuming its uniqueness) depends on the sequence of external assets $\mathbf{x}$. In reality, the mark-to-market

values of $\mathbf{x}$ are affected by portfolios of external assets sold while liquidating insolvent banks. The model in [38] drops the second part of Assumption 2.1 and incorporates the dynamics of the prices of liquidated assets as a function of the dynamics of the insolvency cascade. The equilibrium point resulting by iterating both effects may be understood as giving the long term recovery rates for the debt of defaulting firms.

Case 3) The short term horizon.

In the short term, it has been argued in [48] that under assumptions of distressed liquidation, given below, recovery rates for exposures net of collateral can be approximated by zero.

Assumption 2.2 (Distressed liquidation)**.**

(i) The insolvency cascade happens over a short time horizon.

(ii) A clearing mechanism that redistributes a bank's assets among creditors does not exist in the short term.

In the sequel, we consider the capital sequences exogenously given. We let $\mathbb{D}_0$ the set of initial defaults. Unlike in the previous cases, the set of initial defaults may be specified exogenously as a superset of the set of initially insolvent nodes:

$$\mathbb{D}_0 \supseteq \{i \in \mathbf{v} \ \mid \ c(i) = 0\}, \tag{I.12}$$

allowing thus to account for defaults due to mechanisms other than insolvency.

The default of j induces a loss equal to $e(i,j)$ for its counterparty i. If this loss is greater then i's capital, then i defaults. The set of nodes which become insolvent due to their exposures to initial defaults is

$$\mathbb{D}_1(e,c) = \{i \in \mathbf{v} \mid c(i) < \sum_{j \in \mathbb{D}_0} e(i,j)\}, \tag{I.13}$$

and generally $\mathbb{D}_r$ represents the set of nodes defaulting in round r due to exposures to nodes defaulted in rounds $0, \ldots, r-1$.

(**Definition 2.2** - Insolvency cascade)**.** Starting from the set of fundamental defaults institutions $\mathbb{D}_0 \supseteq \{i \in [1, \ldots, n] \mid c(i) = 0\}$, define $\mathbb{D}_k(\mathbf{e}, \mathbf{c})$, for $k = 1, \ldots, n-1$, as the set of institutions whose capital is insufficient to absorb losses due to defaults of institutions in $\mathbb{D}_{k-1}(\mathbf{e}, \mathbf{c})$:

$$\mathbb{D}_k(\mathbf{e}, \mathbf{c}) = \{i \mid c(i) < \sum_{j \in \mathbb{D}_{k-1}((e,c))} e(i,j)\}. \tag{I.14}$$

It is easy to see that, if the size of the network is n, the cascade finishes at most in $n-1$ rounds. The final set of defaults is given by $\mathbb{D}_{n-1}(\mathbf{e}, \mathbf{c})$.

To fix ideas, let us consider a simple example of a contagion starting by the default of node a on the graph illustrated in Figure I.1. In this simple example, contagion finishes in three rounds, node b defaults in the first round while nodes c and d default in the second round.

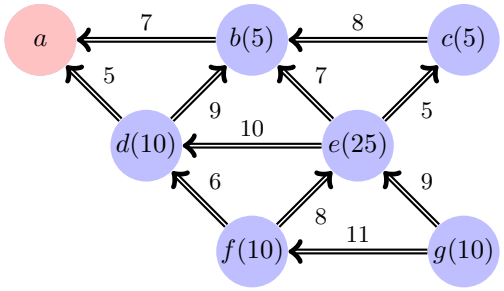

(a) Bank a defaults exogenously. This is called a fundamental default.

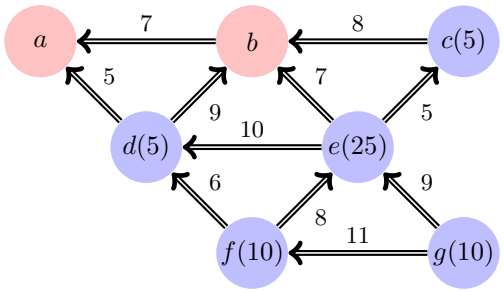

(b) First round of defaults: bank b's capital cannot withstand the loss due to the exposure to a. Bank d writes down the exposure to a from its capital.

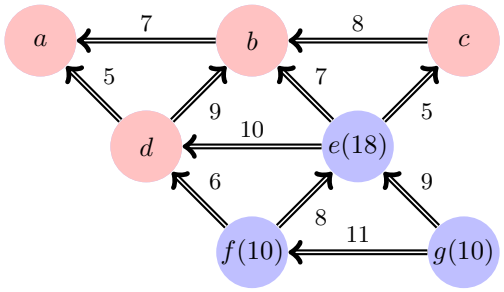

(c) Second round of defaults: banks c and d default due to their respective exposures to b. Bank e writes down the exposure to b from its remaining capital.

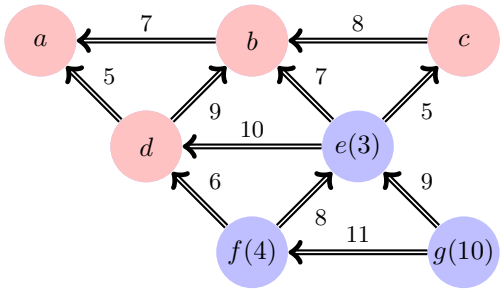

(d) Round 4: no other defaults occur. Bank e writes down the exposure to c and d from its remaining capital, and bank f writes down its exposure to d from its capital. Contagion ends here.

Figure I.1: Contagion on a toy financial network. Links represent exposures net of collateral. Nodes' labels represent capital buffers.

2.2.3 Illiquidity cascades

So far we discussed insolvency cascades that start from a set of exogenous initial bank defaults in a context where all balance sheets were observed at a time 1 after an exogenous shock. The purpose of this section is to explain this shock as well as the emergence of initial defaults as resulting from other distress propagation mechanisms.

This brings us to the previous period, i.e. time 0, at which a snapshot of a bank's balance sheet has been shown in Table I.1a. We now draw more detail in the balance sheet at time 0 by decomposing assets according to their liquidity and maturity.

Distinguishing short-term and long-term claims The non-interbank assets $\tilde{x}(i)$ are decomposed into highly liquid assets, that we assimilate to cash, $m(i)$ and an illiquid portfolio for which the mark-to-market value at time 0 is given by $\phi(i)$. Thus

$$\tilde{x}(i) = m(i) + \phi(i).$$

The illiquid portfolio is assumed to be funded by collateralized short term debt. However, debt cannot finance 100% of the illiquid portfolio. The difference between the market value of the illiquid asset and the value as collateral is called "haircut" and is funded by equity [33]. It follows that the exposure $e(i,j)$ of i to j includes the funding $f(i,j)$ of j's illiquid portfolio. Letting $H(i)$ the haircut applied to i's illiquid assets, we have that

$$\phi(i)(1 - H(i)) = \sum_j f(j,i). \tag{I.15}$$

Furthermore we let $s(i,j)$ the cash flow at time 0 from j to i. This may be a loan arriving at maturity, margin calls on derivatives, coupon payments or other contractual cash flows that is payable at time 0.

Two cases are of particular interest. First, the due cash-flows may be related to a shock in haircuts. If there is a (positive) jump in the haircut of bank i at time 0, equal to $\Delta H(i)$, if follows that the liquidity outflow of bank i includes $\frac{\Delta H(i)}{1-H(i)} \sum_j f(j,i)$. The situation where haircuts jump to 100% is equivalent to the situation where there is a run of short term creditors on bank j and its illiquid asset becomes unusable[33].

Second, the liquidity outflow of a bank i may be related to collateral demands from counterparties on OTC derivatives. The liquidity outflow in this case may be particulary large if a bank has net unidirectional positions with negative mark-to-market. Such a famous example is AIG, who had large net seller positions on CDS contracts.

We can write the net interbank liquidity outflow of bank i as the difference between the total liquidity outflow and the total liquidity inflow of bank i:

$$\Delta m(i) = \sum_j s(j,i) - \sum_j s(i,j). \tag{I.16}$$

Table I.2b shows a balance sheet of a bank, where these details have been added.

We consider that banks with low liquidity have no incentive to sell the illiquid portfolio on the market in a fire sale rather than funding it [59] and that, at our observation time 0 the funding capacity of illiquid portfolios has been attained. Otherwise said, we are in the phase after balance sheets have expanded, so no supplementary liquidity enters the market, but rather banks, anticipating difficulties ahead, start hoarding on liquidity and applying higher margins.

Net cash outflow $\Delta m(i)$	Interbank inflows $\sum_j s(i,j)$
Interbank outflows $\sum_j s(j,i)$	

(a) Cash Flow at time 0.

Interbank assets $\sum_j e(i,j)$ including Short term collateralized lending $\sum_j f(i,j)$	Net worth $c(i)$
	Deposits $D(i)$
Liquidity $m(i)$	Interbank liabilities $\sum_j e(j,i)$ Short term collateralized borrowing $\sum_j f(j,i)$
Illiquid assets $\phi(i)$	
Assets	Liabilities

(b) Stylized balance sheet of a bank.

Table I.2

In this case, the liquidity condition of bank i is given by

$$m(i) - \Delta m(i) \geq 0. \tag{I.17}$$

Remark 2.3. *Let us compare our liquidity Condition (I.17) with the liquidity condition given in the literature that investigates illiquidity due to withdrawal of short term funding alone. If a bank i suffers a liquidity shock in the form of an increase in haircuts (with the convention that haircuts increase to 1 at full funding withdrawal) we have $s(i,j) = \frac{\Delta H(i)}{1-H(i)} f(j,i)$. Condition (I.17) becomes*

$$m(i) - \frac{\Delta H(i)}{1-H(i)} \sum_j f(j,i) > 0, \text{ which can be written as}$$
$$m(i) + (1 - H(i) - \Delta H(i)) \cdot \phi(i) > \sum_j f(j,i).$$

The second inequality is obtained by applying Eq. (I.15). This condition is equivalent to the absence of a run of short term creditors in [115].

Cash flows and illiquidity cascades If a bank j is illiquid because it does not satisfy Condition (I.17), i.e. $m(i) - \Delta m(j) < 0$, then we will call this bank fundamentally illiquid. If there exists a set of fundamentally illiquid banks, than an illiquidity cascade might ensue. Indeed, the net liquidity outflow $\Delta m(i)$ was given in Eq. (I.16) as if all due liquidity inflows were actually received. But, if a counterparty of i, say j is illiquid, then it will default on its due payments to i. As such, the liquidity inflow of bank i is diminished by $s(i,j)$, so bank i may turn illiquid. We can now define an illiquidity cascade similarly to the insolvency cascade

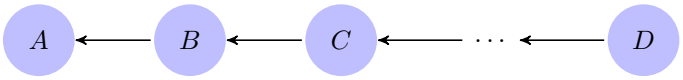

Figure I.2: Chains of intermediaries in OTC markets. Source: Cont and Minca (2011) [45]

in the short term given by Definition 2.2. Keeping the same notations as in Definition 2.2, the final set of illiquid banks is given by

$$\mathbb{D}_{n-1}(\mathbf{s}, \mathbf{m} - \Delta\mathbf{m}),$$

while the total liquidity net outflow is given by

$$\Delta\tilde{m}(i) = \Delta m(i) + \sum_{j \in \mathbb{D}_{n-1}(\mathbf{s}, \mathbf{m}-\Delta\mathbf{m})} s(i,j). \tag{I.18}$$

Note that this liquidity net outflow appears in the balance sheet of the bank under the form of profit and loss, so it is immediately deduced (or added in case it is negative) from capital. Such network effects, are investigated in [45] in the context of OTC derivatives cash flows. Consider for example an institution A that buys protection from an institution B. Institution B will hedge its exposure to the default of the reference entity by buying protection from an institution C, and so on, until reaching an institution D which is a net seller of protection. This is pictured in Figure I.2. All the intermediary institutions seem well hedged and have little incentive to keep a high liquidity position. On the other hand, margin calls may be particulary large following jumps in the spread of the reference entity. If the end net seller of protection defaults, then there is potential of domino effects along the above chain of intermediaries.

2.2.4 Liquidation and price feedback effects

Upon the default of bank j, the holders of its secured debt liquidate the portfolio of illiquid assets. This might trigger important price feedback effects [33, 51].

Consider that there is a finite set of assets on the market whose prices before the distressed selling prices are given by $(S_k)_k \geq 1$. Then the portfolio of bank j can be written as the vector product $\phi(j) = \mathbf{S} \cdot \beta(j)$.

Following [51], we let λ specify the vector of market depths: i.e., the price of asset k moves by 1% when the net supply is equal to $\frac{\lambda}{100}$.

Due to illiquid banks, the price of asset k becomes

$$S'_k = S_k(1 - \frac{1}{\lambda_k} \sum_{j \in \mathbb{D}_{n-1}(\mathbf{s}, \mathbf{m}-\Delta\mathbf{m})} \beta_k(j)). \tag{I.19}$$

This change in price induces a change in the value of the portfolio of a bank i

$$\begin{aligned} \phi'(i) &= \sum_k \beta_k(i) S'_k = \phi(i) - \sum_{j \in \mathbb{D}_{n-1}(\mathbf{s}, \mathbf{m}-\Delta\mathbf{m})} \beta_k(i) \sum_k \beta_k(j) S_k \frac{1}{\lambda_k} \\ &= \phi(i) - \sum_{j \in \mathbb{D}_{n-1}(\mathbf{s}, \mathbf{m})} \rho(i,j), \end{aligned} \tag{I.20}$$

where

$$\rho(i,j) := \sum_k \beta_k(i)\beta_k(i)S_k\frac{1}{\lambda_k} \tag{I.21}$$

can be understood as the impact on the portfolio of i of liquidating the portfolio of j.

As we have seen in the previous subsection, the illiquidity cascade starting from several banks that default on their cash-flows leads to a final set of illiquid banks given by $\mathbb{D}_{n-1}(\mathbf{s}, \mathbf{m} - \Delta\mathbf{m})$.

Now, taking into account the price feedback effects, we have that for every bank i, there will be a supplementary capital loss equal to $\sum_{j\in\mathbb{D}_{n-1}(\mathbf{s},\mathbf{m})}\rho(i,j)$. The shock $\varepsilon(i)$ from section 2.2.1 is now endogenized and equal to $\Delta m + \sum_{j\in\mathbb{D}_{n-1}(\mathbf{s},\mathbf{m})}(\rho(i,j) + s(i,j))$:

$$c(i) = \tilde{c}(i) - \sum_{j\in\mathbb{D}_{n-1}(\mathbf{s},\mathbf{m})}(\rho(i,j) + s(i,j)). \tag{I.22}$$

The set of banks $\mathbb{D}_{n-1}(\mathbf{s}, \mathbf{m} - \Delta\mathbf{m})$ can be seen as the fundamental set of defaults at time 1 when we consider the insolvency cascade.

An important observation is the effective appearance of the exposures $\rho(i,j)$, which on the contrary of all other exposures encountered so far, are not related to contractual claims. A bank i has a hidden exposure to j because they hold similar assets in their portfolio. These exposures reveal themselves at the time of the fire sale and are likely to just as sizeable, or probably even more than exposures related to contractual claims [2].

We have thus seen that distress propagates in a financial network through a sequence of mechanisms. Starting from a liquidity shock, banks may become illiquid. The initial illiquidity and default on payments may transmit to counterparties, which in absence of the inflows from their illiquid counterparties cannot meet their payments and default. A cascade of illiquidity may thus ensue. At the end of this cascade, we obtain a set of illiquid banks. At this point, liquidation of the defaulted bank's portfolios generate a loss in the capital of all banks holding similar assets, irrespective of them having direct claims on defaulted banks. With the set of fundamental defaults given by the set of illiquid banks and the shock on the capital arising from fire sales of illiquid bank's portfolios, we have the premises for an insolvency cascade. This is pictured in Figure I.3. It is then obvious that a necessary condition for the financial network to be resilient to the initial shocks is that both the network of payments $\mathbf{s}$ endowed with the liquidity buffer $\mathbf{m} + \Delta\mathbf{m}$ and the network $\mathbf{e}$ endowed with the capital buffer $\mathbf{c}$, considered after a shock coming from fire sales, are resilient to contagion.

2.3 Random financial network models

2.3.1 Random graphs and complex networks

We have shown in the previous section that various channels of distress propagation - insolvency, illiquidity and price feedback effects - may be modeled as some kind of network epidemics, in the web of interbank exposures, interbank short term lending, the network of derivative cash flows or the network describing the degree of similarity between banks' portfolios. Financial networks generally consist of several thousands of nodes, so an exhaustive analysis of distress propagation in such large networks is not possible. On the other hand, thanks to their size, the behavior of cascades on financial networks can be studied sing a probabilistic approach: we can introduce a random network of which the financial network is a typical sample and analyze, under some mild conditions, the cascading behavior of this random counterpart. The question is

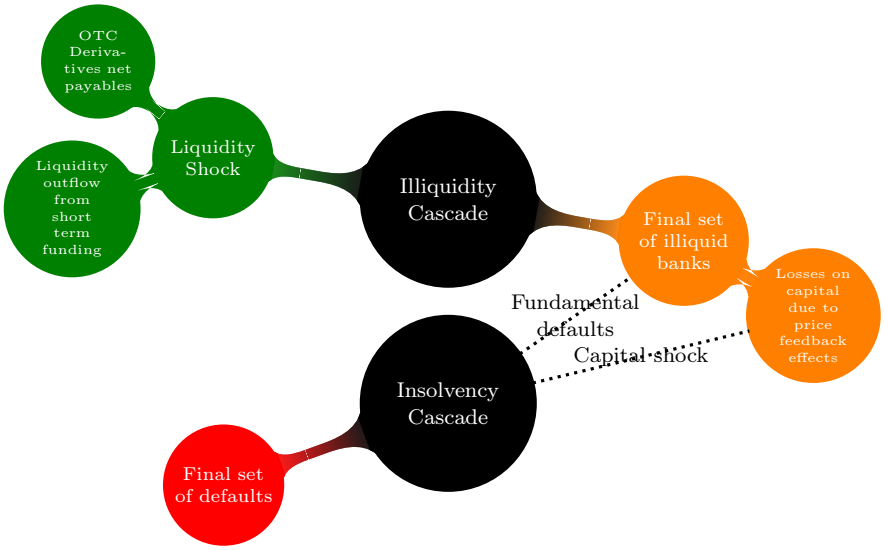

Figure I.3

then what type of random graphs are suitable models for financial networks. Empirical studies like [47, 28] for interbank exposure networks, or [128] for interbank payment flows have pointed out the heterogenous nature of these network's features. First, both the in and out-degree of a node - its number of in-coming and out-going links - are characterized by a power law tail distribution. More precisely, $\mu^+(k)$, defined as the probability that a node chosen uniformly at random has a number k of incident links, is such that for a parameter $\gamma > 0$, $\mu^+(k) \sim k^{-\gamma}$ for k larger than a given constant. A similar empirical result holds for the out-degree. This is known as the *scale-free* property and is a property shared with a plethora of other networks, arising in completely different contexts [117]. Second, the weights on the edges - receivables or exposures - also have a skewed distributions.

These networks are structurally different from the classical **Erdős-Rényi random graphs** [69]. Indeed, in the classical random graphs, each pair of nodes is linked with probability p independently of everything else. If $p = c/n$, the sequence of degrees has an asymptotic Poisson distribution of average c, which is a homogenous distribution. In order to account for the scale free properties of real networks, Newman et al. proposed in a series of papers to use as an underlying graph model the so called random graph with fixed degree distribution [118, 119]. Some of the properties of this random graph had been previously investigated by Molloy and Reed [112, 113]. Their version of the model is in fact different from [118, 119] in the sense that they look at graphs with prescribed degree sequences rather than prescribed degree distributions. The sequences of degrees can be any integers that satisfy certain conditions.

The random graph with prescribed degree sequences denoted by $G_n(\mathbf{d_n})$ is the random graph taken uniformly over all graphs having these degree sequences. Whereas it is difficult to investigate directly the properties of this graph, it is standard to investigate them on the random graph $G_n^*(\mathbf{d_n})$ constructed in the following way [20, 25]: assign to each node i, $d(i)$ half-edges and then choose a pairing of all half edges (belonging to all nodes) uniformly among all pairings. A pair of half edges is forming an edge. Since parallel edges and self-loops may appear,

$G_n^*(\mathbf{d_n})$ is in fact a multi-graph. $G_n(\mathbf{d_n})$ is then obtained by conditioning the multigraph on being a simple. In the literature $G_n^*(\mathbf{d_n})$ is known as the **configuration model** on the given degree sequence $\mathbf{d_n}$.

Although the classical model of Erdős-Rényi cannot capture the properties of real networks, the most important finding in the seminal papers [69, 70] - namely the fact that many graph properties undergo a phase transition with a rather small change in the parameters [96] - has been shown to have corresponding results on the configuration model.

If we denote by $ER(n, c/n)$ the Erdős-Rényi random graph of size n where edges are present independently with probability c/n, the following result holds [27]: If $c < 1$ then with high probability (i.e with probability tending to 1 as $n \to \infty$), every component of $ER(n, c/n)$ has order $O(logn)$. If $c > 1$ then with high probability $ER(n, c/n)$ has a component with $(\alpha(c) + o(1))n$ vertices, where $\alpha(c) > 0$, and all other components have $O(logn)$ vertices.

So, with a slight increase in the average connectivity (which is the only parameter governing Erdős-Rényi random graphs), we a pass to a regime where a giant component (i.e., a connected component representing a positive fraction of the graph) exists. In the case of $G_n(\mathbf{d_n})$, the corresponding question of the existence of a giant component was answered by Molloy and Reed [113] who show that $G_n(\mathbf{d_n})$ contains a giant component w.h.p. if and only if $\sum_k \mu(k)k(k-2) > 0$.

Now consider the case of a simple epidemics on the random graph $ER(n, c/n)$: for any pair of neighbors, there is a symmetric probability p that any of them, if infected, will transmit the infection to the other. The question of whether it is possible for a single node to infect a positive fraction of all nodes, is in fact equivalent to the existence of a giant component in the random graph $ER(n, pc/n)$. Indeed, it is easy to see that the random graph $ER(n, pc/n)$ has the same distribution as the random graph obtained from $ER(n, c/n)$ by removing any edge with probability $1 - p$ independently of everything else (this model in which edges are removed independently with a certain probability is known as bond percolation). Then the spread of the above epidemics on the random graph $ER(n, c/n)$ presents a phase transition stemming from the emergence of the giant component in the random graph $ER(n, pc/n)$: with a slight increase in the 'contagiousness' p of the infection we pass to a regime where a single node can infect a positive fraction of the network. It is clear from this simple example that geometrical properties in networks (i.e., does a giant component exist) are closely related to their dynamic properties like the spread of epidemics.

Bearing this in mind, we turn our attention to the configuration model. The version of Molloy and Reed [112] has been extended by Cooper and Frieze [52] to allow for prescribed sequences of directed degrees. In Chapter III we further extend the model to allow for a prescribed sequences of weights, while relaxing the conditions on the degree sequence given in [52]. The Weighted Configuration Model will be the basis of our model of financial network, on which we will study distress propagation. In numerical applications of Chapters III and IV, we will use another multi-graph model, due to Blanchard [24]. Starting from a prescribed power law distribution of the in-degree and out degree, one can generate, under certain conditions, a random graph with this distributions. We extended the original model to account for the heterogeneity of weights.

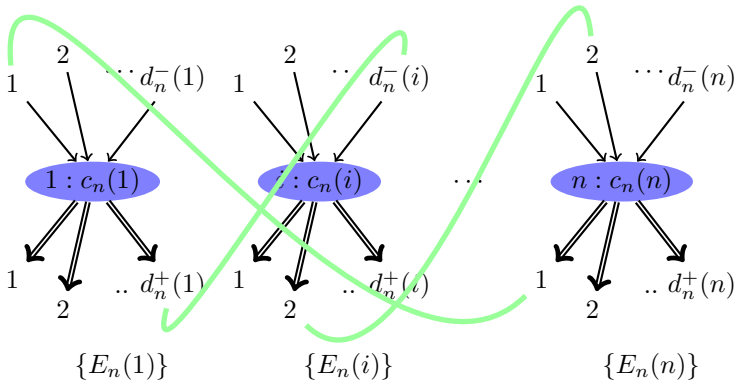

Figure I.4: Configuration model

2.3.2 Weighted Configuration Model

(**Definition 2.5** - Weighted Configuration Model)**.** Given a set of nodes $[1, \ldots, n]$ and a degree sequence $(\mathbf{d_n^+}, \mathbf{d_n^-})$, we associate to each node i two sets, $H_n^+(i)$ representing its out-going half-edges and $H_n^-(i)$ representing its in-coming half-edges, with $|H_n^+(i)| = d_n^+(i)$ and $|H_n^-(i)| = d_n^-(i)$. Let $H_n^+ = \bigcup_i H_n^+(i)$ and $H_n^- = \bigcup_i H_n^-(i)$. A prescribed set of weights $E_n(i)$ where $|E_n(i)| = d_n^+(i)$ is assigned in an arbitrary order to i's out-going half edges. A **configuration** is a matching of H_n^+ with H_n^-. To each configuration we assign a graph. When an out-going half-edge of node i is matched with an in-coming half-edge of node j, a directed edge from i to j appears in the graph. The **configuration model** is the probability space in which all configurations, as defined above, have equal probability. We denote the resulting random directed multigraph by $G_n^*(\mathbf{d_n^-}, \mathbf{d_n^+}, \mathbf{E_n})$, shown in Figure I.4.

2.3.3 Weighted Blanchard model

In Blanchard's random graph model [24], one is given a prescribed degree sequence. Conditionally on the sequence of out-degrees, an arbitrary out-going edge will be assigned to an end-node with probability proportional to the power α of the node's out-degree. For $\alpha > 0$, one obtains positive correlation between in and out-degrees.

The empirical distribution of the out-degree is assumed to converge to a power law with tail coefficient γ^+:

$$\mu_n^+(j) := \#\{i \mid d_n^+(i) = j\} \overset{n\to\infty}{\to} \mu^+(j) \sim j^{\gamma^+ + 1}. \tag{I.23}$$

The main theorem in [24] states that the marginal distribution of the out-degree has a Pareto tail with exponent $\gamma^- = \frac{\gamma^+}{\alpha}$, provided $1 \leq \alpha < \gamma^+$:

$$\mu_n^-(j) := \#\{i \mid d_n^-(i) = j\} \overset{n\to\infty}{\to} \mu^-(j) \sim j^{\gamma^- + 1}.$$

In Chapter V, we extend this model to account for the heterogeneity of weights. The intuition behind our construction can be given by rephrasing the Pareto principle: 20% of the links carry 80% of the weights. Therefore, we will distinguish between two types of links. Links of type A represent a percentage a of the total number of links, but carry a percentage a' of the total mark-to-market value. All other links are said to be of type B.

We can now define the random graph model.

(**Definition 4.3** - Weighted Blanchard Model)**.** *Let $(d_n^+(i))_{i=1}^n$ a prescribed sequence of out-degrees, assumed to verify Condition 4.2. For every node i, its $d_n^+(i)$ in-coming links are partitioned into $d_n^{+,A}(i)$ links of type A and $d_n^{+,B}(i)$ links of type B:*

$$d_n^+(i) = d_n^{+,A}(i) + d_n^{+,B}(i). \tag{I.24}$$

We denote $m^A := \sum_{i=1}^n d_n^{+,A}(i)$ and by $m^B := \sum_{i=1}^n d_n^{+,B}(i)$ the total number of links of type A and type B respectively. We let $F^A : \mathbb{R}_+^{m^A} \to [0,1]$ and $F^B : \mathbb{R}_+^{m^B} \to [0,1]$ the joint probability distributions functions for links of type A and B respectively. The probability distribution functions F^A and F^B are assumed to be invariant under permutation of their arguments.

The random graph is generated then as follows:

- *Generate the weighted subgraph of links of type A by Blanchard's algorithm with prescribed degree sequence $(d_n^{+,A}(i))_{i=1}^n$ and parameter $\alpha > 0$.*
- *Draw m^A random variables from the joint distribution F^A. Assign these exchangeable variables in an arbitrary order to the links of type A.*
- *Proceed similarly for the links of type B.*

3 Contributions of the thesis

We make here a chapter by chapter summary of this thesis' contributions. Part of this overview, referring to the network approach to systemic risk, will be published as a chapter entitled

Mathematical modeling of systemic risk, Financial Networks, Springer Series in Mathematics [110].

The models introduced in Subsections 2.2.3 and 2.2.4 are an original contribution of this thesis. They are intended to provide a base, according to the author's own view, for joint modeling of illiquidiy and insolvency cascades. We model the causal links between these types of cascades as price feedback effects.

3.1 Contributions of Chapter II

Chapter II is dedicated to the reduced approach to default modeling. This work will appear as

Rama Cont and Andreea Minca, Recovering portfolio default intensities implied by CDO quotes, Mathematical Finance (2011) [46].

As we explained in Section 1.3, in Chapter II we propose a rigorous approach to the calibration of "top-down" pricing models for portfolio credit derivatives to a set of observed CDO tranche spreads. First, we show a "mimicking theorem" for point processes which states that the marginal distributions of a loss process with arbitrary stochastic intensity can be matched using a *Markovian* point process. This result implies that, given any risk-neutral loss process with given default intensity we can construct a Markovian loss process which leads to the same prices. This observation allows to narrow down the calibration problem to the search for a Markovian loss process verifying a set of calibration constraints. We formalize this problem in terms of the minimization of relative entropy with respect to the law of a prior loss process under calibration constraints. We use convex duality techniques to solve the problem: the dual problem is shown to be an intensity control problem, characterized in terms of a Hamilton-Jacobi system of differential equations which can be analytically solved.

3.2 Contributions of Chapter III

We overview here the main results which were given in the context of insolvency cascades in financial networks in III, but the model can be used for other types of cascades on a network. We will apply the same model to study illiquidity cascades in chapter V, therefore we prefer to present it in the following form drawn from the game theory literature [101].

We consider a directed network in which nodes can be in one of two states, say 0 and 1. Starting from a set of nodes initially in the state 1, other nodes switch to state 1 according to the weighted influence of their neighbors and a personal threshold.

More precisely, we define the network $\mathbf{w_n}$ on the vertex set $\mathbf{v} = \{1, \dots, n\}$, whereby $w_n(i,j)$ weighs the influence of node j on the state of node i. Each node i has a threshold $q_n(i)$ which determines its capacity to withstand the influence of other nodes. Denoting by $X(j) \in \{0,1\}$ the state of a node j, node i switches to state 1 the first time the following condition is met

$$\sum_j X(j) w_n(i,j) > q_n(i). \tag{I.25}$$

The out-neighbors of a node i are given by the set of nodes having an influence on i and its in-neighbors are given by the set of nodes on which i has an influence. Their respective numbers represent node i's out-degree $d_n^+(i) := \#\{j \mid w_n(i,j) > 0\}$, and respectively in-degree $d_n^-(i) := \#\{j \mid w_n(j,i) > 0\}$. The empirical distribution of the degrees is given by

$$\mu_n(j,k) := \frac{1}{n} \#\{i : d_n^+(i) = j, d_n^-(i) = k\}.$$

We assume that the degree sequences $\mathbf{d_n^+}$ and $\mathbf{d_n^-}$ satisfy the following regularity conditions.

(**Assumption 3.1).** For each $n \in \mathbb{N}$, $\mathbf{d_n^+} = \{(d_n^+(i))_{i=1}^n\}$ and $\mathbf{d_n^-} = \{(d_n^-(i))_{i=1}^n\}$ are sequences of nonnegative integers with $\sum_{i=1}^n d_n^+(i) = \sum_{i=1}^n d_n^-(i)$, and such that, for some probability distribution $\mu(j,k)$, the following hold:

1. *The degree density condition:* the proportion $\mu_n(j,k)$ of nodes with degree (j,k) tends to $\mu(j,k)$, i.e.,

$$\mu_n(j,k) \overset{n\to\infty}{\to} \mu(j,k)$$

2. *Finite expectation property:* $\sum_{j,k} j\mu(j,k) = \sum_{j,k} k\mu(j,k) =: \lambda \in (0,\infty)$;

3. *Second moment property:* $\sum_{i=1}^{n} (d_n^+(i))^2 + (d_n^-(i))^2 = O(n)$.

We turn now our attention to the role of weights and thresholds in the spread of the epidemics. We denote by $\Sigma^{\mathbf{w}}(i)$ the set of permutations of i's out-neighbors and let $\tau \in \Sigma^{\mathbf{w}}(i)$ specify the order in which i's out-neighbors switch to state 1. Then Condition (I.25) is equivalent to saying that node i switches to state 1 precisely after a certain number of its out-neighbors have switched to state 1, where this number is given by

$$\Theta(i, \mathbf{w}, \mathbf{q}, \tau) := \min\{k \geq 0, \sum_j w(i, \tau(j)) > q(i)\}. \tag{I.26}$$

The map Θ gives the *discretized thresholds* that govern the spread of epidemics.
We let

$$p_n(j,k,\theta) := \frac{\#\{(i,\tau) \mid 1 \leq i \leq n,\ \tau \in \Sigma^{\mathbf{e_n}(i)},\ d_n^+(i) = j,\ d_n^-(i) = k,\ \Theta(i, \mathbf{w_n}, \mathbf{q_n}, \tau) = \theta\}}{n\mu_n(j,k)j!}, \tag{I.27}$$

for which we make the following assumption:

(**Assumption 3.4).** *There exists a function* $p : \mathbb{N}^3 \to [0,1]$ *such that for all* $j,k,\theta \in \mathbb{N}$ $(\theta \leq j)$

$$p_n(j,k,\theta) \overset{n\to\infty}{\to} p(j,k,\theta).$$

(**Definition 3.3 - Contagious links).** *We say that a link is 'contagious' if it represents an influence on a node larger than its threshold.*

It is easy to see that $p_n(j,k,1)$ represents the proportion of 'contagious' links leaving nodes with degree (j,k). The limit $p(j,k,1)$ also represents the fraction of nodes with degree (j,k) that switch to 1 as soon as one out-neighbor has switched to 1.

We now define the random network with prescribed degree and weights.

(**Definition 2.4 - Random network ensemble).** Let $\mathcal{G}_n(\mathbf{w_n})$ be the set of all weighted directed graphs with degree sequence $\mathbf{d_n^+}, \mathbf{d_n^-}$ such that, for any node i, the set of weights is given by the non-zero elements of line i in the matrix $\mathbf{w_n}$. On a probability space $(\Omega, \mathcal{A}, \mathbb{P})$, we define $\mathbf{W_n}$ as a random network uniformly distributed on $\mathcal{G}_n(\mathbf{w_n})$.

Then for all $i = 1, \ldots, n$,

$$\{\mathbf{W_n}(i,j), \quad \mathbf{W_n}(i,j) \neq 0\} = \{\mathbf{w_n}(i,j), \quad \mathbf{w_n}(i,j) \neq 0\} \quad \mathbb{P} - a.s.$$

$$\#\{j \in \mathbf{v},\ \mathbf{W_n}(j,i) > 0\} = d_n^+(j), \quad \text{and} \qquad \#\{j \in \mathbf{v},\ \mathbf{W_n}(i,j) \neq 0\} = d_n^-(i).$$

We denote by $\alpha_n(\mathbf{W_n}, \mathbf{q_n})$ the set of defaults at the end of the cascade generated by the set of nodes $\{i \mid q_n(i) = 0\}$.

The following theorems give the asymptotic behavior of this quantity.

(**Theorem 3.8).** *Define the function*

$$I(\pi) := \sum_{j,k} \frac{k\mu(j,k)}{\lambda} \sum_{\theta=0}^{j} p(j,k,\theta)\mathbb{P}(\mathrm{Bin}(j,\pi) \geq \theta), \tag{I.28}$$

where $\mathrm{Bin}(j,\pi)$ *denotes a binomial variable with parameters* j *and* π.

Consider a sequence of weights and thresholds $\{(\mathbf{w_n})_{\mathbf{n\geq 1}}, (\mathbf{q_n})_{\mathbf{n\geq 1}}\}$ *satisfying Assumptions 3.1 and 3.4 and the corresponding sequence of random matrices* $(\mathbf{W_n})_{n\geq 1}$ *defined on* $(\Omega, \mathcal{A}, \mathbb{P})$ *as in Definition 2.4. Let* π^* *be the smallest fixed point of* I *in* $[0,1]$*, i.e.,*

$$\pi^* = \inf\{\pi \in [0,1] \mid I(\pi) = \pi\}.$$

1. *If* $\pi^* = 1$*, i.e., if* $I(\pi) > \pi$ *for all* $\pi \in [0,1)$*, then asymptotically all nodes switch to state* 1*:*
$$\alpha_n(\mathbf{W_n}, \mathbf{q_n}) \xrightarrow{p} 1.$$

2. *If* $\pi^* < 1$ *and furthermore* π^* *is a stable fixed point of* I $(I'(\pi^*) < 1)$*, then the asymptotic fraction of nodes in state* 1 *at the end of the cascade satisfies:*
$$\alpha_n(\mathbf{W_n}, \mathbf{q_n}) \xrightarrow{p} \sum_{j,k} \mu(j,k) \sum_{\theta=0}^{j} p(j,k,\theta)\mathbb{P}(\mathrm{Bin}(j,\pi^*) \geq \theta).$$

(**Definition 4.1 - Resilience measure).** *We define as the resilience measure the following function of the network's features, which takes values in* $(-\infty, 1]$*:*

$$1 - \sum_{j,k} \frac{jk}{\lambda} \mu(j,k) p(j,k,1).$$

(**Theorem 4.3 and Corrolary 4.2).** *Under Assumptions 3.1 and 3.4*

- *If the resilience measure is positive, i.e.,*
$$1 - \sum_{j,k} \frac{jk}{\lambda} \mu(j,k) p(j,k,1) > 0, \tag{I.29}$$
then for every $\varepsilon > 0$*, there exists* N_ε *and* ρ_ε *such that if the initial fraction of nodes in state* 1 *is smaller than* ρ_ε*, then* $\mathbb{P}(\alpha_n(\mathbf{W_n}, \mathbf{q_n}) \leq \varepsilon) > 1 - \varepsilon$ *for all* $n \geq N_\varepsilon$*.*

- *If the resilience measure is negative, i.e.,*
$$1 - \sum_{j,k} \frac{jk}{\lambda} \mu(j,k) p(j,k,1) < 0, \tag{I.30}$$
then there exists a connected set C_n *of nodes representing a positive fraction of the network, i.e.,* $|C_n|/n \xrightarrow{p} c > 0$ *such that, with high probability, any node in the set switching to state* 1 *activates the whole set: for any sequence* $(q_n)_{n\geq 1}$ *such that* $\{i, q_n(i) = 0\} \cap C_n \neq \emptyset$*,*
$$\liminf_n \alpha_n(W_n, q_n) \geq c > 0.$$

Empirical studies on banking networks [28, 128, 48], which reveal that such networks have complex heterogeneous structures, motivated us to study contagion on a weighted and directed network. We embed a financial network in the probability space given by the Weighted Configuration Model, on which we analyze the diffusion contagion.

Our Definition of the Weighted Configuration Model is inspired by our intention to model the network from the perspective of a regulator: many of the network's features are prescribed (otherwise said they are parameters of the model), since the regulator observes the bank's balance sheets. We prescribe the degree sequences, but also the exposure sequences. This model, to our knowledge, is new in the random graph literature and our results generalize previous results on diffusions in random graphs with prescribed degree sequence to the weighted case. Related and well studied problems are the existence of a giant component [52, 113], the k-core problem [36], or bootstrap percolation [6, 7, 17]. Based on a coupling argument allowing to reveal sequentially exposures to defaulted nodes, we are able to identify a multi-dimensional Markov chain which determines at any time the size of contagion. With respect to the history of this Markov chain, the moment when contagion ends is a stopping time. This idea originated in [17] who studied bootstrap percolation on a random regular graph. In our case, several difficulties arise. First, the dimension of the Markov chain is no longer constant like in the case of the regular graph, but depends on the size of the network. Therefore, we generalize to this case the differential equation method in Wormald [134] to show convergence in probability of the trajectory of the rescaled Markov chain to the trajectory of some ordinary differential equations, which can be solved in closed form. Second, we prove the coupling Lemma 6.1, which allows to reduce the case of continuous thresholds to the discretized case. Last, we relax the conditions given in [52] for the directed configuration model. In particular we do not require a strong condition on the maximum degree, rather the condition on the second order moment. This is a crucial requirement in order to apply our results to realistic distributions of degrees of financial networks.

Compared with the existing finance literature, similar cascade conditions have been given previously under branching process approximations by [76], who in turn have extended previous well known work by Watts [133]. The cascade condition, marks the divergence of the **expected** size of a cascade starting from a randomly chosen node, the expectation being taken over the law of the random graph with the given degree distribution.

By comparison, our results are stronger statements on the convergence in probability of the number of defaults for large networks. If the cascade condition is satisfied, this represents a statement holding with probability tending to one as the size of the network tends to infinity, that on a typical sample of our random network, any small fraction of initial defaults chosen uniformly at random triggers a global cascade. More importantly, unlike Gai & Kapadia [76], we do not assume a specific probabilistic model for the degree sequence or the balance sheet data: actual balance sheet data may be used as an input, under mild assumptions. All this is crucial if one wants to identify and monitor the nodes posing the largest systemic risk, or sets of most influential nodes [101].

In summary:

- We obtain an asymptotic expression for the size of a default cascade in a large network, in terms of the characteristics of the network, extending previous results for homogeneous undirected random graphs to heterogeneous, weighted networks. These asymptotic results are shown to be in good agreement with simulations for networks with large but realistic sizes.

- We obtain an analytical criterion for the resilience of a large financial network to the default of one or several institutions, in terms of the characteristics of the network.

- The analytical nature of these results allows to analyze the influence of network characteristics, in a general setting, more explicitly than in previous studies. In particular, our results underline the role played by *contagious exposures* and show that institutions which are both highly connected and overexposed with respect to their capital may act as potential hubs for default contagion.

- Our results show the importance of taking into account the *heterogeneity* of financial networks when discussing issues of financial stability and contagion. In particular we show that, contrarily to the intuition conveyed by examples based on homogeneous networks, in presence of heterogeneity the relation between (average) connectivity of a network and its resilience to contagion is not monotonous.

3.3 Contributions of Chapter IV

This work has appeared as

Hamed Amini, Rama Cont and Andreea Minca, Stress testing the resilience of financial networks, International Journal of Theoretical and Applied Finance" (2011) [9].

We propose a framework for stress testing the resilience of a financial network to external shocks affecting balance sheets. We describe how to take into account contagion effects when designing stress tests and evaluating the magnitude of losses in stress scenarios. Whereas previous studies of contagion effects in financial networks have relied on large scale simulations, our approach uses an analytical criterion for resilience to contagion, based on the asymptotic analysis of default cascades in heterogeneous networks made in Chapter III. In particular, our methodology does not require to observe the whole network but focuses on the characteristics of the network which contribute to its resilience, namely the connectivity of nodes and concentration of contagious links. Applying this framework to a sample network, we observe that the size of the default cascade generated by a macroeconomic shock across balance sheets may exhibit a sharp transition when the magnitude of the shock reaches a certain threshold: beyond this threshold, contagion spreads to a large fraction of the financial system. We show that the regulator can efficiently contain contagion by focusing on fragile nodes, especially those with high connectivity, and their counterparties. Higher capital requirements could be imposed on them to reduce their number of contagious links, and insure that the danger of phase transitions is avoided.

3.4 Contributions of chapter V

The cascade model of Chapter III can accommodate other interpretations. In Chapter V, we interpret the threshold as a liquidity reserve, while the weights represent cash-flows of OTC derivatives. This is an original interpretation, and the problem has been raised from recent regulatory debates on the efficiency of central clearing. The first contribution in Chapter V is to introduce a hierarchical network model for studying illiquidity contagion in OTC derivatives markets, which takes into account public data on the gross and net notional exposures of dealers and their market share for credit default swaps and interest rate derivatives. In such a setting, liquidity shocks may generate contagion due to margin calls across counterparties in a hedging chain.

A second contribution is to introduce a framework for studying the magnitude and dynamics of illiquidity cascades in OTC markets, in a stress test scenario formulated in terms of liquidity shocks. We obtain a criterion for resilience of the network to liquidity shocks; our criterion highlights the role of 'critical cash flows' i.e. cash flows on which an intermediary depends to meet its own short-term obligations. This resilience criterion provides a measure of contagion risk which, unlike the average expected exposure used in previous studies [63], takes into account the structure of the network and the heterogeneity of exposures. We show that this risk measure is directly related to the size of the illiquidity cascade triggered by the initial default of a small number of market participants.

This framework allows to assess the much-debated impact, in terms of systemic risk, of introducing a CDS clearinghouse. Our simulations show that, in absence of a clearing facility for interest rate swaps, an additional clearing facility for CDS does not necessarily have a positive impact on financial stability. On the contrary, when interest rate derivatives (mainly swaps) are centrally cleared –as is currently the case– a CDS clearinghouse can contribute significantly to financial stability by enhancing the resilience of the OTC network to large liquidity shocks, provided all significant dealers are members of the clearing house.

These results, which are somewhat different from Duffie & Zhu's [63] analysis based on expected average exposure in a complete network model with IID exposures, show the importance of taking into account the structure of the network and using a metric based on 'tail events', not just averages, when discussing the benefits of central clearing for systemic risk. Simulations of illiquidity cascades for a large number of networks confirm these conclusions and show that they hold with a high probability across a wide variety of network topologies.

4 Publications and Working Papers

- R. Cont and A. Minca. Recovering portfolio default intensities implied by CDO quotes. *Mathematical Finance*, 2011.
- H. Amini, R. Cont, and A. Minca. Resilience to contagion in financial networks. *Submitted*, 2010.
- H. Amini, R. Cont, and A. Minca. Stress testing the resilience of financial networks. *To appear in the International Journal of Theoretical and Applied Finance*, 2011.
- R. Cont and A. Minca. Credit default swaps and systemic risk. *Working paper*, 2010.
- Mathematical modeling of systemic risk. In *Financial Networks*, Springer Series in Mathematics. Springer, 2011.

Chapter II

Reconstruction of portfolio default intensities

We propose a stable non-parametric algorithm for the calibration of 'top-down' pricing models for portfolio credit derivatives: given a set of observations of market spreads for CDO tranches, we construct a risk-neutral default intensity process for the portfolio underlying the CDO which matches these observations, by looking for the risk neutral loss process 'closest' to a prior loss process, verifying the calibration constraints. We formalize the problem in terms of minimization of relative entropy with respect to the prior under calibration constraints and use convex duality methods to solve the problem: the dual problem is shown to be an intensity control problem, characterized in terms of a Hamilton–Jacobi system of differential equations, for which we present an analytical solution. Given a set of observed CDO tranche spreads, our method allows to construct a default intensity process which leads to tranche spreads consistent with the observations. We illustrate our method on ITRAXX index data: our results reveal strong evidence for the dependence of loss transitions rates on the previous number of defaults, and offer quantitative evidence for contagion effects in the (risk–neutral) loss process. Keywords: collateralized debt obligation, duality, portfolio credit derivatives, reduced-form models, default risk, intensity control, top-down credit risk models, relative entropy, inverse problem, model calibration, stochastic control.

This work will appear as "Rama Cont and Andreea Minca, Recovering portfolio default intensities implied by CDO quotes, Mathematical Finance" (2011) [46].

Contents

1 Introduction

Credit derivatives markets have witnessed an extraordinary activity in the last decade, especially with the development of a large market in portfolio credit derivatives of which collateralized debt obligations (CDOs) are the most well known example [34]. Yet, as illustrated in the recent market turmoil, commonly used static pricing models such as the Gaussian copula model appear to be insufficient for pricing and hedging these complex derivatives [106, 124]. One of the reasons has been the lack of transparency of such pricing methods in which non-intuitive and unobservable "default correlation" parameters are required as an input.

The Gaussian copula model, which has been widely used for the pricing of CDOs, has some well known shortcomings: its inability to reproduce market values of CDO tranche spreads, as exemplified by the base correlation skew, the instability of its "default correlation" parameters –as revealed by the GM/Ford crisis in May 2005 and the subprime crisis in 2007– and, most importantly, the lack of a well-defined dynamics for the risk factors which prevents any model-based assessment of hedging strategies. Other copula-based models may provide better fits to market quotes but share the other drawbacks of the Gaussian copula model, most notably its static character. These shortcomings have inspired a lot of research on alternative approaches to credit risk modeling [106]. On the other hand, a great advantage of static copula models is the ease with which the parameters can be calibrated to market data: this is a feature which many of the more complex, multi-name dynamic models such as Duffie & Garleanu [62], have lacked so far. The key challenge in improving on the Gaussian copula model lies therefore not so much in adding more realistic features to the model but in adding these features while maintaining analytical tractability, especially in regard to the calibration to market data.

To tackle some of these issues while allowing for a parsimonious parametrization of the model, several recent works [32, 124, 77, 71, 10, 108] have proposed a "top-down" approach to the problem, in which one models in "reduced form" the dynamics of the portfolio loss, as a jump process whose intensity λ_t represents the (conditional) rate of occurrence of the next default and whose jump sizes represent losses given default. Though top-down pricing models are typically much simpler to simulate or implement than high-dimensional reduced form models, numerical methods – Laplace transforms, numerical resolution of ODEs– are still required for the pricing of CDO tranches which makes parameter calibration computationally challenging. Existing studies of top-down pricing models [32, 124, 77, 71, 10, 108] address model calibration by applying black box optimization procedures, whose convergence is not guaranteed, to the resulting high-dimensional nonlinear optimization problems. The lack of convexity of the optimization problems involved may lead to multiple solutions and numerical sensitivity of the results, making such results difficult to reproduce and rendering their interpretation delicate.

In this work we propose a rigorous nonparametric approach to the calibration of "top-down" pricing models for portfolio credit derivatives to a set of observed CDO tranche spreads. First,

we show a "mimicking theorem" for point processes which states that the marginal distributions of a loss process with arbitrary stochastic intensity can be matched using a *Markovian* point process. This result implies that, given any risk-neutral loss process with given default intensity we can construct a Markovian loss process which leads to the same prices. This observation allows to narrow down the calibration problem to the search for a Markovian loss process verifying a set of calibration constraints. We formalize this problem in terms of the minimization of relative entropy with respect to the law of a prior loss process under calibration constraints. We use convex duality techniques to solve the problem: the dual problem is shown to be an intensity control problem, characterized in terms of a Hamilton-Jacobi system of differential equations which can be analytically solved using a change of variable.

Given a set of observed CDO tranche spreads, our method allows to construct an implied intensity process λ_t which leads to tranche spreads consistent with the observations. The implied intensity $\lambda_t = f(t, L_t)$ depends on the defaults in the portfolio, which leads to 'contagion' effects and clustering in the occurrence of defaults. The resulting model is parameterized by the probability (per unit time) of the next default in the portfolio, which allows for an intuitive check on parameter values.

The article is structured as follows. Section 2 describes the cash flow structure of a (static) CDO and present a brief review of the "top-down" modeling approach for portfolio credit derivatives. In section 3 we discuss the level of information about the risk-neutral loss process which can be extracted from CDO tranches: we state a "mimicking theorem" for point processes which implies that, in a general setting, the information content of CDO tranche quotations can be represented in the form of an *effective intensity function* allowing for dependence of the default rate on the current number of defaults in the portfolio and calendar time. The model calibration problem is defined in section 4 and formulated in terms of relative entropy minimization under constraints. In section 4.3 we show that the calibration problem maps, via convex duality, into an *intensity control* problem for a point process, which is then solved using dynamic programming. The special structure of our problem allows for analytical solution of this control problem. These results translate into a calibration algorithm which can be used to extract the risk–neutral default intensity from CDO tranche spreads: the algorithm is laid out in detail in section 5 and applied to ITRAXX index data. Section 6 discusses some implications of our results.

2 Portfolio credit derivatives

We model credit events using a filtered probability space $(\Omega, \mathcal{F}, (\mathcal{F}_t)_{t\in[0,T]}, \mathbb{Q})$, where Ω is the set of market scenarios, the filtration $(\mathcal{F}_t)_{t\in[0,T]}$ represents the flow of information up to a terminal date T and $\mathbb{Q}$ is a risk neutral measure. Consider a reference portfolio on which the credit derivatives we consider will be indexed. The main objects of interest are the number of defaults N_t and the (cumulative) *default loss* L_t of this reference portfolio during a period $[0, t]$. We denote by $B(t, u) = \exp(-\int_t^u r(s)ds)$ the discount factor at date t for the maturity $u \geq t$. We shall assume independence between default risk and interest rate risk.

Most *portfolio credit derivatives* can be modeled as contingent claims whose payoff is a (possibly path-dependent) function of the portfolio loss process $(L_t)_{t\in[0,T]}$. The most important example of portfolio credit derivatives are *index default swaps* and *collateralized debt obligations* (CDO) [34].

2.1 Index default swaps

Index default swaps are now commonly traded on various credit indices such as ITRAXX and CDX series, which are equally weighted indices of credit default swaps on European and US names [34]. In an index default swap transaction, a protection seller agrees to pay all default losses in the index (default leg) in return for a fixed periodic spread S paid on the total notional of obligors remaining in the index (premium leg). Denoting by $t_j,\ j = 1, \ldots, J$ the payments dates,

- the default leg pays at t_j the losses $L(t_j) - L(t_{j-1})$ due to defaults in $]t_{j-1}, t_j]$.
- the premium leg pays at t_j an interest (spread) S on the notional of the remaining obligors

$$(t_j - t_{j-1})S(1 - \frac{N_{t_j}}{n}).$$

In particular the cash flows of the index default swap only depend on the portfolio characteristics via N_t and L_t. The value at $t = 0$ of the default leg is

$$\sum_{j=1}^{J} E^{\mathbb{Q}}[B(0, t_j)(L(t_j) - L(t_{j-1})\mathcal{F}_0]$$

while the value at $t = 0$ of the premium leg is

$$S\sum_{j=1}^{J} E^{\mathbb{Q}}[B(0, t_j)(t_j - t_{j-1})(1 - \frac{N_{t_j}}{n})|\mathcal{F}_0].$$

The index default swap spread at $t = 0$ is defined as the (fair) value of the spread which equalizes the two legs at inception:

$$S_{\text{index}} = \frac{\sum_{j=1}^{J} E^{\mathbb{Q}}[B(0, t_j)(L(t_j) - L(t_{j-1})\ )|\mathcal{F}_0]}{\sum_{j=1}^{J} E^{\mathbb{Q}}[B(0, t_j)(t_j - t_{j-1})(1 - \frac{N_{t_j}}{n})|\mathcal{F}_0]}. \tag{II.1}$$

2.2 Collateralized Debt Obligations (CDOs)

Consider a *tranche* defined by an interval $[a, b], 0 \leq a < b < 1$ for the loss process normalized by the total nominal. A CDO tranche swap (or simply CDO tranche) is a bilateral contract in which an investor sells protection on all portfolio losses within the interval $[a, b]$ over some time period $[0, t_J]$ in return for a periodic spread $S(a, b)$ paid on the nominal remaining in the tranche after losses have been accounted for.

The loss of an investor exposed to the tranche $[a, b]$ is

$$L_{a,b}(t) = (L_t - a)^+ - (L_t - b)^+. \tag{II.2}$$

The premium leg is represented by the cash flow payed by the protection buyer to the protection seller. In case of a premium S, its value at time $t = 0$ is

$$S\sum_{j=1}^{J}(t_j - t_{j-1})E^{\mathbb{Q}}[B(0, t_j)((b - L(t_j))^+ - (a - L(t_j))^+\ )\ |\mathcal{F}_0].$$

The default leg is represented by the cash payed by the protection seller to the protection buyer in case of default. Its value at time $t = 0$ is

$$\sum_{j=1}^{J} E^{\mathbb{Q}}[B(0,t_j)(L_{a,b}(t_j) - L_{a,b}(t_{j-1})\ )|\mathcal{F}_0].$$

The "fair spread" (or simply, the tranche spread) of a mezzanine tranche is the premium value $S_0(a,b,t_J)$ that equates the values of the two legs:

$$S_0(a,b,t_J) = \frac{\sum_{j=1}^{J} E^{\mathbb{Q}}[B(0,t_j)\,(L_{a,b}(t_j) - L_{a,b}(t_{j-1}))\ |\mathcal{F}_0]}{\sum_{j=1}^{J} E^{\mathbb{Q}}[B(0,t_j)(t_j - t_{j-1})\,((b - L(t_j))^+ - (a - L(t_j))^+)\,|\mathcal{F}_0]}. \tag{II.3}$$

For an "equity" tranche ($a = 0$) it is customary to require an upfront fee plus a (fixed) periodic spread f (typically 500 bps). The upfront fee $U_0(K,t_J)$ is defined as

$$\begin{aligned} KU_0(K,t_J) = E^{\mathbb{Q}}[&\sum_{j=1}^{J} B(0,t_j)\,(L_{0,K}(t_j) - L_{0,K}(t_{j-1})\ ) \\ &-f\sum_{j=1}^{J} B(0,t_j)(t_j - t_{j-1})(K - L(t_j))^+|\mathcal{F}_0]. \end{aligned} \tag{II.4}$$

Table 1 gives an example of such a tranche structure and the corresponding spreads for a standardized portfolio, the ITRAXX index. Note that these expressions for the tranche spreads depend on the portfolio loss process only through the expected tranche notionals $C_0(t_j,K)$ at date $t = 0$ where

$$C_0(t,K) = E^{\mathbb{Q}}[B(0,t)(K - L_t)^+|\mathcal{F}_0].$$

When the context is clear we will drop the subscript 0 and denote this quantity $C(t,K)$.

2.3 Top-down models for CDO pricing

It is immediately observed that the expressions (II.3) and (II.4) for the spread of a CDO tranche depend on the portfolio characteristics only through the (risk-neutral) law of the loss process L_t. The idea of "top-down" pricing models [10, 71, 77, 108, 124] is to model the risk neutral loss process, either by specifying the dynamics of the cumulative loss [10, 71, 77, 108] or by looking at the forward loss distribution [124]. We adopt here the former approach, which is simpler to implement.

The loss L_t is a piecewise constant process with upward jumps at each default event: its path is therefore completely characterized by the default times $(\tau_j)_{j\geq 1}$, representing default events and the jump sizes ΔL_j representing the loss given default. Here τ_j denotes the j-th default event observed in the portfolio: the index j is *not* associated with the default of a given obligor but with the ordering in time of the events. The idea of aggregate loss models is to represent the rate of occurrence of defaults in the portfolio via the *portfolio default intensity* λ_t. The number of defaults $(N_t)_{t\in[0,T]}$ is modeled as an $\mathcal{F}_t$-adapted point process with $\mathcal{F}_t$-intensity $(\lambda_t)_{t\in[0,T]}$ under $\mathbb{Q}$ i.e.

$$N_t - \int_0^t \lambda_t dt$$

Maturity	Low	High	Bid\ Upfront	Mid\ Upfront	Ask\ Upfront
5Y	0%	3%	11.75%	11.88%	12.00%
	3%	6%	53.75	54.50	55.25
	6%	9%	14.00	14.75	15.50
	9%	12%	5.75	6.25	6.75
	12%	22%	2.13	2.50	2.88
	22%	100%	0.80	1.05	1.30
7Y	0%	3%	26.88%	27.00%	27.13%
	3%	6%	130	131.50	132
	6%	9%	36.75	37.00	38.25
	9%	12%	16.50	17.25	18.00
	12%	22%	5.50	6.00	6.50
	22%	100%	2.40	2.65	2.90
10Y	0%	3%	41.88%	42%	42.13%
	3%	6%	348	350.50	353
	6%	9%	93	94.00	95
	9%	12%	40	41.00	42
	12%	22%	13.25	13.75	14.25
	22%	100%	4.35	4.60	4.85

Table II.1: CDO tranche spreads, in bp, for the ITRAXX index on March 15 2007. For the equity tranche the periodic spread is 500bp and figures represent upfront payments.

is an $\mathcal{F}_t$-local martingale under $\mathbb{Q}$ [29, Ch. II, Theorem T8]. Intuitively, λ_t can be seen as the number of defaults per year conditional on current market information [29, Eq. 3.4, p. 28]:

$$\lambda_t = \lim_{s \downarrow t} \frac{1}{s-t}\, \mathbb{E}[N_s - N_t | \mathcal{F}_t].$$

Here $\mathcal{F}_t$ represents the coarse-grained information resulting from the observation of the aggregate loss process L_t of the portfolio and risk factors affecting it. In the simplest case it corresponds to the information (filtration) generated by the variables $\tau_j,\ \Delta L_j$ but it may also contain information on other market variables. This risk neutral intensity λ_t can be interpreted as the short term credit spread for protection against the next default in the portfolio [124].

λ_t can be modeled as a stochastic process which can depend on the loss process and other randomly evolving factors. The simplest specification is to model the loss L_t as a compound Poisson process [32] where the default intensity is constant and independent of the loss process, but this does not enable to model features such as spread volatility or clustering of defaults [56]. Spread volatility has been introduced by modeling λ_t as an autonomous jump-diffusion process and then constructing N_t as a Cox process: conditional on $(\lambda_t)_{t\in[0,T]}$, N has the law of a Poisson process with intensity $(\lambda_t)_{t\in[0,T]}$. This approach, common in the credit risk literature [104], has been used by Longstaff & Rajan [108] to model aggregate default rates in the CDX index. Default contagion can be incorporated in the model by introducing a dependence of the default intensity on the number of defaults. Ding et al. [60] construct the default process by starting from a birth process with immigration $\lambda_t = c + gN_t$ and applying a time change, while Arnsdorff & Halperin [10] use a two factor specification: $\lambda_t = \lambda_0(N_0 - N_t)Y_t$ where Y_t is a non-negative stochastic process (see also [111]). Finally, one can argue that not only the occurrence of defaults but also their timing and magnitude can affect the default intensity: this feature has been modeled using self-exciting processes [71, 77].

Given the wide variety of models available for the default intensity, the choice of the model class among the above is not easy in practice. Indeed, even at the qualitative level it is not obvious which parametric specifications adequately reproduce observed features of market data. Also, once the class of models has been chosen, it is a nontrivial task to calibrate the model parameters in order to reproduce market spreads of index CDO tranches. In fact, in the models described above, the inverse problem of recovering parameters from market quotes of tranche spreads is both computationally intensive and ill-posed. Finally, these parameterizations mainly stem from analytical convenience, more than from any fundamental economic considerations, so a nonparametric approach which makes fewer arbitrary assumptions on the form of the default intensity can provide some insight for model selection.

3 Identifiability of models from CDO tranche spreads

One issue in the design and calibration of top-down models is how to parameterize the portfolio loss process in a general, yet parsimonious, way which can be flexible enough to accommodate market observations of tranche spreads and remain tractable. The main issue is how to specify the dependence of the default intensity λ_t with respect to other variables in the model: existing models range from a deterministic intensity to full path-dependence with respect to the loss process [71, 77].

While richer models might generate more realistic statistical features, an important issue in model calibration is the *identifiability* of such complex models. Given current prices of portfolio

credit derivatives, what can be inferred from them in terms of the characteristics of the loss process? In this section we present a result which sheds light on this identifiability issue, showing that the marginal distributions of any marked point process with IID marks can be matched by a Markovian jump process. From this "mimicking theorem" we conclude that the retrievable information is exactly given by the conditional expectation of the default intensity given the current loss, which we call the *effective intensity*.

3.1 Mimicking marked point processes with Markovian jump processes

We first prove a "mimicking theorem" which shows that the marginal distributions of any marked point process with IID marks can be matched by a Markovian jump process [1]:

Proposition 3.1. *Consider a marked point process $(L_t)_{t\in[0,T]}$ on a probability space $(\Omega, \mathcal{F}, (\mathcal{F}_t)_{t\in[0,T]}, \mathbb{Q})$ with a (random) $\mathbb{Q}$ - intensity $(\lambda_t)_{t\in[0,T]}$ with respect to $(\mathcal{F}_t)_{t\in[0,T]}$ and IID jumps (marks) with distribution F. Assume there exists a measurable function $\gamma : [0,T] \to [0,\infty[$ such that*

$$\forall t \in [0,T],\ \lambda_t < \gamma_t \text{ a.s. and } \int_0^T \gamma(t)dt < \infty. \tag{II.5}$$

There exists a Markovian jump process $(\tilde{L}_t)_{t\in[0,T]}$ with $\tilde{L}_0 = L_0$, independent jump sizes with distribution F and $\mathbb{Q}$-intensity $\lambda_{\text{eff}}(t, \tilde{L}_{t-})$, where

$$\lambda_{\text{eff}}(t,l) = E^{\mathbb{Q}}[\lambda_t | L_{t-} = l, \mathcal{F}_0], \tag{II.6}$$

such that for any $t \in [0,T]$, L_t and $\tilde{L}_t$ have the same distribution conditional on $\mathcal{F}_0$. In particular, the processes L and $\tilde{L}$ have the same marginal (i.e. one-dimensional) distributions.

This results shows that the flow of marginal distributions of $(L_t)_{t\in[0,T]}$ only depends on the intensity $(\lambda_t)_{t\in[0,T]}$ through its conditional expectation $\lambda_{\text{eff}}(t, L_{t-})$.

The Markov process $\tilde{L}$ is called a *Markovian projection* of L [21]. We call the process $(\lambda_{\text{eff}}(t, L_{t-}))_{t\in[0,T]}$ the *effective intensity* associated to the process L.

The relation between the intensity λ_t and $\lambda_{\text{eff}}(t, L_{t-})$ is analogous to the relation between instantaneous volatility and local volatility in diffusion models [49, 65]. By analogy with the local volatility function in diffusion models [64], we call the function $\lambda_{\text{eff}}(.,.)$ the *local intensity function* associated to the process L.

Proof. Consider any bounded measurable function $f(.)$ and any function $g(.)$ differentiable on $[0,T]$. Using the pathwise decomposition of L into the sum of its jumps and integrating the function $g'(.)$ between jumps we can write

$$f(L_t)g(t) \quad = f(L_0)g(0) + \int_0^t f(L_{s-})g'(s)ds + \sum_{0<s\leq t} g(s)(f(L_{s-} + \Delta L_s) - f(L_{s-}))$$

[1] This result was first pointed out by Brémaud [29, p.30] in the case of queues under the name of "first order equivalence".

so

$$
\begin{aligned}
&E^{\mathbb{Q}}[f(L_t)g(t)|\mathcal{F}_0] \\
&\quad = f(L_0)g(0) + E^{\mathbb{Q}}[\int_0^t f(L_{s-})g'(s)ds + \sum_{0<s\leq t} g(s)(f(L_{s-}+\Delta L_s) - f(L_{s-})\ )|\mathcal{F}_0] \\
&\quad = f(L_0)g(0) + \int_0^t g'(s)ds E^{\mathbb{Q}}[f(L_{s-})|\mathcal{F}_0] \\
&\quad + \int_{\mathbb{R}} F(dy) \int_0^t g(s)ds E^{\mathbb{Q}}[(f(L_{s-}+y) - f(L_{s-})\ )\lambda_s|\mathcal{F}_0],
\end{aligned}
$$

where the second equality is obtained under the IID assumption on the jumps, by integrating over the jump measure of the process L and the third equality by the Fubini Theorem and by [29, Ch. II, Theorem T8].

Denote $\mathcal{G}_t = \sigma(\mathcal{F}_0 \vee L_{t-})$ the information set obtained by adding the knowledge of L_{t-} to the current information set $\mathcal{F}_0$. Noting that $\mathcal{F}_0 \subset \mathcal{G}_t$ we have

$$
\begin{aligned}
E^{\mathbb{Q}}[\ (f(L_{t-}+y) - f(L_{t-})\ )\lambda_t|\mathcal{F}_0] &= E^{\mathbb{Q}}[\ E^{\mathbb{Q}}[\ (f(L_{t-}+y) - f(L_{t-})\ )\lambda_t|\mathcal{G}_t]|\mathcal{F}_0] \\
&= E^{\mathbb{Q}}[\ (f(L_{t-}+y) - f(L_{t-}))E^{\mathbb{Q}}[\lambda_t|\mathcal{G}_t]|\mathcal{F}_0] \\
&= E^{\mathbb{Q}}[\lambda_{\text{eff}}(t, L_{t-})\ (f(L_{t-}+y) - f(L_{t-})\ |\mathcal{F}_0]
\end{aligned}
$$

so, using again the Fubini Theorem,

$$
\begin{aligned}
E^{\mathbb{Q}}[f(L_t)g(t)|\mathcal{F}_0] = f(L_0)g(0) + E^{\mathbb{Q}}[\int_0^t ds f(L_{s-})g'(s)\ |\mathcal{F}_0] \\
+ E^{\mathbb{Q}}[\int_0^t g(s)ds\ \lambda_{\text{eff}}(s, L_{s-}) \int_{\mathbb{R}} F(dy)\ (f(L_{s-}+y) - f(L_{s-})\ )\ |\mathcal{F}_0].
\end{aligned} \tag{II.7}
$$

Consider the time-dependent generator A_t defined by

$$
A_t f(l) = \lambda_{\text{eff}}(t, l) \int_{\mathbb{R}} (f(l+y) - f(l))F(dy).
$$

By [72, Lemma 7.2], under Assumption II.5, there exists a unique family $P(s,t,.,.)$ of (time-inhomogeneous) transition probabilities $P(.,.,.,.)$ solution of

$$
P(s,t,l,\Gamma) = 1_\Gamma(l) + \int_s^t du\ \lambda_{\text{eff}}(u,l) \int_{\mathbb{R}} (P(u,t,l+y,\Gamma) - P(u,t,l,\Gamma))F(dy) \qquad \forall \Gamma \in \mathcal{B}(\mathbb{R})
$$

which defines the law of unique Markov process $(\tilde{L}_t)_{t\in[0,T]}$, whose generator is then given by $(A_t)_{t\in[0,T]}$ [72, Ch. 4, Thm 7.3.]. Thus $\tilde{L}$ has $\mathbb{Q}$-intensity $\lambda_{\text{eff}}(t, \tilde{L}_t)$.

We now show that, for any $t \in [0,T]$, L_t and $\tilde{L}_t$ have the same distribution conditional on $\mathcal{F}_0$. By [72, Ch. 4, Theorem 7.3], the martingale problem for A_t is well posed under the assumption (II.5). Denote for $f \in B(\mathbb{R}), g \in C^1([0,T])$, $(f \otimes g)(l,t) = f(l)g(t)$. We now introduce the operator A^0 on the domain $\mathcal{D}(A^0) = B(\mathbb{R}) \times C^1([0,T])$ by

$$
A^0(f \otimes g)(l,t) = g(t)\lambda_{\text{eff}}(t,l) \int_{\mathbb{R}} (f(l+y) - f(l))F(dy) + f(l)g'(t)
$$

For $t \in [0,T]$, we denote by q_t and respectively $\tilde{q}_t$ the distribution of L_t and respectively $\tilde{L}_t$ conditional on $\mathcal{F}_0$. Then $(\tilde{q}_t)_{s\in[0,T]}$ verifies the forward equation

$$\int f(l)g(t)\nu_t(dl) = \int f(l)g(0)\nu_0(dl) + \int_0^t ds \int A^0(f\otimes g)(l,s)\nu_s(dl). \tag{II.8}$$

By virtue of [72, Ch. 4, Theorem 7.1], the martingale problem on $D([0,T],\mathbb{R})\times[0,T])$ is well posed for A^0 and the process $(\tilde{L}_t,t)$ is a solution. We note that Equation (II.7) can be written as

$$E^{\mathbb{Q}}[f(L_t)g(t)|\mathcal{F}_0] = f(L_0)g(0) + E^{\mathbb{Q}}[\int_0^t A^0(f\otimes g)(L_{s-},s)ds|\mathcal{F}_0] \tag{II.9}$$

so the flow $(q_t)_{t\in[0,T]}$ also verifies Equation (II.8).

Since $q_0 = \tilde{q}_0$, we can apply [72, Ch. 4, Theorem 9.19] to the operator A^0 to find that $q_t = \tilde{q}_t$ for all $t \in [0,T]$, which concludes our proof. □

Remark 3.2. *Proposition 3.1 can be viewed as a "mimicking theorem" [21, 83] for marked point processes: it states that the flow of marginal distributions of a point process with (a random) intensity λ_t can be matched by a Markovian jump process whose intensity is given by (II.6).*

Note that this result also applies regardless of whether the filtration $\mathcal{F}_t$ is the natural filtration of L. In other words, the intensity (λ_t) can depend not only on the history of the (marked) point process itself but also on a richer information set as in the settings where λ_t is constructed through a stochastic differential equation involving an auxiliary Brownian motion W [10, 108, 79]. Even in these cases, however, the construction of $\tilde{L}_t$ does not involve any knowledge of the filtration of the Brownian motion.

Remark 3.3. *The proof of Proposition 3.1 also shows that under the given assumptions, we can replace λ_t by the $\mathcal{G}_t-$measurable process $E^{\mathbb{Q}}[\lambda_t|\mathcal{G}_t]$ i.e. the intensity with respect to the (smaller) filtration $(\mathcal{G}_t)_{t\in[0,T]}$. while retaining the same marginal distributions.*

3.2 Information content of portfolio credit derivatives

Consider now a portfolio loss model defined by a stochastic default intensity process (λ_t) and IID losses given default with distribution F. Applying the above result we obtain the following

Corollary 3.4. *Consider the same assumptions as in Proposition 3.1. Consider a (non path-dependent) portfolio credit derivative whose cash flows at payment dates $t_1,\ldots,t_J$ are of (bounded measurable) functions $f_j(L_{t_j})$ of the aggregate loss L_{t_j} at payment dates. Then its value $E^{\mathbb{Q}}[\sum_{j=1}^J B(0,t_j)f_j(L_{t_j})|\mathcal{F}_0]$ at $t=0$ only depends on the default intensity $(\lambda_t)_{t\in[0,T]}$ through its risk-neutral conditional expectation with respect to the current loss level:*

$$\lambda_{\text{eff}}(t,l) = E^{\mathbb{Q}}[\lambda_t|L_{t-}=l,\mathcal{F}_0]. \tag{II.10}$$

In particular, CDO tranche spreads and mark-to-market value of CDO tranches only depend on the transition rate $(\lambda_t)_{t\in[0,T]}$ through the effective default intensity $\lambda_{\text{eff}}(.,.)$.

Proof. The first claim is a direct application of Proposition 3.1. under the observation that the loss process is positive and bounded from above by 1.

Equation II.3 shows that CDO tranches verify this property with terms of the form $f_j(x) = (x - K_j)_+$. Observing that $L_t \in [0,1]$, we may replace $f_j(x)$ by $f_j(x)1_{x<1} + f_j(1)1_{x\geq 1}$ which is bounded and measurable so the above results apply to the value of each leg of a CDO tranche. Thus CDO tranche spreads and mark to market value of CDO tranches depend only on the marginal (one-dimensional) distribution of L and are thus determined by the effective default intensity. □

Mimicking theorems for marked point processes with general random jump size are considered in [21]. The Markovian projection approach, originally due to [65], has been applied in [111] to the calibration of a top-down portfolio credit models.

In the sequel we shall consider the commonly used setting where the loss is proportional to the number of defaults

$$L_t = \delta N_t, \ \forall t \in [0,T], \tag{II.11}$$

with $\delta = (1-R)/n$ is the fraction of notional lost given a single default.

3.3 Forward equations for expected tranche notionals

Being able to mimick the marginal distribution of the loss processes using a Markovian model allows for considerable simplification of pricing and calibration algorithms. First, for a Markovian jump process the transition probabilities can be computed by solving a Fokker Planck equation. Combined with Proposition 3.1, this shows that the transition probabilities $q_j(0,t) = \mathbb{Q}(N_t = j|\mathcal{F}_0)$ *also* solve the Fokker-Planck equation corresponding to the effective intensity: for $t \geq 0$,

$$\begin{aligned}
\frac{dq_0}{dt}(0,t) &= -\lambda_{\text{eff}}(t,0)q_0(0,t) \\
\frac{dq_j}{dt}(0,t) &= -\lambda_{\text{eff}}(t,j)q_j(0,t) + \lambda_{\text{eff}}(t,j-1)q_{j-1}(0,t) \\
\frac{dq_n}{dt}(0,t) &= \lambda_{\text{eff}}(t,n-1)q_{n-1}(0,t) \quad \text{with initial conditions} \\
q_j(0,0) &= \mathbb{1}_{\{N_0=j\}} \ \forall j = 1,\ldots,n
\end{aligned} \tag{II.12}$$

Moreover, by analogy with the Dupire equation for diffusion models [64], one can show that the expected tranche notional $P(t,K)$ can be obtained by solving a (single) forward equation [49]:

$$\begin{aligned}
&\frac{\partial P(t,K)}{\partial t} - P(t,K-\delta)\lambda_k(t) + \lambda_{k-1}(t)P(t,K) \\
&+ \sum_{j=1}^{k-2}[\lambda_{j+1}(t) - 2\lambda_j(t) + \lambda_{j-1}(t)]\ P(t,j) = 0
\end{aligned} \tag{II.13}$$

where $\lambda_k(t) = \lambda_{\text{eff}}(t,k\delta)$. This is a bidiagonal system of ODEs which can be solved efficiently in order to compute the expected tranche notionals (and thus the values of CDO tranches) given the local intensity function $\lambda_{\text{eff}}(.,.)$ without Monte Carlo simulation.

4 The calibration problem

The model calibration problem for CDO pricing models can be defined as the problem of recovering the law of the portfolio default intensity $(\lambda_t)_{t\in[0,T]}$ from market observations, which consist of spreads for (a small number of) CDO tranches.

Denote by $T_1 <, \ldots, < T_m$ the maturities of the observed CDO tranches (usually $m = 3$ or 4) with $T = T_m$ being the largest maturity and $0, K_1, \ldots, K_I$ the attachment points. We shall use the notations of section 2: the payment dates are denoted $(t_j, j = 1, \ldots, J)$. At $t = 0$ we observe the tranche spreads $(S_0(K_i, K_{i+1}, T_k), i = 1, \ldots, I-1, k = 1, \ldots, m)$ and the upfront fee $(U_0(K_1, T_k), k = 1, \ldots, m)$ for equity tranches.

The calibration problem can be formulated as specifying a law $\mathbb{Q}$ for the loss process such that the spreads computed using the pricing measure $\mathbb{Q}$ match the market observations:

Problem 4.1 (Calibration problem)**.** *Given a set of observed CDO tranche spreads (upfront fee for the equity tranche)* $(S_0(K_i, K_{i+1}, T_k), i = 1, \ldots, I-1, k = 1, \ldots, m)$ *(resp.* $U_0(K_1, T_k), k = 1, \ldots, m$*) for a reference portfolio, construct a pricing measure* $\mathbb{Q}$ *such that the spreads computed under the model* $\mathbb{Q}$ *match the market observations:*

$$S_0(K_i, K_{i+1}, T_k) = \frac{\sum_{t_j \le T_k} E^{\mathbb{Q}}[B(0,t_j)\left(L_{K_i,K_{i+1}}(t_j) - L_{K_i,K_{i+1}}(t_{j-1})\ \right)|\mathcal{F}_0]}{\sum_{t_j \le T_k} E^{\mathbb{Q}}[B(0,t_j)(t_j - t_{j-1})\left((K_{i+1} - L(t_j))^+ - (K_i - L(t_j))^+\right)|\mathcal{F}_0]} \tag{II.14}$$

for all mezzanine tranches $i = 1, \ldots, I-1$ *and maturities* $k = 1, \ldots, m$*, plus the constraint* (II.4) *involving upfront fees for the equity tranches.*

Problem 4.1 is an ill-posed inverse problem, similar to the one which arises in the calibration of pricing models for equity and index derivatives, where one attempts to recover a risk-neutral probability measure from a finite set of option prices: it can be seen as a generalized moment problem for a stochastic process: we want to reconstitute the law $\mathbb{Q}$ of the portfolio loss process given a finite (and typically, small) number of expectations of functions of this process. There is little hope to obtain a unique solution, let alone to compute it in a stable manner. We will now reformulate Problem 4.1 in a manner which makes it well-posed by properly restricting the set of models/ pricing measures and adding information in form of a *prior* probability measure.

4.1 Point processes and intensities

To give a precise formulation of Problem 4.1 we need to specify the set of probability measures in which we seek $\mathbb{Q}$. Proposition 3.1 implies that Problem 4.1 may have infinitely many solutions: if the law $\mathbb{Q}^\lambda$ of a point process with $\mathcal{F}_t-$intensity λ is a solution to Problem 4.1 then its Markovian projection i.e. the loss process with intensity $\lambda_{\text{eff}}(t, L_{t-})$ defined by (II.6) is also a solution. Also, as noted in Section 3.1, if $(\lambda^1_t)_{t\in[0,T]}$ is a solution of Problem 4.1 and λ^2 is a process such that $E^{\mathbb{Q}}[\lambda^1_t|\mathcal{H}_t] = E^{\mathbb{Q}}[\lambda^2_t|\mathcal{H}_t]$ then $(\lambda^2_t)_{t\in[0,T]}$ is also a solution. Therefore we cannot hope for uniqueness of solutions unless the intensity is restricted to be $\mathcal{H}_t-$predictable, where $\mathcal{H}_t$ is the history of the point process N. In fact, using Proposition 3.1 we can even restrict $\mathbb{Q}$ to be the law of a *Markovian* point process.

Recall the following change of measure theorem for point processes [29, Ch VI, Sec. 2]:

Proposition 4.2. *Let $\mathbb{P}$ be a probability measure under which the (canonical) process $(N_t)_{t\in[0,T]}$ is a point process with $\mathcal{H}_t$-intensity $(\gamma_t)_{t\in[0,T]}$. Let $\lambda = (\lambda_t)_{t\in[0,T]}$ be a nonnegative, $\mathcal{H}_t$-predictable process such that*

$$\mathbb{P}(\int_0^T \lambda_s ds < \infty) \quad = 1 \tag{II.15}$$

and $\{t \geq 0, \lambda_t > 0\} = \{t \geq 0, \gamma_t > 0\}$ $\mathbb{P}$-a.s. Define the process

$$Z_t = \left(\prod_{\tau_j \leq t} \frac{\lambda_{\tau_j}}{\gamma_{\tau_j}}\right) \exp\left\{\int_0^t (\gamma_s - \lambda_s)\, ds\right\} \tag{II.16}$$

where $\tau_1 \leq \tau_2 \leq \tau_3 \leq \ldots$ are the jump times of N. If $E^{\mathbb{P}}[Z_T] = 1$ then N is a point process with $\mathcal{H}_t$-intensity $(\lambda_t)_{t\in[0,T]}$ under the probability measure $\mathbb{Q}^\lambda$ defined on $(\Omega, \mathcal{H}_T)$ by

$$\frac{d\mathbb{Q}^\lambda}{d\mathbb{P}} = Z_T \tag{II.17}$$

Taking $\gamma = 1$ (Poisson process) this result can be used to construct (via change of measure) the law $\mathbb{Q}^\lambda$ of a process with a given intensity $(\lambda_t)_{t\in[0,T]}$. The condition $E^{\mathbb{P}}[Z_T] = 1$ is then verified for any bounded $\mathcal{H}_t$-predictable process λ.

The following result is a converse to Proposition 4.2: it shows that *any* equivalent (or, more generally, absolutely continuous) change of measure on $\mathcal{H}_T$ may be represented as a change of intensity:

Proposition 4.3. *Denote by $\mathbb{Q}_0$ the law of a point process $(N_t)_{t\in[0,T]}$ with a strictly positive intensity $(\gamma_t)_{t\in[0,T]}$ verifying*

$$\mathbb{Q}_0(\int_0^T \gamma_t dt < \infty) = 1. \tag{II.18}$$

Then, for any probability measure $\mathbb{Q}$ absolutely continuous with respect to $\mathbb{Q}_0$ there exists a nonnegative predictable process $(\lambda_t)_{t\in[0,T]}$ with $\{t \geq 0, \lambda_t > 0\} \subset \{t \geq 0, \gamma_t > 0\}$ $\mathbb{Q}_0$-a.s. such that

$$\frac{d\mathbb{Q}}{d\mathbb{Q}_0} = \left(\prod_{\tau_j \leq T} \frac{\lambda_{\tau_j}}{\gamma_{\tau_j}}\right) \exp\left\{\int_0^T (\gamma_s - \lambda_s)\, ds\right\}.$$

Furthermore if $\mathbb{Q}$ is equivalent to $\mathbb{Q}_0$ then $\{t \geq 0, \lambda_t > 0\} = \{t \geq 0, \gamma_t > 0\}$ $\mathbb{Q}_0$-a.s. and

$$\mathbb{Q}_0(\int_0^T \lambda_t dt < \infty) = 1$$

Proof. Let $\mathbb{Q} \ll \mathbb{Q}_0$ and $Z_T = \frac{d\mathbb{Q}}{d\mathbb{Q}_0}$. $Z_t = \mathbb{E}^{\mathbb{Q}_0}[Z_T|\mathcal{F}_t]$ is an $\mathcal{F}_t$ martingale under $\mathbb{Q}_0$ with $\mathbb{E}^{\mathbb{Q}_0}(Z_T) = 1$. The martingale representation theorem for point processes [91] then implies the existence of a predictable process Φ such that

$$Z_t = Z_0 + \int_0^t \Phi_s d\tilde{N}_s,$$

where $\tilde{N}_s = N_s - \int_0^t \gamma_s ds$.

Define $\lambda_t := (1 + \frac{\Phi_t}{Z_{t^-}})\ \gamma_t \mathbb{1}_{Z_{t^-}>0}$. Solving for Φ and substituting in the above equation shows that Z_t verifies the following SDE

$$dZ_t = \mathbb{1}_{\lambda_t>0} Z_{t^-} (\frac{\lambda_t}{\gamma_t} - 1) d\tilde{N}_t.$$

Since Z is a positive martingale, if there exists $t_0 \geq 0$ such that $Z_{t_0} = 0$ then $\forall t \geq t_0, Z_t = 0$: this remark allows to remove the $\mathbb{1}_{\lambda_t>0}$ in the SDE. Z is thus a stochastic exponential given by (II.16). Since $Z \geq 0$ (II.16) implies that $\mathbb{Q}_0(\lambda_{\tau_j} \geq 0) = 1$ so $\mathbb{Q}_0(\cap_{j\geq 1}\{\lambda_{\tau_j} \geq 0\}) = 1$. Since under $\mathbb{Q}_0$, N has a strictly positive intensity $\gamma_t > 0$ verifying (II.18), $\bigcup_{j\geq 1} \mathrm{supp}(\tau_j) = [0, T]$ so $\mathbb{Q}_0(\forall t \in [0, T], \lambda_t \geq 0) = 1$: λ is nonnegative.

If $\mathbb{Q} \sim \mathbb{Q}_0$ then $Z > 0$ so all the indicator functions in the above equations are equal to 1, which entails that $\{t \geq 0, \lambda_t > 0\} = \{t \geq 0, \gamma_t > 0\}$ $\mathbb{Q}_0$-a.s. Moreover, since Z is given by (II.16) the strict positivity of Z implies that $\exp(-\int_0^T \lambda_t dt) > 0$ i.e.

$$\mathbb{Q}_0(\int_0^T \lambda_t dt < \infty) = 1$$

□

Consider now a *prior* probability measure $\mathbb{Q}_0$ under which the (canonical) process $(N_t)_{t\in[0,T]}$ is a Markov point process with (predictable) intensity $(\gamma_t)_{t\in[0,T]}$ with respect to $\mathcal{H}_t$, where $\gamma_t = g(t, N_{t-})$ is given by a local intensity function $g(.,.)$. For example, if g is a constant function then $\mathbb{Q}_0$ is the law of a Poisson process on $[0, T]$ with intensity g. More generally, we assume that g is bounded and non-negative; $\mathbb{Q}_0$ can then be constructed as the solution of a martingale problem. We also assume the following non-degeneracy condition:

$$\exists a > 0, \quad \forall k < n, \quad \forall t \in [0, T[, \quad g(t, k) > a > 0 \tag{II.19}$$

Taking $\mathbb{P} = \mathbb{Q}_0$ in Proposition 4.2, any bounded predictable process λ satisfies $E^{\mathbb{Q}_0}[Z_T] = 1$ [29, Ch VI, Thm T4].

Define the set $\mathbb{M}$ of probability measures on $(\mathcal{H}_T)$ absolutely continuous with respect to $\mathbb{Q}_0$:

$$\mathbb{M} = \{\mathbb{Q} \in \mathcal{P}(\Omega, \mathcal{H}_T),\ \mathbb{Q}_{|\mathcal{H}_T} \ll \mathbb{Q}_{0|\mathcal{H}_T}\} \tag{II.20}$$

and $\mathbb{M}_{\mathrm{eq}}$ the subset of measures in $\mathbb{M}$ *equivalent* to $\mathbb{Q}_0$.

Proposition 4.3 shows that elements of $\mathbb{M}$ are of the form $\mathbb{Q}^\lambda$ with a default intensity process $\lambda \in \Lambda$ where Λ is the set of all non-negative $\mathcal{H}_t$-predictable processes $\lambda = (\lambda_t)_{t\in[0,T]}$ such that

$$\mathbb{Q}_0(\int_0^T \lambda_t\ dt < \infty) = 1.$$

4.2 Formulation via relative entropy minimization

Even after restricting to $\mathcal{H}_0-$measurable intensities, Problem 4.1 remains ill-posed if only a finite number of observations constrain the choice of the pricing measure $\mathbb{Q}$. A commonly used solution strategy in such ill-posed inverse problems is to restore uniqueness and stability by adding some information in the form of a prior model $\mathbb{Q}_0$ and looking for the risk-neutral loss process verifying the calibration constraints (II.14) which is the "closest" to $\mathbb{Q}_0$ in some sense.

Following similar approaches to the model calibration problem in the context of equity derivatives [12, 16, 13, 50, 129] we use as a measure of proximity the *relative entropy*, defined as $\mathbb{Q}$ with respect to $\mathbb{Q}_0$, defined as

$$I(\mathbb{Q},\mathbb{Q}_0) = E^{\mathbb{Q}_0}[\frac{d\mathbb{Q}}{d\mathbb{Q}_0}\ln\frac{d\mathbb{Q}}{d\mathbb{Q}_0}]$$

and reformulate the calibration problem as the minimization of relative entropy with respect to the prior under calibration constraints:

Problem 4.4 (Calibration via relative entropy minimization)**.** *Given a prior loss process with law $\mathbb{Q}_0$, find a loss process with law $\mathbb{Q}^\lambda$ and default intensity $(\lambda_t)_{t\in[0,T^*]}$ which minimizes*

$$\inf_{\mathbb{Q}^\lambda\in\mathbb{M}} E^{\mathbb{Q}_0}[\frac{d\mathbb{Q}^\lambda}{d\mathbb{Q}_0}\ln\frac{d\mathbb{Q}^\lambda}{d\mathbb{Q}_0}] \quad \text{under} \quad E^{\mathbb{Q}^\lambda}[H_{i,k}|\mathcal{F}_0]=0, \quad i=0,\dots,I-1, \qquad k=1,\dots,m \tag{II.21}$$

where,

$$\begin{aligned} H_{ik} &= S_0(K_i,K_{i+1},T_k)\sum_{t_j\le T_k} B(0,t_j)(t_j-t_{j-1})[(K_{i+1}-L(t_j))^+-(K_i-L(t_j))^+] \\ &+ \sum_{t_j\le T_k} B(0,t_j)[(K_{i+1}-L(t_j))^+-(K_i-L(t_j))^+-(K_{i+1}-L(t_{j-1}))^+ +(K_i-L(t_{j-1}))^+)\ ] \end{aligned} \tag{II.22}$$

$$\begin{aligned} H_{0k} &= K_1U_0(K_1,T_k)+f\sum_{t_j\le T_k} B(0,t_j)(t_j-t_{j-1})[(K_1-L(t_j))^+] \\ &+ \sum_{t_j\le T_k} B(0,t_j)[(K_1-L(t_j))^+-(K_1-L(t_{j-1}))^+)\ ] \end{aligned} \tag{II.23}$$

This approach to model calibration allows for an information-theoretic interpretation [53] and is linked via duality to exponential utility maximization problems [81].

The following result shows that this formulation of the calibration problem is now well-posed:

Proposition 4.5 (Existence and uniqueness of a solution to the calibration problem)**.** *Assume*

$$\exists\mathbb{P}\in\mathbb{M}_{\text{eq}}, I(\mathbb{P},\mathbb{Q}_0)<\infty \quad E^{\mathbb{P}}[H_{i,k}|\mathcal{F}_0]=0,\ \forall i=0,\dots,I-1\ \forall k=1,\dots,m \tag{II.24}$$

Then Problem 4.4 admits a unique solution $\mathbb{Q}^*\in\mathbb{M}$.

Proof. The primal problem can be characterized as the I-projection (in the sense of [53]) of $\mathbb{Q}_0$ on the set

$$\mathcal{E} := \{\mathbb{Q}\ll\mathbb{Q}_0, E^{\mathbb{Q}}[H_{i,k}]=0\ \forall i=0,\dots,I-1,\forall k=1,\dots,m\}.$$

Then $\mathcal{E}$ is a convex set of measures which is closed under convergence in total variation distance. For two measures $\mathbb{Q}^i,\mathbb{Q}^j\in\mathcal{E}$ with $Z^i=\frac{d\mathbb{Q}^i}{d\mathbb{Q}_0}, Z^j=\frac{d\mathbb{Q}^j}{d\mathbb{Q}_0}$ the total variation distance is given by

$$|\mathbb{Q}^i-\mathbb{Q}^j| = E^{\mathbb{Q}_0}[|Z^i-Z^j|].$$

Consider now a sequence $(\mathbb{Q}_j)_{j\ge1}$ converging in total variation. Then the sequence $(Z^j=\frac{d\mathbb{Q}^j}{d\mathbb{Q}_0})_{j\ge1}$ converges in $L^1(\Omega,\mathbb{Q}_0)$ to a limit Z

$$\mathbb{E}^{\mathbb{Q}_0}[\ |Z^j-Z|\ ]\underset{j\to\infty}{\to}0.$$

We have that $\mathbb{E}^{\mathbb{Q}_0}(Z) = 1$, $0 \leq Z < \infty$. Define the probability measure $\mathbb{P}$ by the density $\frac{d\mathbb{P}}{d\mathbb{Q}_0} = Z$. $\mathbb{P}$ is absolutely continuous with respect to $\mathbb{Q}_0$.

Furthermore, since $E^{\mathbb{Q}_0}(|Z^j - Z|) \to 0$ as $j \to \infty$ and the random variables H_{ik} are bounded, we also have that

$$E^{\mathbb{Q}_0}(|(Z^j - Z)H_{ik}|) \overset{j\to\infty}{\to} 0.$$

so $E^{\mathbb{P}}(H_{ik}) = 0$. Hence $\mathcal{E}$ is convex and variation closed. A result of Csiszar [53, Theorem 2.1.] then guarantees the existence of the I-projection on $\mathcal{E}$. The solution is unique since the relative entropy $\mathbb{Q} \mapsto I(\mathbb{Q}, \mathbb{Q}_0)$ is a strictly convex functional. □

The rest of the paper is devoted to the solution of Problem 4.4. We will see that the choice of relative entropy as calibration criterion makes the problem tractable and exhibit an efficient numerical method for solving the problem and apply this method to data sets of index CDOs to extract implied default intensities from index CDO tranche spreads.

4.3 Dual problem as an intensity control problem

The primal problem (Problem 4.4) is an infinite-dimensional constrained optimization problem whose solution does not seem obvious. A key advantage of using the relative entropy as a calibration criterion is that it can be computed explicitly in the case of point processes. The constrained optimization problem (II.21) can then be simplified by introducing Lagrange multipliers and using convex duality methods [54].

Proposition 4.6 (Computation of relative entropy)**.** *Denote by $\mathbb{Q}^\lambda$ the law on $[0,T]$ of the point process with intensity $\lambda = (\lambda_t)_{t\in[0,T]} \in \Lambda$. We assume the non-degeneracy condition II.19 holds. The relative entropy of $\mathbb{Q}^\lambda$ with respect to $\mathbb{Q}_0$ is given by:*

$$E^{\mathbb{Q}_0}[\frac{d\mathbb{Q}^\lambda}{d\mathbb{Q}_0} \ln \frac{d\mathbb{Q}^\lambda}{d\mathbb{Q}_0}] = E^{\mathbb{Q}^\lambda}[\int_0^T (\lambda_t \ln \frac{\lambda_t}{\gamma_t} dt - \lambda_t + \gamma_t)dt]. \tag{II.25}$$

Proof. It is a straightforward application of Proposition 4.2.

$$E^{\mathbb{Q}_0}[\frac{d\mathbb{Q}^\lambda}{d\mathbb{Q}_0} \ln \frac{d\mathbb{Q}^\lambda}{d\mathbb{Q}_0}] = E^{\mathbb{Q}^\lambda}[\sum_{\tau_i \leq T} \ln \frac{\lambda_{\tau_i}}{\gamma_{\tau_i}} + \int_0^T (\gamma_t - \lambda_t)dt].$$

The intensity $(\lambda_t)_{t\in[0,T]}$ of the loss L under $\mathbb{Q}^\lambda$ is characterized [29] by the property that for any $\mathcal{H}_t-$predictable process $C(t)$,

$$E^{\mathbb{Q}^\lambda}[\sum_{0<\tau_i\leq T} C(\tau_i)] = E^{\mathbb{Q}^\lambda}[\int_0^T \lambda_t C(t)dt].$$

Since λ, γ are $\mathcal{H}_t-$predictable it follows that

$$E^{\mathbb{Q}^\lambda}(\sum_{0<\tau_i\leq T} \ln \frac{\lambda_{\tau_i}}{\gamma_{\tau_i}}) = E^{\mathbb{Q}^\lambda}(\int_0^T \ln \frac{\lambda_s}{\gamma_s} dN_s) = E^{\mathbb{Q}^\lambda}(\int_0^T \lambda_s \ln \frac{\lambda_s}{\gamma_s} ds). \tag{II.26}$$

□

Proposition 4.7 (Duality). *Under the condition* (II.24)*, the primal problem (II.21) is equivalent to*

$$\sup_{\mu\in\mathbb{R}^{m.I}}\inf_{\lambda\in\Lambda}E^{\mathbb{Q}^\lambda}[\int_0^T(\lambda_s\ln\frac{\lambda_s}{\gamma_s}+\gamma_s-\lambda_s)ds-\sum_{i=0}^{I-1}\sum_{k=1}^{m}\mu_{i,k}H_{ik} \tag{II.27}$$

Proof. First, we note that by Proposition 4.3, the optimization in (II.21) may be done over $\mathbb{Q}\in\mathbb{M}$ or $\mathbb{Q}^\lambda,\lambda\in\Lambda$. The relative entropy $I(\mathbb{Q},\mathbb{Q}_0)$ is then given by (II.25). Define now the Lagrangian

$$\mathcal{L}(\lambda,\mu)=E^{\mathbb{Q}^\lambda}[\int_0^T(\lambda_s\ln\frac{\lambda_s}{\gamma_s}+\gamma_s-\lambda_s)ds-\sum_{i=0}^{I-1}\sum_{k=1}^{m}\mu_{i,k}H_{ik} \tag{II.28}$$

where μ_{ik} are the Lagrange multiplier for the inequality constraints (II.22). The primal problem (II.21) is then equivalent to

$$\inf_{\lambda\in\Lambda}\sup_{\mu\in\mathbb{R}^{m.I}}E^{\mathbb{Q}^\lambda}[\int_0^T(\lambda_s\ln\frac{\lambda_s}{\gamma_s}+\gamma_s-\lambda_s)ds-\sum_{i=0}^{I-1}\sum_{k=1}^{m}\mu_{i,k}H_{ik} \tag{II.29}$$

Under (II.24), Proposition 4.5 ensures that the primal problem (II.21) is finite-valued. Under condition (II.24), [54, Theorem 2] then ensures that the primal problem (II.21) has the same value as the associated dual problem (II.29). □

The inner optimization problem

$$J(\mu)=\mathcal{L}(\lambda^*(\mu),\mu)=\inf_{\lambda\in\Lambda}\mathcal{L}(\lambda,\mu)$$

is an example of an *intensity control* problem [23, 29]: the optimal choice of the intensity of a jump process in order to minimize a criterion of the type

$$E^{\mathbb{Q}^\lambda}[\int_0^T\varphi(t,\lambda_t,N_t)dt+\sum_{j=1}^{J}\Phi_j(L_{t_j})\quad], \tag{II.30}$$

where $t_j,\ j=1,\dots,J$ are the spread payment dates, $\varphi(t,\lambda_t,N_t)$ is a *running cost* and $\Phi_j(L)$ represents a "terminal" cost. In our case

$$\varphi(t,x,k)=x\ln\frac{x}{g(t,k)}+g(t,k)-x \text{ and } \Phi_j(L)=\sum_{i=1}^{I-1}M_{ij}(K_i-L)^+\qquad, \tag{II.31}$$

where

$$\begin{aligned}M_{ij}=&B(0,t_{j+1})\sum_{T_k\geq t_{j+1}}(\mu_{ik}-\mu_{i-1,k})+\\&B(0,t_j)\sum_{T_k\geq t_j}[\mu_{ik}(-1-\Delta S(K_i,K_{i+1},T_k))-\mu_{i-1,k}(1-\Delta S(K_{i-1},K_i,T_k)],\end{aligned} \tag{II.32}$$

with $\Delta = t_j - t_{j-1}$ is the interval between payments and $S(K_0, K_1, T_k) = f$.

The solution of an intensity control problem can be obtained using a dynamic programming principle and is characterized in terms of a system of Hamilton-Jacobi equations [29, Ch. VII]. We will now use these properties to solve (II.30).

Once the inner optimization/ intensity control problem has been solved we have to solve the outer problem by optimizing $J(\mu)$ over the Lagrange multipliers $\mu \in \mathbb{R}^{mI}$: the corresponding optimal control λ^* then yields precisely the default intensity which calibrates the observations. The problem setting is similar to the one formulated by Avellaneda et al. [16] in the context of diffusion models. We will observe however that, unlike the setting of [16], we are able to solve the stochastic control problem in (II.30) analytically thereby greatly simplifying the algorithm.

Standard formulations of intensity control problems involve a single horizon ($J = 1$); we will first examine this case in the next section and then discuss how to extend the analysis to the case of several maturities in section 4.5.

4.4 Hamilton Jacobi equations

Let us consider first the case where $J = 1$ i.e a single time horizon is involved. The dual problem is then to minimize

$$\inf_{\lambda \in \Lambda} E^{\mathbb{Q}^\lambda}[\int_0^T \varphi(t, \lambda_t, N_t)dt + \Phi(T, L_T)] \tag{II.33}$$

where $\Phi(.)$ is of the form (II.31) (and thus depends on the Lagrange multipliers μ). The solution of the stochastic control problem (II.29) can be obtained using dynamic programming methods [23, 29]. The idea is to define a family of optimization problems indexed by the initial condition (t, n),

$$V(t, N_t) = \inf_{\lambda \in \Lambda([t,T])} E^{\mathbb{Q}^\lambda}[\int_t^T (\lambda_s \ln \frac{\lambda_s}{\gamma_s} + \gamma_s - \lambda_s)ds + \Phi(T, \delta N_T))|\mathcal{H}_t] \tag{II.34}$$

where $\delta = (1 - R)/n$ is the loss given a single default and $\Lambda([t, T])$ is the set of restrictions to $[t, T]$ of elements of Λ. The value function $V(t, k)$ then solves the dynamic programming equation [29]:

$$\frac{\partial V}{\partial t}(t, k) + \inf_{\lambda \geq 0}\{\lambda[V(t, k + 1) - V(t, k)] + \lambda \ln \frac{\lambda}{g(t, k)} - \lambda + g(t, k)\} = 0 \tag{II.35}$$

$$\text{for} \quad t \in [0, T] \quad \text{and} \quad V(T, k) = \Phi(T, k\delta)) \tag{II.36}$$

The value function of (II.33) is then given by $V(0, 0)$ and the optimal intensity control is obtained by maximizing over λ in the nonlinear term [29]:

Proposition 4.8 (Verification theorem)**.** *If $V : [0, T] \times \mathbb{N}$ is a bounded solution of (II.35)–(II.36), differentiable in t then $\mathcal{L}(\lambda^*_\mu, \mu) = V(0, 0)$ and the optimal control λ^*_μ is given by the minimizer of*

$$\lambda^*_\mu(t, k) = \arg\min_{\lambda \geq 0} \ \lambda[V(t, k + 1) - V(t, k)] + (\lambda \ln \frac{\lambda}{g(t, k)} + g(t, k) - \lambda),$$

for each t and $0 \leq k \leq n$.

In this case the maximum in the nonlinear term can be explicitly computed:

$$\lambda^*_\mu(t,k) = g(t,k)e^{-[V(t,k+1)-V(t,k)]} \tag{II.37}$$

$$\frac{\partial V}{\partial t}(t,k) + g(t,k)(1 - e^{-[V(t,k+1)-V(t,k)]}) = 0. \tag{II.38}$$

To solve the dual problem we need to solve the Hamilton–Jacobi equations (II.35)–(II.36). This is a system of n nonlinear ODEs which may seem daunting at first glance. Remarkably, in this case a logarithmic change of variable yields an explicit solution:

Proposition 4.9 (Value function)**.** *Consider a function Φ such that $\Phi(x) = 0$ for $x \geq n\delta$. The solution of (II.35)-*(II.36) *has the probabilistic representation*

$$V(t,k) = -\ln[1 + \sum_{j=0}^{n-k} \mathbb{Q}_0(N_T = k+j | N_t = k)(e^{-\Phi(T,(k+j)\delta)} - 1)]. \tag{II.39}$$

Corollary 4.10 (Case of Poisson prior)**.** *If the prior process is a Poisson process with intensity γ_0 stopped at n, then the value function V is given by*

$$V(t,k) = \Phi(T,n\delta) - \ln[1 + \sum_{j=0}^{n-k-1} \frac{\gamma_0^j (T-t)^j e^{-\gamma_0(T-t)}}{j!}(e^{\Phi(T,n\delta)-\Phi(T,(k+j)\delta)} - 1)].$$

Proof. If we consider $u(t,k) = e^{-V(t,k)}$ then u solves a *linear* equation

$$\frac{\partial u(t,k)}{\partial t} + g(t,k)(u(t,k+1) - u(t,k)) = 0 \qquad \text{with} \quad u(T,k) = \exp(-\Phi(T,k\delta))$$

which is recognized as the backward Kolmogorov equation associated with the Markovian point process with intensity function $g(t,k)$ (i.e. the prior process, with law $\mathbb{Q}_0$). The solution is thus given by the Feynman-Kac formula

$$u(t,k) = E^{\mathbb{Q}_0}[e^{-\Phi(T,\delta N_T)} | N_t = k].$$

The expectation is easily computed using the transition probabilities of the prior process, where the sum over jumps can be truncated using the fact that $\Phi(x) = 0$ for $x \geq n\delta$:

$$\begin{aligned}
u(t,k) &= \sum_{j=0}^{n-k} \mathbb{Q}_0(N_T = k+j | N_t = k) e^{-\Phi(T,(k+j)\delta)} + \sum_{j>n-k} \mathbb{Q}_0(N_T = k+j | N_t = k) \\
&= \sum_{j=0}^{n-k} \mathbb{Q}_0(N_T = k+j | N_t = k) e^{-\Phi(T,(k+j)\delta)} + 1 - \sum_{j=0}^{n-k} \mathbb{Q}_0(N_T = k+j | N_t = k) \\
&= 1 + \sum_{j=0}^{n-k} \mathbb{Q}_0(N_T = k+j | N_t = k)[e^{-\Phi(T,(k+j)\delta)} - 1]
\end{aligned}$$

which leads to (II.39). These transitions probabilities can be explicitly computed for a (stopped) Poisson process which then leads to the result. □

The fact that a logarithmic change of variable linearizes the Hamilton Jacobi equation is not a coincidence: this is a common feature of stochastic control problems related to exponential utility maximization [136]. This result can also be derived using the dual representation of the entropic risk measure as in [123].

4.5 Handling payment dates

In the (realistic) case where several payment dates $0 \leq t_1 \leq t_2, \ldots, \leq t_J$ are involved, the criterion to be optimized in the dual problem is of the form

$$E^{\mathbb{Q}^\lambda}[\int_0^{t_J} \varphi(t, \lambda_t, N_t)dt + \Phi_1(L_{t_1}) + \Phi_2(L_{t_2}) + \ldots \Phi_J(L_{t_J})].$$

We will now show that this problem can be treated as a sequence of single-horizon intensity control problems in a recursive manner using a dynamic programming principle. Denote by $\Lambda([t_j, t_{j+1}])$ the restriction to $t \in [t_j, t_{j+1}]$ of elements in Λ. Consider the value function:

$$V(t, k; \mu) = \inf_{\Lambda([t,t_J])} E^{\mathbb{Q}^\lambda}[\int_t^{t_J} \varphi(t, \lambda_t, N_t)dt + \sum_{t_j > t} \Phi_j(L_{t_j})|N_t = k]$$

We will compute V going backwards from t_J. First, we note that $V(t_{J-1}, k; \mu)$ is of the form (II.33) and can be computed using the formula (II.39) with $\Phi = \Phi_J$. Assume now we have computed $V(t, k; \mu)$ for $t \geq t_{j+1}$. Then

$$\begin{aligned} V(t_j, k; \mu) = \inf_{\Lambda([t_j,t_J])} E^{\mathbb{Q}^\lambda}[&\int_{t_j}^{t_{j+1}} \varphi(t, \lambda_t, N_t)dt + \Phi_{j+1}(L_{t_{j+1}}) \\ &+ \int_{t_{j+1}}^{t_J} \varphi(t, \lambda_t, N_t)dt + \sum_{i=j+2}^{J} \Phi_j(L_{t_j})|N_{t_j} = k]. \end{aligned} \tag{II.40}$$

The dynamic programming principle can be stated by saying that the cost functional is a martingale when computed at the optimal policy λ^*, hence:

$$\begin{aligned} &V(t_j, k; \mu) = \\ &E^{\mathbb{Q}^*}[\int_{t_j}^{t_{j+1}} \varphi(t, \lambda_t^*, N_t^*)dt + \Phi_{j+1}(L_{t_{j+1}}) + \int_{t_{j+1}}^{t_J} \varphi(t, \lambda_t^*, N_t^*)dt + \sum_{i=j+2}^{J} \Phi_j(L_{t_j})|N_{t_j} = k] \\ &= \inf_{\Lambda([t_j,t_J])} E^{\mathbb{Q}^\lambda}[\int_{t_j}^{t_{j+1}} \varphi(t, \lambda_t, N_t)dt + \Phi_{j+1}(L_{t_{j+1}}) + V(t_{j+1}, k; \mu)|N_{t_j} = k] \end{aligned}$$

Therefore on $[t_j, t_{j+1}[$ we also have a problem of the form (II.33) with $\Phi = F_{j+1} = \Phi_{j+1} + V(t_{j+1}, .)$: $V(t_j, k; \mu)$ can therefore be computed using the formula (II.39) with $\Phi = F_{j+1}$. This results in the following method for computing recursively the value function $V(t, k; \mu)$:

1. Start from the last payment date $j = J$ and set $F_J(k) = \Phi_J(t_J, \delta k)$.
2. Solve the Hamilton–Jacobi equations (II.35) on $]t_{j-1}, t_j]$ backwards starting from the terminal condition

   $$V(t_j, k, \mu) = F_j(k). \tag{II.41}$$

   $V(t, k, \mu)$ can be explicitly computed for $t \in [t_{j-1}, t_j]$ using (II.39) with $\Phi = F_J$.
3. Set $F_{j-1}(k) = V(t_{j-1}, k, \mu) + \Phi_{j-1}(t_{j-1}, k\delta)$

4. Decrease j to j-1, go to step 2 and repeat until $j = 0$ is reached.

The value function of the dual problem is then given by $V(0, 0, \mu)$. This procedure yields an explicit (although lengthy) formula for $V(0, 0, \mu)$, which is obtained by nesting J times the expression (II.39). In particular this formula can be used to compute $\nabla V(0, 0, \mu)$ and to use gradient-based methods to maximize $V(0, 0, \mu)$ with respect to μ in the last step of the algorithm.

5 Recovering market-implied default rates

5.1 Calibration algorithm

The above results lead to a non-parametric algorithm for recovering a market-implied portfolio default intensity from CDO spreads. The algorithms consists of the following steps:

1. Solve the dynamic programming equations (II.35)–(II.36) for $\mu \in \mathbb{R}^{m.I}$ to compute $V(0, 0, \mu)$.

2. Solve the maximization problem

$$\sup_{\mu \in \mathbb{R}^{m.I}} V(0, 0, \mu) + \sum_{k=1}^{m} \mu_{0k} U_0(K_1, T_k)$$

   using a gradient–based method to obtain the Lagrange multipliers μ^*.

3. Compute the calibrated default intensity (optimal control) as follows:

$$\lambda^*(t, k) = \gamma(t, k) e^{V^*(t,k) - V^*(t,k+1)}. \tag{II.42}$$

4. Compute the term structure of loss probabilities by solving the Fokker-Planck equations (II.12).

5. The calibrated default intensity $\lambda^*(., .)$ can then be used to compute CDO spreads for different tranches, forward tranches, etc.: first we compute the expected tranche notionals $P(T, K)$ by solving the forward equation (II.13) and then use the expected trance notionals to evaluate CDO tranche spreads, mark to market value, etc. In particular the calibrated default intensity can be used to "fill the gaps" in the base correlation surface in an arbitrage-free manner, by first computing the expected tranche loss for all strikes and then computing the base correlation for that strike.

Remark 5.1. *Unlike other calibration methods based on nonlinear least squares, for typical sets of data, the calibration problem is an unconstrained concave maximization in* $\mathbb{R}^{18}$ *and the gradient-based algorithm is guaranteed to compute the optimum efficiently with quadratic convergence rate.*

Maturity	Low	High	Bid\ Upfront	September 26, 2005	March 25, 2008
5Y	0%	3%	29.50%	29.875%	38.67 %
	3%	6%	96	98	454.08
	6%	9%	33	34.5	280.22
	9%	12%	13	14	189.40
	12%	22%	7.50	8.125	110.74
	22%	100%	2.25	3.125	46.87
7Y	0%	3%	47.1%	47.55 %	43.97%
	3%	6%	193	196.5	514.76
	6%	9%	52	54.5	312.50
	9%	12%	29	31.5	206.53
	12%	22%	12	13.5	115.47
	22%	100%	5.25	6.25	48.55
10Y	0%	3%	58.25%	58.75%	48.43%
	3%	6%	505	512.5	633.16
	6%	9%	100	103	362.40
	9%	12%	48	51.5	238.54
	12%	22%	22	23.5	25
	22%	100%	8.25	9.5	10.75

Table II.2: ITRAXX IG Europe tranche spreads (mid), September 26, 2005 vs March 25, 2008.

5.2 Application to ITRAXX tranches

We have applied the above methodology to several data sets of CDO quotes; we present here only the results for three data sets, consisting of ITRAXX Europe IG tranche quotes on Sept 26, 2005, March 15, 2007 and March 25, 2008.

Figure II.2 displays the local intensity function $\lambda(t, k)$ as a function of time t and the number of defaults k.

Several features deserve to be commented. First, we note the strong dependence of the default intensity on the portfolio loss level: once a few defaults occur, the default intensity sharply increases. Figure II.2 shows the dependence of the default intensity with respect to the number of defaults at two different dates (in 2005 and 2008). We observe a similar pattern in both cases: while the initial default rate is close to 1 (which means on average one default every year), it quickly increases as defaults occur in the portfolio, which leads to default contagion. Contagion stems from the fact that λ_{eff} steeply increases with the number of defaults after the first few defaults. The jump in the default intensity at each new default may result in clustering of defaults: an example is shown in figure II.5 which displays a sample path of N_t and the default intensity simulated using the effective intensity function in figure II.2. Such contagion effects, which lead to the clustering of defaults, have been observed in historical time series [56]: our results indicated that their effect is also detectable in the *implied* default intensity, i.e. that contagion risk is effectively priced into market quotes of CDO tranches. In pricing terms, this steep initial slope means that in this period (2005-2007) equity tranches were priced relatively cheaply with respect to mezzanine or senior tranches. The values of $\lambda(t, k)$ for small k also

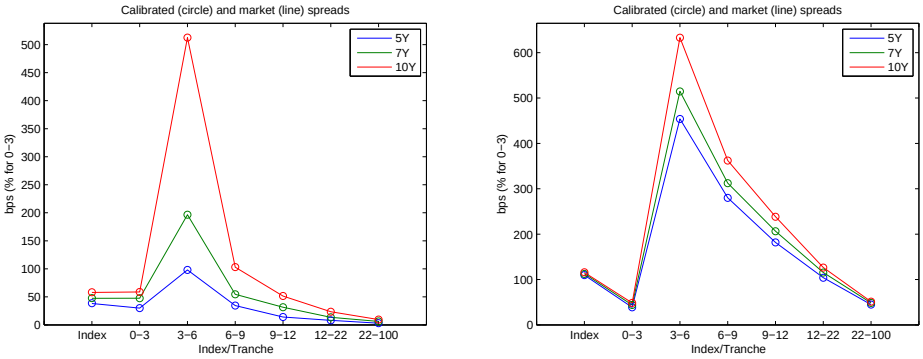

Figure II.1: Model vs market spreads: ITRAXX September 26, 2005 (left) Sept 2008 (right).

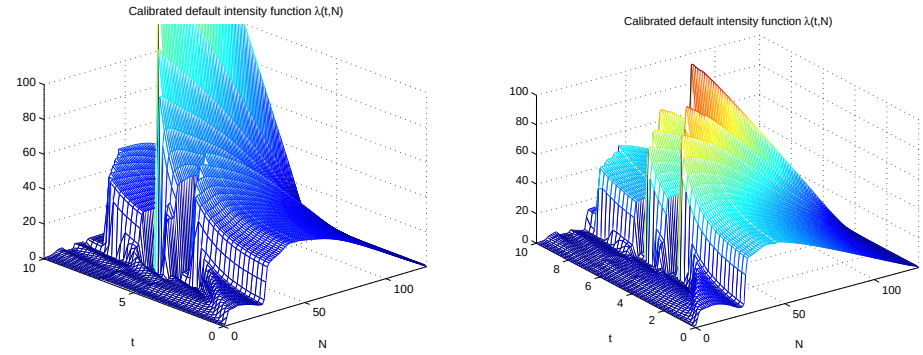

Figure II.2: Implied ITRAXX default intensity functions: September 2005 (left) vs Sept 2008 (right).

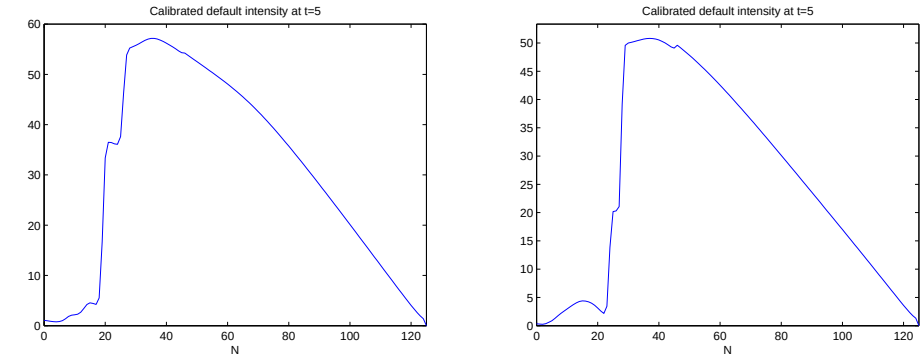

Figure II.3: Implied default intensity as a function of number of defaults at a 2 year horizon: Sept 2005 (left) and Sept 2008 (right).

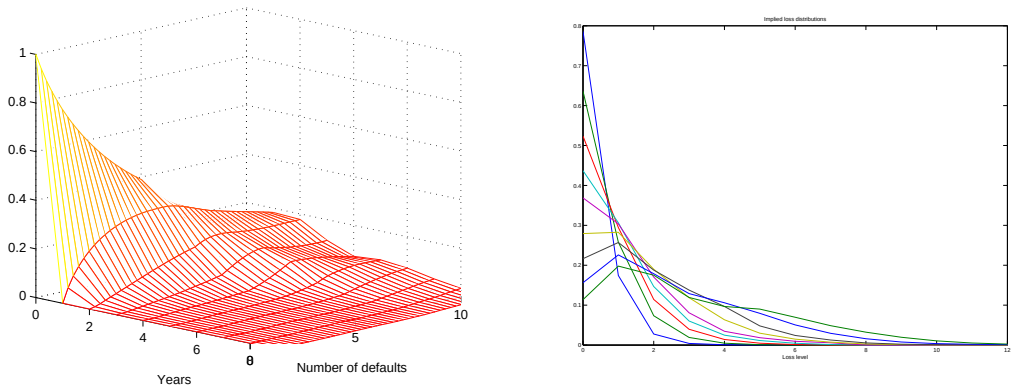

Figure II.4: Left: term structure of loss distributions implied by ITRAXX Europe Series 6, March 15 2007. Right: loss distributions at various maturities.

give interesting insights for the pricing of first-to-default and $k-$th to default swaps. Once the equity tranche of the portfolio is wiped out by defaults, we observe in figure II.2 a plateau where the default intensity remains relatively insensitive to the number of defaults: in this regime, in fact, a Poisson approximation seems to work well. This regime corresponds to the bulk of the portfolio, composed of obligors whose default risk is well represented by the average spread of the portfolio. From a pricing perspective, this flat region implied that, in these examples, apart from the equity tranche, the other tranches were priced assuming a constant (and high) value of the default intensity once the equity tranche has been wiped out. The steep decline of the $\lambda(t,k)$ for large k can be understood as corresponding to the group of obligors in the index with the lowest spreads/ default risk and which are the least exposed to systemic risk: they are the last to default, with a very low probability.

Finally we note that, as illustrated in Figures II.1, II.2 and II.3, both the precision of the calibration the qualitative features of the default intensity function remain the same throughout the period 2005-2008, a particularly turbulent period during which base correlations computed using Gaussian copula models have been notoriously unstable and sometimes impossible to calibrate to market spreads. This shows that the instability of such "default correlations" parameters is linked more to model mis-specification than to genuine non-stationarity: using a richer model structure along with a stable calibration algorithm restores a greater degree of parameter stability. This aspect is of course essential if the model is to be used for hedging [43].

We also note that there is a discontinuity in the dependence on t at each observed maturity: this discontinuity is a structural feature related to properties of the dynamic programming equation and does not have any informational content. Such discontinuities are not present in quantities such as default probabilities (Figure II.4).

The above approach can be used to construct an arbitrage-free interpolation/extrapolation of 'base correlations', by first calibrating the local intensity function to the observed tranche spreads then computing expected tranche losses for a fine grid of detachment points/maturities and converting them into a base correlation figure. Note that, unlike the usual linear interpolation of base correlations, this method also provides an arbitrage-free extrapolation of base

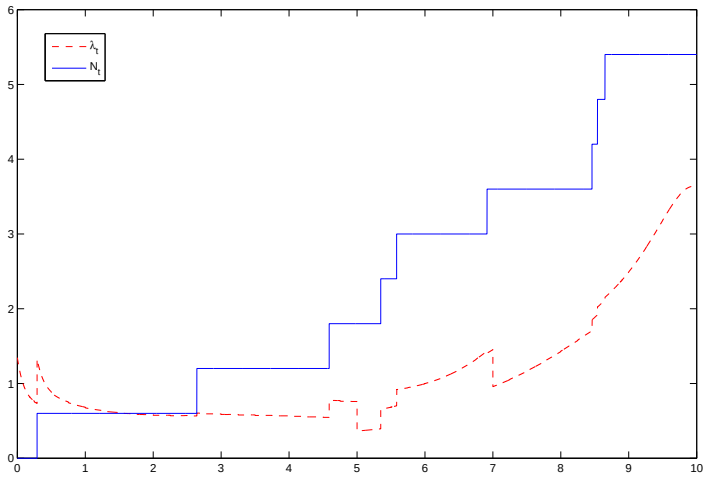

Figure II.5: Simulated sample path of number of defaults (solid line) and default intensity (dotted line) in the Markovian default model defined by the intensity function shown in Figure II.2. Note the clustering of defaults and the jump in the default intensity at default events.

correlations beyond the largest detachment point and below the smallest attachment point. Figure II.6 shows the result of such an interpolation for the ITRAXX data, compared with the linear interpolation method used by many market participants. The difference between the two methods is striking, especially for senior tranches.

6 Conclusion

We have proposed a rigorous methodology for calibrating a CDO pricing model to market data, by formulating the calibration problem as a relative entropy minimization problem under constraints and mapping it into an intensity control problem for a point process, which can be solved analytically.

By contrast with other calibration methods proposed for top-down CDO pricing models in the literature, our method is *nonparametric*: it does not assume any arbitrary functional form for the default intensity. Another feature of algorithm proposed is that it does not require preliminary interpolation or smoothing of CDO data in maturity or strike (which may violate arbitrage constraints), nor does it require a preliminary (model-dependent) "stripping" of CDO spreads into expected tranche notionals. In particular, our algorithm yields meaningful and stable results even for sparse data sets such as the ones available in CDS index markets.

Our method allows to compute portfolio default rates implied by index CDO quotes. Results obtained on ITRAXX tranche spreads point to default contagion effects in the risk-neutral loss process and also illustrate that the implied default intensity corresponding to the first few defaults are very different from those of the bulk of the portfolio.

The model obtained from our calibration is a Markovian loss process where the default

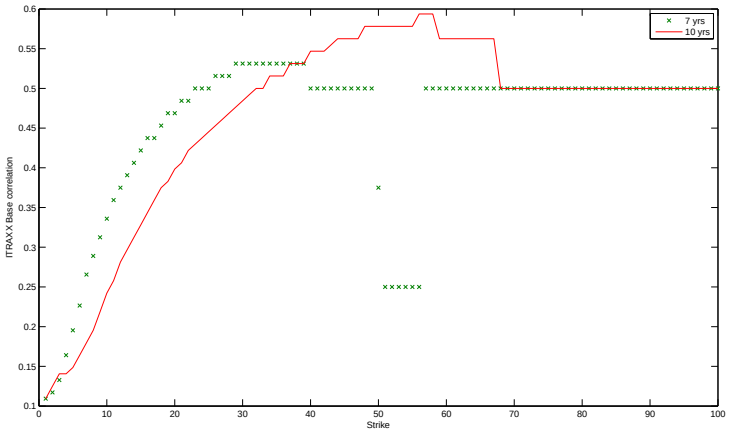

Figure II.6: Base correlation surface generated by the calibrated model: ITRAXX Europe Series 6, March 15 2007.

intensity depends on the current loss level and time. When compared with other possible specifications of top-down pricing models, the Markovian loss process considered here is of course quite simple in structure. Though it does account for clustering of defaults, it does not include, for instance, spread risk and the influence of other factors such as interest rates. Although more complex specifications are possible, as shown in Proposition 3.1, the information content of CDO spreads does not allow to identify such models uniquely. Recently, Lopatin & Misirpashayev [111] have suggested to use a Markovian loss model as an intermediate step in the calibration of a two-factor model with richer dynamics, using a relation such as (II.6) to link the parameters of the full two dimension model to the calibrated effective intensity. In this context our algorithm can be used as the first phase of a calibration algorithm for more complex models, provided the computation of the effective intensity is tractable [42].

Chapter III

Resilience to contagion in financial networks

Contagion of losses across financial institutions may be modeled as a cascade process on a network representing their mutual exposures. We derive rigorous asymptotic results for the magnitude of balance-sheet contagion in a large financial network and give an analytical expression for the asymptotic fraction of defaults, in terms of network characteristics. Our results extend previous studies on contagion in random graphs to inhomogeneous directed graphs with a given degree sequence and arbitrary distribution of weights. We introduce a criterion for the resilience of a large financial network to the default of a small group of financial institutions and quantify how contagion amplifies small shocks to the network. Our results emphasize the role played by "contagious exposures" and show that institutions which contribute most to network instability in case of default are highly connected institutions to whom their counterparties are highly exposed. The asymptotic results show good agreement with simulations for networks with realistic sizes.[1]

Keywords: *systemic risk, default contagion, random graphs, macro-prudential regulation.*

[1]This work was presented at the MITACS Workshop on Financial Networks and Risk Assessment (Toronto, May 2010), the Workshop on financial derivatives and risk management (Toronto, May 2010), the 6th Bachelier World Congress (Toronto, June 2010), the Workshop on Systemic Risk and Central Counterparties (Paris, Sept 2010) and the Conference Modeling and managing Financial Risks (Paris, January 2011). We thank D. Bienstock, M. Crouhy, J. Gleeson for helpful comments and discussions. Andreea Minca's work was supported by a doctoral grant from the Natixis Foundation for Quantitative Research.

Contents

1 Introduction

The recent financial crisis has highlighted the interconnectedness of financial institutions worldwide and led to an increased awareness of the impact of network externalities when considering financial stability [4, 41, 84, 87].

The interrelations among financial institutions may be modeled in terms of a network whose characteristics turn out to be heterogeneous and complex in nature [28, 48]. The network approach for contagion modeling has been used extensively both in theoretical [5, 4, 19, 41, 66, 76, 120] and empirical studies [48, 68, 132, 116]. In these models, the default of certain banks due to exogenous shocks may propagate to their counterparties as these write down from their capital the exposures to the defaulted banks.

Contagion effects and network externalities in banking systems have been investigated in the literature from various standpoints. Network externalities are –implicitly or explicitly– present in various early discussions of systemic risk (see e.g. Hellwig [86], Kiyotaki & Moore [100], Rochet & Tirole [122] through the interlinkages between balance sheets. Allen and Gale

[5] pioneered the use of network models in the study the stability of a system of interconnected financial institutions. Their results, extended in various directions by subsequent studies based on stylized network structures, such as Lagunoff and Schreft (2001) [103], Leitner (2005) [105], point to the crucial role played by network structure in the tradeoff between risk sharing and contagion. However, the simplicity of the network structures assumed in these studies has raised questions about the robustness of their conclusions when applied to banking systems [19].

Contagion in graphs has also been investigated in a more general context; relevant references include Morris [114], Kleinberg [101] and Watts [133]. These models consider, in one form or another, a mechanism in which an agent decides to adopt one of two states as a function of the state of its neighbors and a threshold which measures its susceptibility to this direct influence. Insolvency cascades in banking networks fall under the irreversible version of this model [133, 101] – becoming insolvent is not reversible, unlike the case of agents playing a network game who can revise their decisions [114] – in which the solvency threshold of a given bank depends on its level of capital, the state of solvency of its direct counterparties and its exposures to them. Gai and Kapadia [76] apply the results of Watts [133] to financial networks, assuming exposures are equally distributed across counterparties.

However, empirical studies [28, 128, 48] reveal that banking networks have a complex heterogeneous structure which turns out to be quite different from those studied in the aforementioned works. These networks exhibit heavy tailed distributions for both connectivity and exposures, which seem to play an important role when analyzing systemic risk [48]. In particular, the heterogeneity of exposures - weights associated to the links - prevents from reducing the analysis of contagion in banking networks to the case where a node's aggregate exposure is distributed uniformly across counterparties, as in [76, 109].

More complex network structures, based on random graph models, have been studied using a simulation-based approach by Nier et al. [120] and Cont & Moussa [47]. These studies allow to investigate a wide variety of network structures and provide interesting insights into the interplay between network properties and contagion. However, the numerical complexity of such large scale simulations and the inherent difficulty to repeat them for a large number of parameter values, makes it difficult to understand the specific influence of those parameters. Finally, whereas full information on counterparty exposures may not be available, the opposite point of view in which all important features of the financial network – degree of connectivity and balance sheets – are random is equally, if not more, unrealistic. Data on balance sheets and the magnitude of counterparty exposures cannot be ignored when analyzing financial stability of banking networks.

In this paper, we place ourselves between these two extremes and develop techniques for analyzing default cascades in weighted directed networks, with arbitrary degree sequences and in which one can prescribe an arbitrary set of exposures –or weights attached to the links– for each node in the network. Our results provide analytical insights into the nature of the relation between network structure and contagion in large-scale networks, without the need for undesirable restrictions on the topology and structure of the network.

1.1 Summary

We propose a model for the contagion of losses across financial institutions, in terms of a cascade process on a network representing their mutual exposures. Our setting allows for arbi-

trary network structures and heterogeneous networks which mimic the empirically properties of banking systems. Our contribution is to derive rigorous asymptotic results for the magnitude of contagion in large network and give an analytical expression for the asymptotic fraction of defaults, in terms of network characteristics.

We formulate our results in terms of insolvency cascades in a network of financial institutions with interlinked balance sheets, where losses flow out from the liability side of the balance sheets; however, similar techniques may be used for analyzing cascades of illiquidity in which losses propagate through the asset side.[2]

Our proof is based on a coupling argument: we construct a related multigraph –a weighted configuration model– which leads to the same number of defaults as in the original contagion process but is easier to study because of its independence properties. The contagion process in this model may then be described by a Markov chain. Generalizing the differential equation method of Wormald [134] to the case where the dimension of the Markov chain depends on size of the network we show that, as the network size increases, the rescaled Markov chain converges in probability to a limit described by a system of ordinary differential equations, which can be solved in closed form. This enables us to obtain analytical results on the final fraction of defaults in the network. As a corollary, we obtain a characterization of the (modified) contagion threshold defined by Morris [114] for a large class of graphs.

These results generalize previous ones on diffusions in random graphs with prescribed degree sequence to the case of inhomogeneous, weighted random graphs with arbitrary degree sequences. Related problems are the problem of existence of a giant component in random graphs [52, 113], the k-core problem [35] and the bootstrap percolation problem [6, 7, 17].

Based on these results, we introduce a global criterion of resilience of the financial network to small initial shocks, in which the contribution to systemic risk of every node becomes apparent. This criterion allows to study the influence of the network topology on the magnitude of contagion, and may be used as a tool for stress testing the resilience of interbank networks [9].

Our approach allows us to obtain several new results:

- We obtain an asymptotic expression for the size of a default cascade in a large network, in terms of the characteristics of the network, extending previous results for homogeneous undirected random graphs to heterogeneous, weighted networks. These asymptotic results are shown to be in good agreement with simulations for networks with large but realistic sizes.

- We obtain an analytical criterion for the resilience of a large financial network to the default of one or several institutions, in terms of the characteristics of the network.

- The analytical nature of these results allows to analyze the influence of network characteristics, in a general setting, more explicitly than in previous studies. In particular, our results underline the role played by *contagious exposures* and allow to identify institutions which may act as potential hubs for default contagion.

- Our results show the importance of taking into account the *heterogeneity* of financial networks when discussing issues of financial stability and contagion. In particular we show that, contrarily to the intuition conveyed by examples based on homogeneous networks,

[2]For an illuminating discussion, albeit not in a network framework, on the relation between illiquidity and insolvency see [115].

in presence of heterogeneity the relation between (average) connectivity of a network and its resilience to contagion is not monotonous.

These results provide new insights into the link between network structure and the resilience of a network to small shocks characterized in terms of the default of one or several financial institutions, a question of interest in the context of macroprudential regulation of banking systems. In particular, we are able to obtain analytical results which complement and extend previous theoretical results obtained for simpler network structures and the simulation results obtained using data on interbank claims.

Conditions for stability of networks with respect to contagion have been previously derived in the literature [133, 76], using mean field approximations or heuristic methods, in terms of the **expected** size of a cascade starting from a randomly chosen node, the expectation being taken over the law of the random graph with given degree distribution. Our results yield stronger statements on the convergence in probability of the number of defaults, allow for heterogeneity in network structure and, unlike the setting of Gai & Kapadia [76], take into account the non-uniform distribution of exposures across counterparties.

1.2 Outline

Section 2 introduces a model for a network of financial institutions which allows for various features empirically observed in interbank networks and describes a mechanism for default contagion in such a network. Section 3 gives our main result, which is a rigorous asymptotic analysis of the magnitude of contagion in large networks. Section 4 uses this result to define a measure of resilience for a financial network: we show that when this indicator of resilience crosses a threshold, small initial shocks to the network –in the form of the exogenous default of a small set of nodes– may generate a large-scale cascade of failure, a signature of *systemic risk*.

Section 5 illustrates, through concrete examples, how our results allow to relate the magnitude of contagion and the resilience of the network to various features of the network such as capital ratios and connectivity properties. We observe that networks with the same average connectivity may amplify initial shocks in very different manners and their resilience to contagion can vastly differ. In particular, the relation between 'connectivity' and 'contagion' is not monotonous. Technical proofs are given in Section 6.

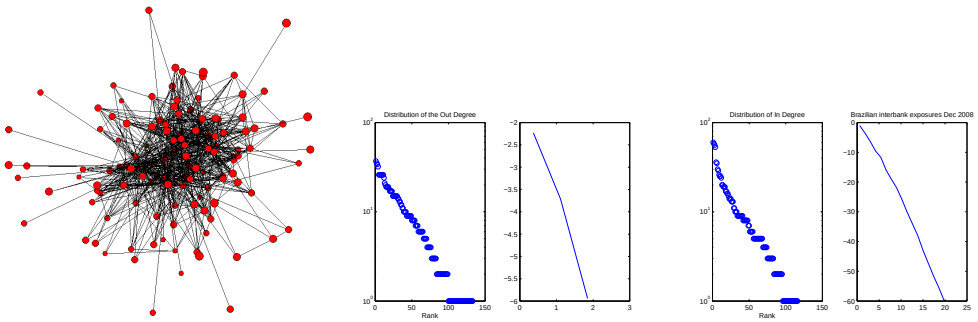

Figure III.1: (a) The Brazilian interbank network, (b) The out-degree (number of debtors) has a Pareto tail distribution with exponent ≈ 1.7, (c) The in-degree (number of creditors) has a Pareto tail distribution with exponent ≈ 3 . Source: Cont et al. [48].

Assets	Liabilities
Interbank assets $A(i) = \sum_j e(i,j)$	Interbank liabilities $L(i) = \sum_j e(j,i)$ Deposits $D(i)$
Other assets $x(i)$	Net worth $c(i) = \gamma(i)A(i)$

Table III.1: Stylized balance sheet of a bank.

2 A network model of default contagion

2.1 Counterparty networks

Interlinkages across balance sheets of financial institutions may be modeled by a weighted directed graph $\mathbf{g} = (\mathbf{V}, \mathbf{e})$ on the vertex set $\mathbf{V} = [1, \ldots, n]$, whose elements represent financial institutions. Table III.1 displays a stylized balance sheet of a financial institution: denoting by $e(i,j)$ the exposure (in monetary units) of institution i to institution j, the interbank assets of i are given by $A(i) = \sum_j e(i,j)$, whereas $L(i) = \sum_j e(j,i)$ represents the interbank liabilities of i. In addition to these interbank assets and liabilities, a bank may hold other assets and liabilities (such as deposits).

The net worth of the bank, given by its **capital** $c(i)$, represents its capacity for absorbing losses while remaining solvent. We will refer to the ratio

$$\gamma(i) = \frac{c(i)}{A(i)}.$$

$\gamma(i)$ as the "capital ratio" of institution I although technically it is the ratio of capital to interbank assets and not total assets. An institution is *insolvent* if its net worth is negative or zero, in which case we set $\gamma(i) = 0$.

Definition 2.1. A **financial network** $(\mathbf{e}, \gamma)$ is defined by

- a matrix of exposures $\{e(i,j)\}_{1 \le i,j \le n}$,
- a set of capital ratios $\{\gamma(i)\}_{1 \le i \le n}$.

In this network, the *in-degree* of a node i

$$d^-(i) = \#\{j \in \mathbf{V} \ \mid \ e(j,i) > 0\},$$

represents the number of nodes exposed to i while its *out-degree*

$$d^+(i) = \#\{j \in \mathbf{V} \ \mid \ e(i,j) > 0\}$$

represents the number of institutions i is exposed to. The set of initially insolvent institutions is represented by

$$\mathbb{D}_0(e, \gamma) = \{i \in \mathbf{V} \ \mid \ \gamma(i) = 0\}.$$

2.2 Default contagion

In a network $(\mathbf{e}, \gamma)$ of counterparties, the default of one or several nodes may lead to the insolvency of other nodes, generating a *cascade* of defaults.

Starting from the set of initially insolvent institutions

$$\mathbb{D}_0(e, \gamma) = \{i \in \mathbf{V} \mid \gamma(i) = 0\},$$

which represent *fundamental defaults*, we define a contagion process as follows.

Denoting by $R(j)$ the recovery rate on the assets of j at default, the default of j induces a loss equal to $(1 - R(j))e(i, j)$ for its counterparty i. If this loss exceeds the capital of i, then i becomes in turn insolvent. The set of nodes which become insolvent due to their exposures to initial defaults is

$$\mathbb{D}_1(e, \gamma) = \{i \in \mathbf{V} \mid \gamma(i)A(i) < \sum_{j \in \mathbb{D}_0} (1 - R(j))e(i, j)\},$$

This procedure may be iterated to define the *default cascade* initiated by a set of initial defaults.

Definition 2.2 (Default cascade)**.** Given a set $\mathbb{D}_0(\mathbf{e}, \gamma) = \{i \in [1, \dots, n] \mid \gamma(i) = 0\}$ of insolvent institutions, the increasing sequence $(\mathbb{D}_k(e, \gamma), k \geq 1)$ of subsets of $\mathbf{V}$ defined by

$$\mathbb{D}_k(\mathbf{e}, \gamma) = \{i \mid \gamma(i)A(i) < \sum_{j \in \mathbb{D}_{k-1}(\mathbf{e}, \gamma)} (1 - R(j))e(i, j)\}.$$

is called the *default cascade* initiated by $\mathbb{D}_0(e, \gamma)$.

$\mathbb{D}_k(\mathbf{e}, \gamma)$ represents the set of institutions whose capital is insufficient to absorb losses due to defaults of institutions in $\mathbb{D}_{k-1}(\mathbf{e}, \gamma)$

It is easy to see that, in a network of size n, the cascade ends after at most $n - 1$ iterations, so $\mathbb{D}_{n-1}(e, \gamma)$ represents the set of all nodes which become insolvent starting from the initial set of defaults $\mathbb{D}_0(e, \gamma)$.

Definition 2.3. The fraction of defaults in the network $(\mathbf{e}, \gamma)$ initiated by $\mathbb{D}_0(e, \gamma)$ is given by

$$\alpha_n(\mathbf{e}, \gamma) = \frac{|\mathbb{D}_{n-1}(\mathbf{e}, \gamma)|}{n}.$$

The recovery rates $R(i)$ may be exogenous or, as in Eisenberg and Noe [66], determined endogenously by redistributing assets of a defaulted entity among debtors, proportionally to their outstanding debt. As noted in [131, 48], the latter scenario is too optimistic since in practice liquidation takes time and assets may depreciate in value due to fire sales during liquidation.

As argued in [48, 68], when examining the short term consequences of default, the most realistic assumption on recovery rates is zero: assets held with a defaulted counterparty are frozen until liquidation takes place, a process which can in practice take months to terminate.

2.3 A random network model

Figure 1 displays the example of the Brazilian interbank network, studied in [48]. Empirical studies on interbank exposures [28, 48] show such networks to have a complex, heterogeneous

structure characterized by heavy-tailed cross-sectional distributions of degrees (number of counterparties) and exposures.

Given a description of the large-scale structure of the network in statistical terms, it is natural to model the network as a *random graph* whose statistical properties correspond to these observations.

Consider a sequence $(e_n, \gamma_n)_{n\geq 1}$ of financial networks, indexed by the number of nodes n , where $\mathbf{d_n^+} = \{d_n^+(i)\}_{i=1}^n$ (respectively $\mathbf{d_n^-} = \{d_n^-(i)\}_{i=1}^n$) represents the sequence of in-degrees (resp. out-degrees) of nodes in e_n. We now construct a random network $\mathbf{E}_n$ such that e_n may be considered as a typical sample of $\mathbf{E}_n$.

Definition 2.4 (Random network ensemble)**.** Let $\mathcal{G}_n(\mathbf{e_n})$ be the set of all weighted directed graphs with degree sequence $\mathbf{d_n^+}, \mathbf{d_n^-}$ such that, for any node i, the set of exposures is given by the non-zero elements of line i in the exposure matrix $\mathbf{e_n}$. Let $(\Omega, \mathcal{A}, \mathbb{P})$ be a probability space. We define $\mathbf{E_n} : \Omega \to \mathcal{G}_n(\mathbf{e_n})$ as a random directed graph uniformly distributed on $\mathcal{G}_n(\mathbf{e_n})$.

We endow the nodes in $\mathbf{E_n}$ with the capital ratios $\gamma_\mathbf{n}$. Then for all $i = 1, \ldots, n$,

$$\{\mathbf{E_n}(i,j), \quad \mathbf{E_n}(i,j) \neq 0\} = \{\mathbf{e_n}(i,j), \quad \mathbf{e_n}(i,j) \neq 0\} \quad \mathbb{P} - a.s.$$

$$\#\{j \in \mathbf{V},\ \mathbf{E_n}(j,i) > 0\} = d_n^+(j), \quad \text{and} \qquad \#\{j \in \mathbf{V},\ \mathbf{E_n}(i,j) \neq 0\} = d_n^-(i).$$

Definition 2.4 is equivalent to the representation of the financial system by an unweighted graph chosen uniformly among all graphs with the degree sequence $(\mathbf{d_n^+}, \mathbf{d_n^-})$, in which we assign to the links emanating from node i the set of weights $W_n(i) := \{e_n(i,j) > 0\}$.

2.4 Link with the configuration model

A standard method for studying random graphs with prescribed degree sequence is to consider (see e.g., [26, 113, 92]) a related random multigraph with the same degree sequence, known as the *configuration model* [26], then condition on this multigraph being simple. The configuration model in the case of random directed graphs has been studied by Cooper and Frieze [52]. Proceeding analogously, we introduce a multigraph with the same degrees and exposures as the network defined above, but which is easier to study because of the independence properties of the variables involved. Conditioned on being a simple graph, it has the same law as the random financial network defined above.

Definition 2.5 (Configuration Model)**.** Given a set of nodes $[1, \ldots, n]$ and a degree sequence $(\mathbf{d_n^+}, \mathbf{d_n^-})$, we associate to each node i two sets, $H_n^+(i)$ representing its out-going half-edges and $H_n^-(i)$ representing its in-coming half-edges, with $|H_n^+(i)| = d_n^+(i)$ and $|H_n^-(i)| = d_n^-(i)$. Let $H_n^+ = \bigcup_i H_n^+(i)$ and $H_n^- = \bigcup_i H_n^-(i)$. A **configuration** is a matching of H_n^+ with H_n^-. To each configuration we assign a graph. When an out-going half-edge of node i is matched with an in-coming half-edge of node j, a directed edge from i to j appears in the graph. The **configuration model** is the random directed multigraph $G_n^*(\mathbf{e_n})$ which is uniformly distributed across all configurations (Figure III.2.

It is easy to see that, conditional on being a simple graph, $G_n^*(\mathbf{e_n})$ is uniformly distributed on $\mathcal{G}_n(\mathbf{e_n})$. Thus, the law of $G_n^*(\mathbf{e_n})$ conditional on being a simple graph is the same as the law of $\mathbf{E}_n$.

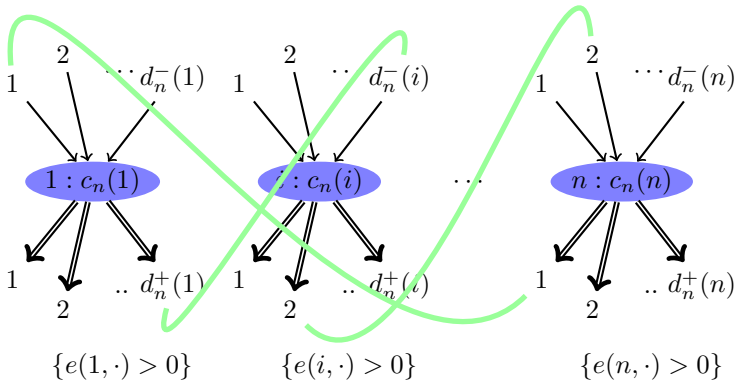

Figure III.2: Configuration model

In particular any property that holds with high probability (with probability tending to 1 as $n \to \infty$) for the random multigraph $G_n^*(\mathbf{e_n})$, holds with high probability on the random network $\mathbf{E}_n$ provided

$$\liminf_{n\to\infty} \mathbb{P}(G_n^*(\mathbf{e_n}) \; is \; simple) > 0. \tag{III.1}$$

In particular (see [93]), the condition $\sum_{i=1}^n (d_n^+(i))^2 + (d_n^-(i))^2 = O(n)$ implies (III.1).

Remark 2.6. Janson [93] has studied, in the case of undirected graphs, the probability of the random multigraph to be simple. One can adapt the proof to the directed case and show that the condition $\sum_{i=1}^n (d_n^+(i))^2 + (d_n^-(i))^2 = O(n)$ implies (III.1). Indeed, in the non-directed case, Janson [93] proves that when $m_n := \sum_{i=1}^n d_n(i) \to \infty$, ($d_n(i)$ is the degree of node i) one has

$$\mathbb{P}(G^*(n,(d_n(i))_1^n) \text{ is simple}) = \exp\left(-\frac{1}{2}\sum_i \lambda_{ii} - \sum_{i<j}(\lambda_{ij} - \log(1+\lambda_{ij}))\right) + o(1),$$

where for $1 \le i,j \le n$; $\lambda_{ij} := \frac{\sqrt{d_n(i)(d_n(i)-1)d_n(j)(d_n(j)-1)}}{m_n}$. The proof of these results is based on counting vertices with at least one loop and pairs of vertices with at least two edges between them, disregarding the number of parallel loops or edges. The same argument applies to the directed case, and one can show that when $m_n := \sum_{i=1}^n d_n^+(i) = \sum_{i=1}^n d_n^-(i) \to \infty$, then

$$\mathbb{P}(G_n^*(\mathbf{e_n}) \text{ is simple}) = \exp\left(-\frac{1}{2}\sum_i \lambda_{ii} - \sum_{i<j}(\lambda_{ij} - \log(1+\lambda_{ij}))\right) + o(1),$$

where for $1 \le i,j \le n$; $\lambda_{ij} = \frac{\sqrt{d_n^+(i)d_n^-(i)d_n^+(j)d_n^-(j)}}{m_n}$.

One can observe that a uniform matching of half-edges can be obtained sequentially: choose an in-coming half-edge according to any rule (random or deterministic), and then choose the corresponding out-going half-edge uniformly over the unmatched out-going half-edges. The configuration model is thus particularly appropriate for the study of contagion, as we will see in the proofs, since we can restrict the matching process to choosing only in-coming half-edges entering defaulted nodes. In doing so, on constructs directly the contagion cluster in the random graph given by the configuration model and endowed with the sequence of capital ratios.

Due to this property, it is easier to study contagion on $G_n^*(\mathbf{e_n})$ under conditions on the degree sequence for the assumption above (III.1) to hold, then translate all results holding with high probability to the initial network E_n defined in Definition 2.4.

3 Asymptotic results

We consider a sequence of random financial networks as introduced above. Our goal is to study the behavior of $\alpha_n(\mathbf{E_n}, \gamma_\mathbf{n})$ which represents the size of the cascade generated by the default of initially insolvent institutions $\mathbb{D}_0(\mathbf{E_n}, \gamma_\mathbf{n}) = \{i, \gamma_n(i) = 0\}$.

Notations. Let a_n be a sequence of positive numbers. For a non-random sequence b_n we say

- $b_n = O(a_n)$ if there exist constants C and n_0 such that $|b_n| \leq Ca_n$ for $n \geq n_0$.
- $b_n = o(a_n)$ if $\frac{b_n}{a_n} \overset{n\to\infty}{\to} 0$.

A sequence of events $\mathcal{A}_n$ is said to occur w.h.p. (with high probability) if $\lim_{n\to\infty} \mathbb{P}(\mathcal{A}_n) = 1$. $\overset{p}{\to}$ denotes convergence in probability. For a sequence (X_n) of random variables, we say

- $X_n = O_p(a_n)$ if for every $\varepsilon > 0$ there exist constants C_ε and n_ε such that $\mathbb{P}(|X_n| \leq C_\varepsilon a_n) > 1 - \varepsilon$ for $n \geq n_\varepsilon$.
- $X_n = o_p(a_n)$ if for every $\varepsilon > 0$ there exists n_ε such that $\mathbb{P}(|X_n| \leq \varepsilon a_n) > 1 - \varepsilon$ for $n \geq n_\varepsilon$. This is equivalent [95, Lemma 2] to

$$\frac{X_n}{a_n} \overset{p}{\to} 0.$$

We also denote

- w.h.p. $X_n = O(a_n)$ if there exists a constant C such that $|X_n| \leq Ca_n$ w.h.p.
- w.h.p. $X_n = o(a_n)$ equivalently to $X_n = o_p(a_n)$.

3.1 Assumptions

Denote by

$$m_n := \sum_{i=1}^n d_n^+(i) = \sum_{i=1}^n d_n^-(i)$$

the total number of links in the network $\mathbf{e_n}$. The **empirical distribution of the degrees** is defined by

$$\mu_n(j,k) := \frac{1}{n}\#\{i : d_n^+(i) = j, d_n^-(i) = k\}.$$

We assume that the degree sequences $\mathbf{d_n^+}$ and $\mathbf{d_n^-}$ satisfy the following conditions.

Assumption 3.1. For each $n \in \mathbb{N}$, $\mathbf{d_n^+} = \{(d_n^+(i))_{i=1}^n\}$ and $\mathbf{d_n^-} = \{(d_n^-(i))_{i=1}^n\}$ are sequences of nonnegative integers with $\sum_{i=1}^n d_n^+(i) = \sum_{i=1}^n d_n^-(i)$, and such that, for some probability distribution μ on $\mathbb{N}^2$,

1. $\mu_n(j,k) \to^{n\to\infty} \mu(j,k)$;
2. *Finite expectation property:* $\sum_{j,k} j\mu(j,k) = \sum_{j,k} k\mu(j,k) =: \lambda \in (0,\infty)$;
3. $\sum_{i=1}^n (d_n^+(i))^2 + (d_n^-(i))^2 = O(n)$.

In particular these assumptions imply that $m_n/n \to \lambda$, as $n \to \infty$.

Denote by $\Sigma^{\mathbf{e}}(i)$ the set of permutations of the counterparties of i in the network $\mathbf{e}$, i.e., permutations of the set $\{j \mid e(i,j) > 0\}$. For the purpose of studying contagion, the exposures and capital ratios of different nodes may be summarized in terms of *default thresholds* for each node:

Definition 3.2 (Default threshold)**.** For a node i and permutation $\tau \in \Sigma^{\mathbf{e}}(i)$ which specifies the order in which i's counterparties default, the default threshold

$$\Theta(i, \mathbf{e}, \gamma, \tau) := \min\{k \geq 0, \gamma(i)A(i) < \sum_{j=1}^{k} (1-R)e_{i,\tau(j)}\}, \tag{III.2}$$

measures how many counterparty defaults i can tolerate before it becomes insolvent, if its counterparties default in the order specified by τ.

We also define

$$p_n(j,k,\theta) := \frac{\#\{(i,\tau) \mid 1 \leq i \leq n,\ \tau \in \Sigma^{\mathbf{e_n}(i)},\ d_n^+(i) = j,\ d_n^-(i) = k,\ \Theta(i, \mathbf{e_n}, \gamma_{\mathbf{n}}, \tau) = \theta\}}{n\mu_n(j,k)j!} \tag{III.3}$$

We will see in Section 6.1 that, for n large, $p_n(j,k,\theta)$ gives the fraction of nodes with degree (j,k) which have the default threshold equal to θ, in the random financial network $\mathbf{E}_n$. In particular, for $\theta = 1$,

$$n\mu_n(j,k)jp_n(j,k,1)$$

is the number of exposures of nodes with degree (j,k) which exceed the capital of the exposed node i.e. exposures which, in case of default of the initial node always lead to the insolvency of the exposed node. These links play a special role: we will call them *contagious exposures* (or contagious links):

Definition 3.3 (Contagious exposure)**.** We call an exposure (or link) $(i \to j)$ *contagious* if it exceeds the capital of the exposed node:

$$e_n(i,j) > c_n(i).$$

We will assume that $p_n(j,k,\theta)$ has a limit when $n \to \infty$:

Assumption 3.4. There exists a function $p : \mathbb{N}^3 \to [0,1]$ such that for all $j,k,\theta \in \mathbb{N}$ $(\theta \leq j)$

$$p_n(j,k,\theta) \overset{n\to\infty}{\to} p(j,k,\theta).$$

Under this assumption, we will see in Section 6 that $p(j,k,\theta)$ is also the limit in probability of the fraction of nodes with degree (j,k) which become insolvent after θ of their counterparties default. In particular,

- $p(j,k,0)$ represents the proportion of initially insolvent nodes with degree (j,k);
- $p(j,k,1)$ represents the proportion of nodes with degree (j,k) which are 'vulnerable' i.e. may become insolvent due to the default of a single counterparty.

We now present examples of models for counterparty networks which satisfy Assumption 3.4.

Example 3.5 (Independent exposures)**.** Assume for all n, the exposures of all nodes $i \in [1,\dots,n]$ with the same degree (j,k), $\{e_n(i,l) > 0 \mid d_n^+(i) = j, d_n^-(i) = k\}$, are i.i.d. random variables, with a law depending on j and k, but not on n, denoted $F_X(j,k)$. We assume the same for the sequence of capital ratios i.e. $\{\gamma_n(i) \mid d_n^+(i) = j, d_n^-(i) = k\}$ are i.i.d. variables with a law $F_\gamma(j,k)$ which may depend on (j,k), but not on n. Then it is easy to see that, by the law of large numbers, Assumption 3.4 holds and the limit $p(j,k,\theta)$ is known,

$$p(j,k,\theta) = \mathbb{P}(X_\theta > \gamma \sum_{l=1}^{j} X_l - \sum_{l=1}^{\theta-1}(1-R)X_l \geq 0),$$

with $(X_l)_{l=1}^j$ random i.i.d. variables with law $F_X(j,k)$ and γ an independent random variable with law $F_\gamma(j,k)$.

Example 3.6 (Exchangeable exposures)**.** Empirical observations of banking networks [48, 28, 128] show that they are hierarchical, 'disassortative' networks [109], with a few large and highly interconnected dealer banks and many small banks, connected predominantly to dealer banks. This can be modeled in a stylized way by partitioning the set of nodes into two sets, a set $\mathcal{D}$ of n^D dealer banks, and a set $\mathcal{N}$ of n^N non-dealer banks.

We assume that the exposures $\{e_n(i,l) > 0 \mid i \in \mathcal{D}\}$, and $\{e_n(i,l) > 0 \mid i \in \mathcal{N}\}$ are restrictions corresponding to the first m_n^D, respectively m_n^N, elements of infinite sequences of exchangeable variables, where m_n^D and m_n^N denote the total number of exposures belonging to dealer and respectively non-dealer banks. Similarly, the capital ratios $\{\gamma_n(i) \mid i \in \mathcal{D}\}$ and $\{\gamma_n(i) \mid i \in \mathcal{N}\}$ are restrictions to the first n^D (respectively n^N) elements of the sequence, independent of the sequence of exposures.

We can extend this example to a finite number of classes of nodes, represented by their degrees, and also drop the assumption of independence between exposures and capital ratios, replacing it by the assumption that, within each class, the sequence of a node's exposures and capital ratios are exchangeable random variables.

For each node i with $d_n^+(i) = j, d_n^-(i) = k$ we let

$$Y_n(i) := (\{e_n(i,j) > 0\}, \gamma_n(i))$$

be a multivariate random variable with state space $\Im^{j,k} \subset \mathbb{R}_+^j \otimes \mathbb{R}$ and we assume that the law of the finite sequence

$$\big\{Y_n(i) \mid i \in [1,\dots,n], d_n^+(i) = j, d_n^-(i) = k\big\}$$

is invariant under permutation.

Then the family $\{Y_n(i) \mid i \in [1,\dots,n], d_n^+(i) = j, d_n^-(i) = k\}_{0\le j,k\le M}$ represents a family of finite multi-exchangeable systems, as defined by Graham [82]. We let the empirical measure sequence

$$\left\{\Lambda_n^{j,k} := \frac{\sum_i \mathbb{1}_{\{\ d_n^+(i)=j,\ d_n^-(i)=k\}}\delta_{Y_n(i)}}{n\mu_n(j,k)}\right\}_{0\le j,k\le M}.$$

We suppose that the family $\{Y_n(i) \mid i \in [1,n], d_n^+(i) = j, d_n^-(i) = k\}_{0\le j,k\le M}$ converges in law when $n \to \infty$ to an infinite multi-exchangeable system

$$\lim_{n\to\infty} \left\{Y_n(i) \mid i \in [1,\dots,n], d_n^+(i) = j, d_n^-(i) = k\right\}_{0\le j,k\le M} \overset{\mathcal{L}}{=} \left\{Z_l^{j,k} \mid l \ge 1\right\}_{0\le j,k\le M}. \quad \text{(III.4)}$$

By [82, Theorem], the empirical measure converges in law to

$$\lim_{n\to\infty} \left\{\Lambda_n^{j,k}\right\}_{0\le j,k\le M} \overset{\mathcal{L}}{=} \left\{\Lambda^{j,k}\right\}_{0\le j,k\le M}. \quad \text{(III.5)}$$

For an arbitrary $Z \in \Im^{j,k}$ we define the function

$$h(Z,\theta) = \frac{\#\{\tau \mid \tau \in \Sigma(j), \Theta(Z,\tau) = \theta\}}{j!},$$

with $\Theta(Z,\tau)$ being the equivalent on the space $\Im^{j,k}$ of $\Theta(i,\mathbf{e},\gamma,\tau)$ in Definition 3.2. Then, by Equation (III.5) giving the convergence of empirical measures and the fact that the function h is bounded, we have

$$p_n(j,k,\theta) = \mathbb{E}^{\Lambda_n^{j,k}}(h(\mathbf{Z},\theta)) \overset{n\to\infty}{\to} \mathbb{E}^{\Lambda^{j,k}}(h(\mathbf{Z},\theta)) = p(j,k,\theta),$$

with $\mathbf{Z}$ a random element of $\Im^{j,k}$. A last observation is that Equation (III.4) is verified in our two tiered example since the sequences used to construct the network of size n are restrictions of infinite exchangeable sequences.

3.2 The asymptotic magnitude of contagion

We consider the representation of the financial network by a random graph as described in Section 2.3. Denote by

$$\beta(j,\pi,\theta) := \mathbb{P}(\mathrm{Bin}(j,\pi) \ge \theta) = \sum_{l\ge\theta}^{j} \binom{j}{l} \pi^l (1-\pi)^{j-l},$$

the distribution function of a binomial random variable $\mathrm{Bin}(j,\pi)$ with parameters j and π. Consider $p(j,k,\theta)$ defined in Assumption 3.4. (By Lemma 6.4 in Appendix 6 this quantity represents the asymptotic fraction of nodes with out-degree j and in-degree k that will default when θ of their debtors default.) We define the function $I : [0,1] \to [0,1]$ as

$$I(\pi) := \sum_{j,k} \frac{\mu(j,k)k}{\lambda} \sum_{\theta=0}^{j} p(j,k,\theta)\beta(j,\pi,\theta). \quad \text{(III.6)}$$

$I(\pi)$ has the following interpretation: if the end node of a randomly chosen edge defaults with probability π, $I(\pi)$ is the expected fraction of counterparty defaults after one iteration of the cascade.

Let π^* be the smallest fixed point of I in $[0,1]$, i.e.

$$\pi^* = \min\{\pi \in [0,1] \mid I(\pi) = \pi\}.$$

The value π^* represents the probability that an edge taken at random ends in a defaulted node at the end of the contagion process.

Remark 3.7. I admits at least one fixed point. Indeed, I is a continuous increasing function and

$$I(1) = \sum_{j,k} \frac{\mu(j,k)k}{\lambda} \sum_{\theta=0}^{j} p(j,k,\theta) \leq 1,$$

since $\sum_{\theta=0}^{j} p(j,k,\theta) \leq 1$. Moreover,

$$I(0) = \sum_{j,k} \frac{\mu(j,k)k}{\lambda} p(j,k,0) \geq 0$$

represents the probability that an edge taken at random ends in a fundamentally defaulted node. So the function I has at least a fixed point in $[0,1]$.

We can now announce our main theorem.

Theorem 3.8. *Consider a sequence of exposure matrices and capital ratios* $\{(\mathbf{e_n})_{\mathbf{n}\geq\mathbf{1}}, (\gamma_\mathbf{n})_{\mathbf{n}\geq\mathbf{1}}\}$ *satisfying Assumptions 3.1 and 3.4 and the corresponding sequence of random matrices* $(\mathbf{E_n})_{n\geq 1}$ *defined on* $(\Omega, \mathcal{A}, \mathbb{P})$ *as in Definition 2.4. Let* π^* *be the smallest fixed point of* I *in* $[0,1]$*, i.e.*

$$\pi^* = \min\{\pi \in [0,1] \mid I(\pi) = \pi\}.$$

1. *If* $\pi^* = 1$*, i.e. if* $I(\pi) > \pi$ *for all* $\pi \in [0,1)$*, then asymptotically all nodes default during the cascades*
$$\alpha_n(\mathbf{E_n}, \gamma_\mathbf{n}) \xrightarrow{p} 1.$$

2. *If* $\pi^* < 1$ *and furthermore* π^* *is a stable fixed point of* I $(I'(\pi^*) < 1)$*, then the asymptotic fraction of defaults*
$$\alpha_n(\mathbf{E_n}, \gamma_\mathbf{n}) \xrightarrow{p} \sum_{j,k} \mu(j,k) \sum_{\theta=0}^{j} p(j,k,\theta)\beta(j,\pi^*,\theta).$$

A proof of this theorem is given in Appendix 6.

4 Resilience to contagion

4.1 A simple measure of network resilience

The resilience of a network to small shocks is a global property of the network which depends on is detailed structure, not just the average connectivity. However, the above results allow to introduce a rather simple and easy to compute indicator for the resilience of a network to small shocks.

Definition 4.1 (Network resilience)**.** Define the network resilience as

$$1 - \sum_{j,k} \frac{jk}{\lambda} \mu(j,k) p(j,k,1) \in (-\infty, 1].$$

The following result, which is a consequence of Theorem 3.8, shows that this indicator measures the resilience of a network to the initial default of a small fraction ε of the nodes:

Proposition 4.2. *Consider a sequence of financial networks* $(\mathbf{E_n}, \gamma_\mathbf{n})$ *satisfying Assumption* (3.1) *and* (3.4)*. If*

$$1 - \sum_{j,k} \frac{jk}{\lambda} \mu(j,k) p(j,k,1) > 0 \tag{III.7}$$

then for every $\varepsilon > 0$*, there exists* N_ε *and* ρ_ε *such that if the initial fraction of defaults is smaller than* ρ_ε*, then the final fraction of defaults is negligible with high probability*

$$\forall n \geq N_\varepsilon, \qquad \mathbb{P}(\alpha_n(\mathbf{E_n}, \gamma_\mathbf{n}) \leq \varepsilon) > 1 - \varepsilon$$

Proof. Consider ρ bounding from above the fraction of fundamental defaults

$$\sum_{j,k} \mu(j,k) p(j,k,0) \leq \rho.$$

We have

$$I(\alpha) = \sum_{j,k} \frac{\mu(j,k)k}{\lambda} \sum_{\theta=0}^{j} p(j,k,\theta) \beta(j,\alpha,\theta).$$

Using a first order expansion of $\beta(j,\alpha,\theta)$ in α at 0:

$$\beta(j,\alpha,\theta) = 1_{\{\theta=0\}} + \alpha j 1_{\{\theta=1\}} + o(\alpha).$$

Then,

$$I(\alpha) = \sum_{j,k} \frac{\mu(j,k)k}{\lambda} (p(j,k,0) + \alpha j p(j,k,1)) + o(\alpha).$$

Let α^* be the smallest fixed point of $I(\alpha)$. Given Condition III.7, for $\alpha > 0$ and small enough,

$$\lim_{\rho \to 0} I(\alpha) = \alpha \sum_{j,k} \frac{\mu(j,k)jk}{\lambda} p(j,k,1) + o(\alpha) < \alpha,$$

where we use the fact that if the fraction of fundamental defaults tends to zero, so does the fraction of out-going links belonging to fundamentally defaulted nodes. On the other hand we have seen that $I(0) \geq 0$. Thus $\lim_{\rho \to 0} \alpha^* = 0$.

Let us now fix ε. By continuity of the function g defined by $g(\alpha) = \sum_{j,k} \mu(j,k) \sum_{\theta=0}^{j} p(j,k,\theta) \beta(j,\alpha,\theta)$ appearing in Theorem 3.8, there exists ρ_ε such that $g(\alpha^*) < \varepsilon/2$ as soon as $\rho < \rho_\varepsilon$. By Theorem 3.8 we have that there exists an integer N_ε such that, for $n \geq N_\varepsilon$,

$$\mathbb{P}(|\alpha_n(\mathbf{E_n}, \gamma_\mathbf{n}) - g(\alpha^*)| < \varepsilon/2) > 1 - \varepsilon,$$

which completes the proof. □

Theorem 4.3. *Consider a sequence of financial networks* $(\mathbf{E_n}, \gamma_\mathbf{n})$ *satisfying Assumption 3.1 and 3.4. If*

$$1 - \sum_{j,k} \frac{\mu(j,k)jk}{\lambda} p(j,k,1) < 0, \tag{III.8}$$

then with high probability there exists a set of nodes representing a positive fraction of the financial system, strongly interlinked by contagious links (i.e. there is a directed path of contagious links from any node to another in the component), such that any node belonging to this set can trigger the default of all nodes in the set.

Given the network topology, the Condition III.7 sets limits on the fraction of contagious links $p_n(j,k,1)$, i.e. on the magnitude of exposures relative to capital.

Remark 4.4. *(Branching process approximation).* Condition III.7 may be justified using the following heuristic argument. We describe an approximation of the local structure of the graph by a branching process, the children being the in-coming neighbors: the root ϕ with probability $\mu^-(k_\phi) := \sum_j \mu(j,k_\phi)$ has an in-degree equal to k_ϕ. Each of these k_ϕ vertices with probability $\frac{\mu(j,k)j}{\lambda}$ has degree (j,k), and with probability equal to $p(j,k,1)$ default when their parent defaults. Let y be the extinction probability, given by the smallest solution of

$$y = \sum_{j,k} \frac{\mu(j,k)j}{\lambda} p(j,k,1) y^k. \tag{III.9}$$

If $\sum_{j,k} \frac{\mu(j,k)jk}{\lambda} p(j,k,1) < 1$, then the smallest solution of (III.9) is $y = 1$, whereas if

$$\sum_{j,k} \frac{\mu(j,k)jk}{\lambda} p(j,k,1) > 1,$$

there is a unique solution with $y \in (0,1)$.

Similar results have been obtained using heuristic methods or mean-field approximations in epidemic models on unweighted graphs with arbitrary degree distributions. Gai & Kapadia [76], give the following condition for the appearance of global cascades,

$$1 - \sum_{j,k} \frac{jk}{\lambda} \mu(j,k) v(j) < 0, \tag{III.10}$$

with $v(j)$ being the probability that a bank with out-degree j is vulnerable, exposed to the default of a single neighbor. This condition can be seen as a special case of Condition (III.8) in which the assets and capital buffers are i.i.d. sequences verifying a law of large numbers. In such case the convergence Assumption 3.4 is satisfied by the law of large numbers. The model of [76] is an extension of the model of global cascades proposed by Watts[133], with a definition of the probability of a node to be vulnerable in terms of the distribution of the size of assets and capital buffers. These results are derived using generating function methods (see Newman [119]): under the assumption that component sizes are finite, one finds the generating function of the size of a connected component; the point at which the expected size of a connected component diverges marks the phase transition when the giant component appears. Note that the arguments used by Gai & Kapadia [76] are only valid for graphs without cycles i.e. trees.

In Theorem 4.3, the quantity $v(j)$ is replaced in our condition by $p(j,k,1)$, the asymptotic fraction of contagious links, a directly observable quantity.

Remark 4.5 (Too interconnected to fail?)**.** We suppose that the resilience condition given by Equation (III.7) is satisfied. Let π^*_ε be the smallest fixed point of I in $[0,1]$, when a fraction ε of all nodes represent fundamental defaults, i.e. $p(j,k,0)=\varepsilon$ for all j,k.

We obtain then, by a first order approximation of the function I, that

$$\pi^*_\varepsilon = \frac{\varepsilon}{1-\sum_{j,k}\frac{\mu(j,k)jk}{\lambda}p(j,k,1)} + o(\varepsilon).$$

By a first order approximation of the function $\pi \to \sum_{j,k}\mu(j,k)\sum_{\theta=0}^{j}p(j,k,\theta)\beta(j,\pi,\theta)$ giving the asymptotic fraction of defaults in Theorem 3.8, we obtain that, for any ρ there exists ε_ρ and n_ρ such that for all $\varepsilon<\varepsilon_\rho$ and $n>n_\rho$

$$\mathbb{P}(|\alpha_n(\mathbf{E_n},\gamma_\mathbf{n}) - \varepsilon(1+\frac{\sum_{j,k}j\mu(j,k)p(j,k,1)}{1-\sum_{j,k}\frac{\mu(j,k)jk}{\lambda}p(j,k,1)})| < \rho) > 1-\rho. \tag{III.11}$$

Suppose now that initially insolvent fraction involves only nodes with degree (d^+,d^-), and we denote $\pi^*_\varepsilon(d^+,d^-)$ the smallest fixed point of I in $[0,1]$ in the case where $p(d^+,d^-,0)=\varepsilon$ and $p(j,k,0)=0$ for all $(j,k)\neq(d^+,d^-)$. Then we obtain that, for any ρ there exists ε_ρ and n_ρ such that for all $\varepsilon<\varepsilon_\rho$ and $n>n_\rho$,

$$\mathbb{P}\left(|\alpha_n(\mathbf{E_n},\gamma_\mathbf{n}) - \varepsilon\mu(d^+,d^-)(1+\frac{d^-}{\lambda}\frac{\sum_{j,k}\frac{\mu(j,k)jk}{\lambda}p(j,k,1)}{1-\sum_{j,k}\frac{\mu(j,k)jk}{\lambda}p(j,k,1)})| < \rho\right) > 1-\rho. \tag{III.12}$$

This simple expression shows that there are basically two factors that determine how small initial shocks are amplified by the financial network: the interconnectedness of the node represented by its in-degree d^- and the average number of contagious links in the network, the 'frailty' of a node being its average number of contagious exposures, represented by the term $jp(j,k,1)$.

4.2 Relation with the Contagion threshold of a graph

Morris [114] considers a model of contagion on an arbitrary graph where a node 'defaults' when a proportion q of its neighbors have defaulted and defines the 'modified contagion threshold' [114, Sec. 7.2.] as the largest q such that contagion will spread from a "small" randomly chosen fraction of nodes to the whole population. This case corresponds to a special case of our model where all links have equal weights (equal exposures) and equal capital ratios $\gamma(i)=q$. In this case

$$p(j,k,\theta) = 1_{\{\theta=\lceil qj\rceil\}}, \tag{III.13}$$

where $\lceil qj\rceil$ denotes the integer part of qj. We consider the situation where a fraction ε of independently chosen nodes are insolvent:

$$\forall j,k,\ p(j,k,0)=\varepsilon. \tag{III.14}$$

We define, as in [114, Sec. 7.2.], the contagion threshold:

$$\xi = \max\{q \mid \text{for all } \varepsilon>0,\ \alpha_n(\mathbf{E_n},\gamma_\mathbf{n}) \xrightarrow{p} 1\}, \tag{III.15}$$

which assesses whether an arbitrarily small group can trigger the default of a fraction tending to 1 with high probability as the size of the network tends to infinity. Morris [114, Sec. 7.2] gives an upper bound for ξ in a given graph. The following result expresses ξ, in terms of π^*, for a heterogeneous random graph:

Corollary 4.6. *Under the assumptions of Theorem 3.8, and denoting by $\pi^*(q,\varepsilon)$ the smallest stable fixed point of function I under the conditions Equation (III.13) and (III.14). The contagion threshold is given by*

$$\xi = \lim_{\varepsilon \to 0} \max\{q \mid \pi^*(q,\varepsilon) = 1\}.$$

Note there that the "δ-uniformity condition" on the graph structure is replaced by the Assumption 3.1.

It is easy to see that this threshold can be also characterized qualitatively as in [114]. We say that a group is p-cohesive if every node in the group has at least proportion p of its out-neighbors within the group.

Proposition 4.7. *The contagion threshold ξ is the smallest q such that for any set $X_n = o(n)$, its complementary $\bar{X}_n$ contains an (1 - q) – cohesive subgroup, representing a positive fraction of all nodes.*

Remark 4.8. Proposition 4.7 follows immediately from the above result. Let us denote by X_n the initial set of defaults and suppose that nodes default when a proportion q of their counterparties default. The defaults triggered by X_n are the nodes belonging to the set $\mathcal{D}_f$. The complementary set $\bar{\mathcal{D}}_f$ is a $(1-q)$ cohesive group. Contagion is avoided if and only if this group represents a positive fraction of the network, i.e. if $\pi^* < 1$.

5 Contagion in finite networks

The results of Section 3 hold in the limit of large network size. In order to assess whether these results still hold for networks whose size is large but finite, we now compare our theoretical results with numerical simulations for networks with realistic sizes. In particular, we investigate the effect of heterogeneity in network structure and the relation between resilience and connectivity.

5.1 Relevance of asymptotics

Interbank networks in developed countries may contain several thousands of nodes. The Federal Deposit Insurance Corporation insured 7969 institutions as of 3/18/2010, while the European Central Bank reports 8350 monetary financial institutions in the Euro zone (80% credit institutions and 20% money market funds). To assess the relevance of asymptotic formulae for studying contagion in networks with such sizes, we generate a scale-free network of 10000 nodes with Pareto distributed exposures using the random graph model introduced by Blanchard [24], which can be seen as a static version of the preferential attachment model. In this model, given the sequence of out-degrees, an arbitrary out-going edge is assigned to an end-node i with probability proportional to the power $d_n^+(i)^\alpha$ where $\alpha > 0$. This leads to positive correlation between in-degrees and out-degrees.

The distribution of the out-degree in this model is a Pareto law with tail exponent γ^+:

$$\mu_n^+(j) := \#\{i \mid d_n^+(i) = j\} \overset{n\to\infty}{\to} \mu^+(j) \sim j^{\gamma^+ + 1}.$$

and the conditional limit law of the in-degree is a Poisson distribution

$$P(d^- = k | d^+ = j) = e^{-\lambda(j)} \frac{\lambda(j)^k}{k!},$$

with $\lambda(j) = \frac{j^\alpha \mathbb{E}(D^+)}{\mathbb{E}((D^+)^\alpha)}$, where D^+ denotes a random variable with law μ^+. The main theorem in [24] states that the marginal distribution of the in-degree has a Pareto tail with exponent $\gamma^- = \frac{\gamma^+}{\alpha}$, provided $1 \leq \alpha < \gamma^+$.

The distribution of this simulated network's degrees and exposures is given in Figure III.3 and is based on the empirical analysis of the Brazilian network in June 2007 [48]. On one hand

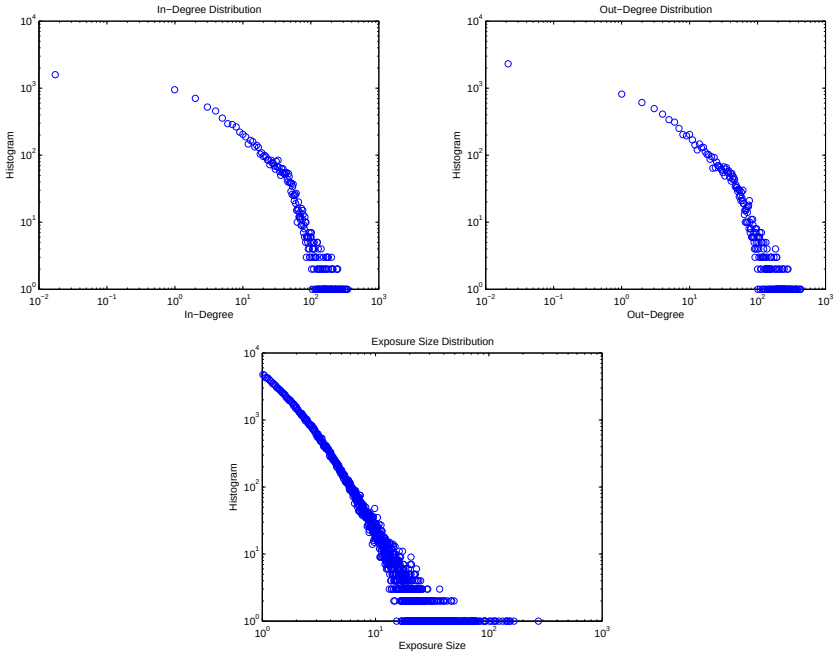

Figure III.3: (a) The distribution of out-degree has a Pareto tail with exponent 2.19, (b) The distribution of the in-degree has a Pareto tail with exponent 1.98, (c) The distribution of the exposures (tail-exponent 2.61).

we make a simulation of the default contagion starting with a random set of defaults representing 0.1% of all nodes (chosen uniformly among all nodes). On the other hand we plug the empirical distribution of the degrees and the fraction of contagious links into Equation (III.11) for the amplification of a small number of initial defaults. Figure III.4 plots these values for varying values of the minimal capital ratios. We find a good agreement between the theoretical and the simulated default amplification ratios. We can clearly see that for minimal capital ratios γ_{min} less than the critical value γ^*_{min}, the amplification ratio increases dramatically. Figure III.5 plots the simulated fraction of defaults in a scale free network, starting from the initial default

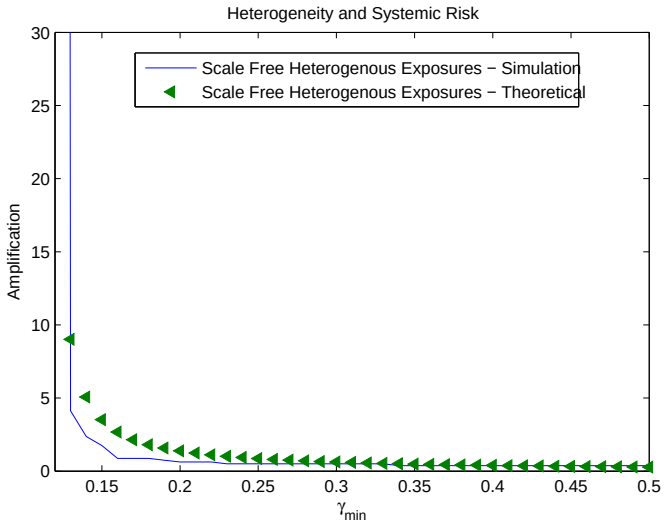

Figure III.4: Amplification of the number of defaults in a Scale-Free Network. The in and in-degree of the scale-free network are Pareto distributed with tail coefficients 2.19 and 1.98 respectively, the exposures are Pareto distributed with tail coefficient 2.61, $n = 10000$.

of a single node, as a function of the in-degree of the defaulting node, versus the theoretical slope given in Equation (III.12).

5.2 The impact of heterogeneity

In the examples of the previous section we can compute the minimal capital ratio γ^*_{min} such that the network is resilient under Condition (III.7). Two factors contribute to the sum in Condition (III.7), connectivity of the node, and its frailty. We compare, in Figure III.6, the ratio by which contagion amplifies the number of initial default in three cases: a scale free network with heterogeneous weights, a scale free network with equal weights (exposures) and a 'homogeneous' random network, the Erdös-Rényi random graphs, with equal weights. All three networks are parameterized to have the same average degree i.e. the same total number of links. It is interesting to note that the most heterogeneous network is also the least resilient, as opposed to the homogeneous Erdös–Rényi network with the same distribution of exposures.

5.3 Average connectivity and contagion

A recurrent question in the literature on financial networks is the impact of connectivity on resilience to contagion has [5, 19]. While Allen & Gale [5] find that resilience increases with connectivity, Battiston et al [19] exhibit different model settings where this relation is non-monotonous. An immediate conclusion of the Section 5.2 is that the average connectivity alone cannot be a good indicator of contagion or network stability. We can easily see this by considering a simple example and using the asymptotic formula (III.11).

Consider a network with equal exposures and $1/3 \leq \gamma_{min} < 1/2$ such that $p_n(j,k,\theta) = 1_{\{j\in 1,2\}}$. We first consider the case $\mu_n(1,3) = \mu_n(2,3) = \mu_n(6,3) = 1/3$. Then we consider two

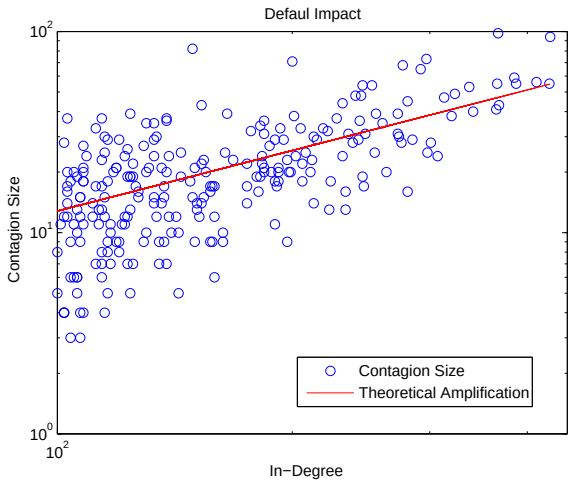

Figure III.5: Number of defaulted nodes

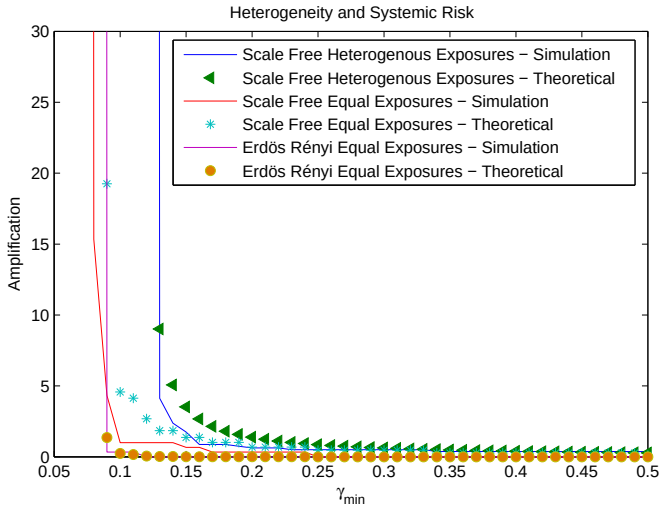

Figure III.6: Amplification of the number of defaults in a Scale-Free Network (in and in-degree of the scale-free network are Pareto distributed with tail coefficients 2.19 and 1.98 respectively, the exposures are Pareto distributed with tail coefficient 2.61), the same network with equal weights and an Erdös Rényi Network with equal exposures $n = 10000$.

more cases, defined by their respective degree distributions: $\tilde{\mu}_n(1,2) = 2/3, \tilde{\mu}_n(4,2) = 1/3$ and $\hat{\mu}_n(4,4) = 1$ (i.e. a regular graph with degree 4). In all three cases the network is resilient and we easily notice that in the case of the graph with degree distribution $\tilde{\mu}$ an increase of the resilience measure of the network is associated with a decrease in average connectivity while in the case of $\hat{\mu}$ it is associated with an increase in connectivity. Therefore, we observe that both the resilience measure and the magnitude of contagion do not depend on the average connectivity in a monotonous way. While in the case of [19] this non-monotonicity is obtained by introducing an ad-hoc mechanism of 'financial accelerators' introduced on top of the network contagion effects, in our case it stems from an intrinsic trade-off between risk-sharing and contagion which is inherent in the model.

These examples show that the resilience of a network cannot be simply assessed by examining an aggregate measure of connectivity such as the average degree or the number of links, as sometimes naively suggested in the literature, but requires a closer examination of features such as the distribution of degrees and the structure of the subgraph of contagious links.

6 Appendix: proofs

6.1 Coupling

We are given the set of nodes $[1,\dots,n]$ and their sequence of degrees $(\mathbf{d_n^+}, \mathbf{d_n^-})$. For each node i, we fix an indexing of its out-going and in-coming half-edges, ranging in $[1,\dots,d_n^+(i)]$ and $[1,\dots,d_n^-(i)]$ respectively. Furthermore, all out-going half-edges are given a global label in the range $[1,\dots,m_n]$, with m_n the total number of out-going (in-coming) half-edges. Similarly, all in-coming half-edges are given a global label in the range $[1,\dots,m_n]$.

For a set A, we denote by Σ_A the set of permutations of A. For the sequence of edge weights and capital ratios, $(\mathbf{e_n}, \gamma_\mathbf{n})$, we generate the random graph $\tilde{G}_n(\mathbf{e_n}, \gamma_\mathbf{n})$, by the following algorithm:

1. For each node i, choose a permutation $\tau_n(i) \in \Sigma_{H_n^+(i)}$ uniformly at random among all permutations of node i's out-going half edges.

2. Color all in-coming and out-going half-edges in black. Define the set of initially defaulted nodes
$$\mathcal{D}_0 := \bigcup_{i,\gamma_n(i)=0} \{i\}.$$
Set for all nodes in $[1,\dots,n]\backslash\mathcal{D}_0$, $c(i) = \gamma_n(i)\sum_{w\in W_n(i)} w$.

3. At step $k \geq 1$, if the set of in-coming black half-edges belonging to nodes in $\mathcal{D}_{k-1}$ is empty, denote $\mathcal{D}_f$ the set $\mathcal{D}_{k-1}$. Otherwise:

   (a) Choose among all in-coming black half-edges of the nodes in $\mathcal{D}_{k-1}$ the in-coming half-edge with the lowest global label and color it in red.

   (b) Choose a node i with probability proportional to its number of black out-going half-edges and set $\pi_n(k) = i$. Let i have $l-1$ out-going half-edges colored in red. Choose its $\tau_i(l)$-th out-going half-edge and color it in red. Let its weight be w. If the node $i \notin \mathcal{D}_{k-1}$ and $(1-R)w$ is larger than i's remaining capital then $\mathcal{D}_k = \mathcal{D}_{k-1}\bigcup\{i\}$. Otherwise, the capital of node i becomes $c(i) - (1-R)w$.

(c) Match node i's $\tau_i(l)$-th out-going half-edge to the in-coming half-edge selected at step (3a) to form an edge.

4. Choose a random uniform matching of the remaining out-going half-edges and match them to the remaining in-coming half-edges in increasing order and color them all in red.

Lemma 6.1. *The random graph $\tilde{G}_n(\mathbf{e_n}, \gamma_\mathbf{n})$ has the same distribution as $G^*_n(\mathbf{e_n})$. Furthermore the set $\mathcal{D}_f$ at the end of the above algorithm is the final set of defaulted nodes in the graph $\tilde{G}_n(\mathbf{e_n}, \gamma_\mathbf{n})$, endowed with capital ratios $\gamma_\mathbf{n}$.*

Proof. The second claim is trivial. Let us prove the first claim. We denote by σ_n^+ and σ_n^- the random permutations in $\Sigma_{[1,\dots,m_n]}$, representing the order in which the above algorithm selects the in-coming / out-going edges. At step k of the above construction, in-coming half-edge with global label $\sigma_n^-(k)$ is matched to out-going half-edge with global label $\sigma_n^+(k)$ to form an edge. The permutation σ_n^+ is determined by the set of permutations $(\tau_n(i))_{i=1,\dots,n}$ and the sequence π_n of size m_n, representing the sequence of nodes selected at Step (k-3b) of the algorithm (each node i appears in sequence π_n exactly $d_n^+(i)$ times). It is easy to see that σ_n^+ is a uniform permutation among all permutations in $\Sigma_{[1,\dots,m_n]}$, since $(\tau_n(i))_{i=1,\dots,n}$ are uniformly distributed and at each step of the algorithm we choose a node with probability proportional to its black out-going half-edges. On the other hand, the value of $\sigma_n^-(k)$ depends in a deterministic manner on

$$(\mathbf{e_n}, \gamma_\mathbf{n}, \sigma_n^+(1), \dots, \sigma_n^+(k-1)).$$

The out-going half-edge with global label j is matched with the in-coming half-edge with global label $(\sigma_n^- \circ (\sigma_n^+)^{-1})(j)$. In order to prove our claim it is enough to prove that the permutation $(\sigma_n^- \circ (\sigma_n^+)^{-1})$ is uniformly distributed among all permutations of m_n. Indeed, for an arbitrary permutation ξ belonging to the set $\Sigma_{[1,\dots,m_n]}$ we have that

$$\mathbb{P}\left(\sigma_n^+(j) = \xi^{-1}(\sigma_n^-(j)) \mid \sigma_n^+(1), \dots, \sigma_n^+(j-1)\ ,\ \sigma_n^+(k) = \xi^{-1}(\sigma_n^-(k)) \text{ for all } k < j\right) = \frac{1}{m_n - j + 1}.$$

Conditional on the knowledge of $(\sigma_n^+(1), \dots, \sigma_n^+(j-1))$, $\sigma_n^-(j)$ is deterministic. Also, by conditioning on $\forall k < j,\ \sigma_n^+(k) = \xi^{-1}(\sigma_n^-(k))$, then $\xi^{-1}(\sigma_n^-(j)) \in \mathcal{T} := [1, \dots, m] \backslash \{\sigma_n^+(1), \dots, \sigma_n^+(j-1)\}$, of cardinal $m_n - j + 1$. In the above algorithm, $\sigma_n^+(j)$ has uniform law over $\mathcal{T}$. Then the probability to choose $\xi^{-1}(\sigma_n^-(j))$ is $\frac{1}{m_n - j + 1}$.

By the law of iterated expectations, we obtain that

$$\mathbb{P}(\sigma_n^- \circ (\sigma_n^+)^{-1} = \xi) = \mathbb{P}(\sigma_n^+ = \xi^{-1} \circ \sigma_n^-) = \frac{1}{m_n!}.$$

This and the fact that the last step of the algorithm is a conditionally uniform match conclude the proof. □

We can find the final set of defaulted nodes $\mathcal{D}_f$ of the above algorithm in the following manner: once the permutation $\tau_n(i)$ is chosen, assign to each node its corresponding threshold $\theta_n(i) = \Theta(i, \mathbf{e_n}, \gamma_\mathbf{n}, \tau_n(i))$ as in Definition 3.2 and forget everything about $(\mathbf{e_n}, \gamma_\mathbf{n})$.

Definition 6.2. Denote by $\tilde{G}_n(\mathbf{d}_\mathbf{n}^+, \mathbf{d}_\mathbf{n}^-, \theta_\mathbf{n})$ the random graph resulting from Algorithm 6.1, in which we replace Step 3b of the algorithm by the fact that node i defaults the first time it has $\theta_n(i)$ out-going half-edges colored in red, i.e. at step $\inf\{k \geq 1, \text{ such that } \theta_n(i) = \#\{1 \leq l \leq k,\ \pi_n(l) = i\}\}$.

Corollary 6.3. *$\tilde{G}_n(\mathbf{d}_\mathbf{n}^+, \mathbf{d}_\mathbf{n}^-, \theta_\mathbf{n})$ has the same law as the unweighted skeleton of $\tilde{G}_n(\mathbf{e}_\mathbf{n}, \gamma_\mathbf{n})$.*

Let $N_n(j, k, \theta)$ denote the number of nodes with degree (j, k) and threshold θ after choosing uniformly the random permutations $\tau_\mathbf{n}$ in the above construction.

Lemma 6.4.

$$\frac{N_n(j,k,\theta)}{n} \underset{n\to\infty}{\overset{p}{\to}} \mu(j,k)p(j,k,\theta),$$

Proof. For any node i with with degree (j, k), the probability that its default threshold $\Theta(i, \mathbf{e}_\mathbf{n}, \gamma_\mathbf{n}, \tau_n(i))$, is equal to θ is

$$\nu_n(i,\theta) := \frac{\#\{\tau \in \Sigma(i)^\mathbf{e} \mid \Theta(i, \mathbf{e}_\mathbf{n}, \gamma_\mathbf{n}, \tau) = \theta\}}{j!}.$$

Then we have

$$N_n(j,k,\theta) = \sum_{i,\ d_n^+(i)=j,\ d_n^-(i)=k} Ber(\nu_n(i,\theta)),$$

where $Ber(\cdot)$ denotes a Bernoulli variable. By Assumption 3.4 we have

$$\mathbb{E}[N_n(j,k,\theta)/n] = \mu_n(j,k)p_n(j,k,\theta) \overset{n\to\infty}{\to} \mu(j,k)p(j,k,\theta),$$

$$\text{and} \qquad \mathrm{Var}[N_n(j,k,\theta)/n] = \frac{\sum_{i,\ d_n^+(i)=j,\ d_n^-(i)=k} \nu_n(i,\theta)(1-\nu_n(i,\theta))}{n^2} \overset{n\to\infty}{\to} 0.$$

Now it is easy to conclude the proof by Chebysev's inequality.

□

6.2 A Markov chain description of contagion dynamics

In the previous section, we have replaced the description based on default rounds given in section (2.2) by an equivalent one based on successive bilateral interactions. By **interaction** we mean coupling an in-coming edge with an out-going edge. At each step of Algorithm 6.1 we have one interaction only between two banks, yielding at most one default. This allows for a simpler Markov chain which leads to the the same set of final defaults.

We describe now the contagion process on the unweighted graph $\tilde{G}_n(\mathbf{d}_\mathbf{n}^+, \mathbf{d}_\mathbf{n}^-, \theta_\mathbf{n})$ with thresholds $(\theta_n(i) = \Theta(i, \mathbf{e}_\mathbf{n}, \gamma_\mathbf{n}), \tau_n(i))_{1\leq i\leq n}$ in terms of the dynamics of a Markov chain.

At each iteration we partition the nodes according to their state of solvency, degree, threshold and number of defaulted neighbors and define $S_n^{j,k,\theta,l}(t)$, the number of solvent banks with degree (j, k), default threshold θ and l defaulted debtors before time t. We introduce the additional variables of interest:

- $D_n^{j,k,\theta}(t)$, the number of defaulted banks at time t with degree (j, k) and default threshold θ,

- $D_n(t)$: the number of defaulted banks at time t,
- $D_n^-(t)$: the number of black in-coming edges belonging to defaulted banks,

for which it is easy to see that the following identities hold:

$$\begin{aligned} D_n^{j,k,\theta}(t) &= \mu_n(j,k)p_n(j,k,\theta) - \sum_{0\le l<\theta} S_n^{j,k,\theta,l}(t), \\ D_n^-(t) &= \sum_{j,k,0\le\theta\le j} kD_n^{j,k,\theta}(t) - t, \\ D_n(t) &= \sum_{j,k,0\le\theta\le j} D_n^{j,k,\theta}(t). \end{aligned}$$

Because at each step we color in red one out-going edge and the number of black out-going edges at time 0 is m_n, the number of black out-going edges at time t will be $m_n - t$ and we have

$$D_n^+(t) + S_n^+(t) = m_n - t.$$

By construction, $\mathbf{Y_n}(t) = \left(S_n^{j,k,\theta,l}(t)\right)_{j,k,0\le l<\theta\le j}$ represents a Markov chain. The iteration (3-k) of the cascade process 6.1 corresponds to the evolution of the Markov chain at date k.

Let $(\mathcal{F}_{n,t})_{t\ge 0}$ be its natural filtration. We define the operator $\wedge$ as

$$x \wedge y = \max(x, y).$$

The length of the default cascade is given by

$$T_n = \inf\{0 \le t \le m_n,\ D_n^-(t) = 0\} \wedge m_n, \tag{III.16}$$

The total number of defaults is $D_f := D_n(T_n)$.

Let us now descrive the transition probabilities of the Markov chain. For $t < T_n$, there are three possibilities for the partner B of an in-coming edge of a defaulted node A at time $t+1$:

1. B is in default, the next state is $\mathbf{Y_n}(t+1) = \mathbf{Y_n}(t)$.
2. B is solvent, has degree (j,k) and default threshold θ and this is the $(l+1)$-th deleted out-going edge and $l+1 < \theta$. The probability of this event is $\frac{(j-l)S_n^{j,k,\theta,l}(t)}{m_n - t}$. The changes for the next state will be

$$\begin{aligned} S_n^{j,k,\theta,l}(t+1) &= S_n^{j,k,\theta,l}(t) - 1, \\ S_n^{j,k,\theta,l+1}(t+1) &= S_n^{j,k,\theta,l+1}(t) + 1. \end{aligned}$$

3. B is solvent, has degree (j,k) and default threshold θ and this is the θ-th deleted out-going edge. Then with probability $\frac{(j-\theta+1)S_n^{j,k,\theta,\theta-1}(t)}{m_n - t}$ we have

$$S_n^{j,k,\theta,\theta-1}(t+1) = S_n^{j,k,\theta,\theta-1}(t) - 1.$$

Let Δ_t be the difference operator: $\Delta_t Y := Y(t+1) - Y(t)$. We obtain the following equations for the expectation of $\mathbf{Y_n}(t+1)$, conditional on $\mathcal{F}_{n,t}$, by averaging over the possible transitions:

$$\begin{aligned}\mathbb{E}\left[\Delta_t S_n^{j,k,\theta,0}|\mathcal{F}_{n,t}\right] &= -\frac{jS_n^{j,k,\theta,0}(t)}{m_n - t},\\ \mathbb{E}\left[\Delta_t S_n^{j,k,\theta,l}|\mathcal{F}_{n,t}\right] &= \frac{(j-l+1)S_n^{j,k,\theta,l-1}(t)}{m_n - t} - \frac{(j-l)S_n^{j,k,\theta,l}(t)}{m_n - t}. \end{aligned} \tag{III.17}$$

The initial condition is

$$S_n^{j,k,\theta,l}(0) = N_n(j,k,\theta)\mathbb{1}(l=0)\mathbb{1}(0<\theta\leq j).$$

Remark 6.5. We are interested in the value of D_f as defined in (III.16). In case $T_n < m_n$, the Markov chain can still be well defined for $t \in [T_n, m_n)$ by the same transition probabilities. However, after T_n it will no longer be related to the contagion process and the value $D^-(t)$, representing for $t \leq T_n$ the number of in-coming half-edges belonging to defaulted banks, becomes negative. We consider from now on that the above transition probabilities hold for $t < m_n$.

We will show in the next section that the trajectory of these variables for $t \leq T_n$ is close to the solution of the deterministic differential equations suggested by equations (III.17) with high probability (i.e. with probability tending to 1 as $n \to \infty$).

6.3 A law of large numbers for the contagion process

Define the following set of differential equations denoted by (DE):

$$\begin{aligned}(s^{j,k,\theta,0})'(\tau) &= -\frac{js^{j,k,\theta,0}(\tau)}{\lambda - \tau},\\ (s^{j,k,\theta,l})'(\tau) &= \frac{(j-l+1)s^{j,k,\theta,l-1}(\tau)}{\lambda-\tau} - \frac{(j-l)s^{j,k,\theta,l}(\tau)}{\lambda-\tau}, \qquad \text{(DE)},\end{aligned}$$

with initial conditions

$$s^{j,k,\theta,l}(0) = \mu(j,k)p(j,k,\theta)\mathbb{1}(l=0)\mathbb{1}(0<\theta\leq j).$$

Lemma 6.6. *The system of differential equations (*DE*) admits the unique solution*

$$y(\tau) := \left(s^{j,k,\theta,l}(\tau)\right)_{j,k,0\leq l<\theta\leq j},$$

in the interval $0 \leq \tau < \lambda$*, with*

$$s^{j,k,\theta,l}(\tau) := \mu(j,k)p(j,k,\theta)\binom{j}{l}(1-\frac{\tau}{\lambda})^{j-l}(\frac{\tau}{\lambda})^l\mathbb{1}_{\{0<\theta\leq j\}}. \tag{III.18}$$

Proof. We denote by DE^K the set of differential equations defined above, restricted to $j\wedge k < K$ and by $b(K)$ the dimension of the restricted system. Since the derivatives of the functions $\left(s^{j,k,\theta,l}(\tau)\right)_{j\wedge k<K,0\leq l<\theta\leq j}$ depend only on τ and the same functions, by a standard result in the theory of ordinary differential equations [88, Ch.2, Thm 11], there is an unique solution of DE^K in any domain of the type $(-\varepsilon,\lambda)\times R$, with R a bounded subdomain of $\mathbb{R}^{b(K)}$ and

$\varepsilon > 0$. The solution of (DE) is defined to be the set of functions solving all the finite systems $(DE^K)_{K\geq 1}$.

We solve now the system DE. Let $u = u(\tau) = -ln(\lambda - \tau)$. Then $u(0) = -ln(\lambda)$, u is strictly monotone and so is the inverse function $\tau = \tau(u)$. We write the system of differential equations (DE) with respect to u:

$$\begin{aligned}(s^{j,k,\theta,0})'(u) &= -js^{j,k,\theta,0}(u),\\ (s^{j,k,\theta,l})'(u) &= (j-l+1)s^{j,k,\theta,l-1}(u) - (j-l)s^{j,k,\theta,l}(u).\end{aligned}$$

Then we have

$$\frac{d}{du}(s^{j,k,\theta,l+1}e^{(j-l-1)(u-u(0))}) = (j-l)s^{j,k,\theta,l}(u)e^{(j-l-1)(u-u(0))},$$

and by induction, we find

$$s^{j,k,\theta,l}(u) = e^{-(j-l)(u-u(0))}\sum_{r=0}^{l}\binom{j-r}{l-r}\left(1-e^{-(u-u(0))}\right)^{l-r}s^{j,k,\theta,r}(u(0)).$$

By going back to τ, we have

$$s^{j,k,\theta,l}(\tau) = (1-\frac{\tau}{\lambda})^{j-l}\sum_{r=0}^{l}s^{j,k,\theta,r}(0)\binom{j-r}{l-r}(\frac{\tau}{\lambda})^{l-r}.$$

Then, by using the initial conditions, we find

$$s^{j,k,\theta,l}(\tau) = \mu(j,k)p(j,k,\theta)\binom{j}{l}(1-\frac{\tau}{\lambda})^{j-l}(\frac{\tau}{\lambda})^{l}\mathbb{1}_{\{\theta>0\}}.$$

□

A key idea is to approximate, following Wormald [134], the Markov chain by the solution of a system of differential equations in the large network limit [134, 113]. We summarize here the main result of [135].

For a set of variables $Y^1, ..., Y^b$ and for $U \subset \mathbb{R}^{b+1}$, define the stopping time $T_U = T_U(Y^1, ..., Y^b) = \inf\{t \geq 1, (t/n; Y^1(t)/n, ..., Y^b(t)/n) \notin U\}$.

Lemma 6.7 (Theorem 5.1. in [135]). *Let $b \geq 2$ be an integer and consider a sequence of real valued random variables $(\{Y_n^l(t)\}_{1\leq l\leq b})_{t\geq 0}$ and its natural filtration $\mathcal{F}_{n,t}$. Assume that there is a constant $C_0 > 0$ such that $|Y_n^l(t)| \leq C_0 n$ for all n, $t \geq 0$ and $1 \leq l \leq b$. For all $l \geq 1$ let $f_l : \mathbb{R}^{b+1} \to \mathbb{R}$ be functions and assume that for some bounded connected open set $U \subseteq \mathbb{R}^{b+1}$ containing the closure of*

$$\{(0, z_1, ..., z_b) : \exists\ n \text{ such that } \mathbb{P}(\forall\ 1 \leq l \leq b,\ Y_n^l(0) = z_l n) \neq 0\},$$

the following three conditions are verified:

1. (Boundedness). *For some function $\beta(n) \geq 1$ we have for all $t < T_U$*

$$\max_{1\leq l\leq b}|Y_n^l(t+1) - Y_n^l(t)| \leq \beta(n).$$

2. (Trend). *There exists* $\lambda_1(n) = o(1)$ *such that for* $1 \leq l \leq b$ *and* $t < T_U$

$$|\mathbb{E}[Y_n^l(t+1) - Y_n^l(t)|\mathcal{F}_{n,t}] - f_l(t/n, Y_n^1(t)/n, ..., Y_n^l(t)/n)| \leq \lambda_1(n).$$

3. (Lipschitz). *The functions* $(f_l)_{1\leq l\leq b}$ *are Lipschitz-continuous on* U.

Then the following conclusions hold:

(a) *For* $(0, \hat{z}_1, ..., \hat{z}_b) \in U$, *the system of differential equations*

$$\frac{dz_l}{ds} = f_l(s, z_1, ..., z_l), \quad l = 1, ..., b,$$

has a unique solution in U, $z_l : \mathbb{R} \to \mathbb{R}$, *which passes through* $z_l(0) = \hat{z}_l$, *for* $l = 1, \ldots, b$, *and which extends to points arbitrarily close to the boundary of* U.

(b) *Let* $\lambda > \lambda_1(n)$ *with* $\lambda = o(1)$. *For a sufficiently large constant* C, *with probability* $1 - O\left(\frac{b\beta(n)}{\lambda}\exp\left(-\frac{n\lambda^3}{\beta(n)^3}\right)\right)$, *we have*

$$\sup_{0\leq t\leq\sigma(n)n} (Y_n^l(t) - nz_n^l(t/n)) = O(\lambda n),$$

where $\mathbf{z}_n(t) = (z_n^1(t), \ldots, z_n^b(t))$ *is the solution of*

$$\frac{d\mathbf{z}_n}{dt} = f(t, \mathbf{z}_n(t)) \qquad z_n(0) = \mathbf{Y}_n(0)/n$$

$$\text{and} \qquad \sigma(n) = \sup\{t \geq 0, \quad d_\infty(\mathbf{z}_n(t), \partial U) \geq C\lambda\}.$$

We apply this lemma to the contagion model described in Section 6.2. Let us define, for $0 \leq \tau \leq \lambda$

$$\begin{aligned}
\delta^{j,k,\theta}(\tau) &:= \mu(j,k)p(j,k,\theta) - \sum_{0\leq l<\theta} s^{j,k,\theta,l}(\tau), \\
\delta^-(\tau) &:= \sum_{j,k,\theta} k\delta^{j,k,\theta}(\tau) - \tau, \quad \text{and} \\
\delta(\tau) &:= \sum_{j,k,\theta} \delta^{j,k,\theta}(\tau),
\end{aligned}$$

with $s^{j,k,\theta,l}$ given in Lemma 6.6. With $\text{Bin}(j,\pi)$ denoting a binomial variable with parameters j and π, we have

$$\delta^{j,k,\theta}(\tau) = \mu(j,k)p(j,k,\theta)\mathbb{P}\left(\text{Bin}(j, \frac{\tau}{\lambda}) \geq \theta\right), \tag{III.19}$$

$$\begin{aligned}
\delta^-(\tau) &= \sum_{j,k,\theta} k\delta^{j,k,\theta}(\tau) - \tau \\
&= \sum_{j,k,\theta\leq j} k\mu(j,k)p(j,k,\theta)\mathbb{P}\left(\text{Bin}(j, \frac{\tau}{\lambda}) \geq \theta\right) - \tau \qquad \text{(III.20)} \\
&= \lambda(I(\frac{\tau}{\lambda}) - \frac{\tau}{\lambda}),
\end{aligned}$$

and

$$\delta(\tau) := \sum_{j,k,0\leq\theta\leq j} \mu(j,k)p(j,k,\theta)\mathbb{P}\left(\text{Bin}(j, \frac{\tau}{\lambda}) \geq \theta\right). \tag{III.21}$$

6.4 Proof of Theorem 3.8

We now proceed to the proof of Theorem 3.8 whose aim is to approximate the value $D_n(T_n)/n$ as $n \to \infty$. We base the proof on Theorem 6.7. However, several difficulties arise since in our case the number of variables depends on n. We first need to bound the contribution of higher order terms in the infinite sums (III.20) and (III.21). Fix $\varepsilon > 0$. By Condition 3.1, we know

$$\lambda = \sum_{j,k} k\mu(j,k) = \sum_{j,k} j\mu(j,k) \in (0,\infty).$$

Then, there exists an integer K_ε, such that

$$\sum_{k \geq K_\varepsilon} \sum_{j} k\mu(j,k) + \sum_{j \geq K_\varepsilon} \sum_{k} j\mu(j,k) < \varepsilon,$$

which implies that

$$\sum_{j \wedge k \geq K_\varepsilon} k\mu(j,k) < \varepsilon.$$

It follows that

$$\forall\ 0 \leq \tau \leq \lambda, \sum_{j \wedge k \geq K_\varepsilon, 0 \leq \theta \leq j} k\mu(j,k)p(j,k,\theta)\mathbb{P}\left(\mathrm{Bin}(j, \frac{\tau}{\lambda}) \geq \theta\right) < \varepsilon. \tag{III.22}$$

The number of vertices with degree (j,k) is $n\mu_n(j,k)$. Again, by Condition 3.1,

$$\sum_{j,k} k\mu_n(j,k) = \sum_{j,k} j\mu_n(j,k) \to \lambda \in (0,\infty).$$

Therefore, for n large enough, $\sum_{j \wedge k \geq K_\varepsilon} k\mu_n(j,k) < \varepsilon$, and

$$\forall\ 0 \leq t \leq m_n, \sum_{j \wedge k \geq K_\varepsilon, 0 \leq \theta \leq j} kD^{j,k,\theta}(t)/n < \varepsilon. \tag{III.23}$$

For $K \geq 1$, we denote

$$\mathbf{y}^K := \left(s^{j,k,\theta,l}(\tau)\right)_{j \wedge k < K,\ 0 \leq l < \theta \leq j} \text{ and}$$
$$Y_n^K := \left(S_n^{j,k,\theta,l}(\tau)\right)_{j \wedge k < K,\ 0 \leq l < \theta \leq j},$$

both of dimension $b(K)$, where $\delta^{j,k,\theta}(\tau), s^{j,k,\theta,l}(\tau)$ are solutions to a system (DE) of ordinary differential equations. Let

$$\pi^* = \min\{\pi \in [0,1] | I(\pi) = \pi\}.$$

For the arbitrary constant $\varepsilon > 0$ we fixed above, we define the domain U_ε as

$$U_\varepsilon = \{\left(\tau, y^{K_\varepsilon}\right) \in \mathbb{R}^{b(K_\varepsilon)+1}\ :\ -\varepsilon < \tau < \lambda - \varepsilon\ ,\ -\varepsilon < s^{j,k,\theta,l} < 1\}. \tag{III.24}$$

The domain U_ε is a bounded open set which contains the support of all initial values of the variables. Each variable is bounded by a constant times n ($C_0 = 1$). By the definition of our process, the Boundedness condition is satisfied with $\beta(n) = 1$. The second condition of the theorem is satisfied by some $\lambda_1(n) = O(1/n)$. Finally the Lipschitz property is also satisfied since $\lambda - \tau$ is bounded away from zero. Then by Lemma 6.7 and by using Lemma 6.4 for convergence of initial conditions, we have :

Corollary 6.8. *For a sufficiently large constant C, we have*

$$\mathbb{P}(\forall t \leq n\sigma_C(n), \mathbf{Y}_n^{K_\varepsilon}(t) = n\mathbf{y}^{K_\varepsilon}(t/n) + O(n^{3/4})) = 1 - O(b(K_\varepsilon)n^{-1/4}exp(-n^{-1/4})) \quad \text{(III.25)}$$

uniformly for all $t \leq n\sigma_C(n)$ where

$$\sigma_C(n) = \sup\{\tau \geq 0, d(\mathbf{y}^{K_\varepsilon}(\tau), \partial U_\varepsilon\ ) \geq Cn^{-1/4}\}.$$

When the solution reaches the boundary of U_ε, it violates the first constraint in III.24, determined by $\hat{\tau} = \lambda - \varepsilon$. By convergence of $\frac{m_n}{n}$ to λ, there is a value n_0 such that $\forall n \geq n_0$, $\frac{m_n}{n} > \lambda - \varepsilon$, which ensures that $\hat{\tau}n \leq m_n$. Using (III.22) and (III.23), we have, for $0 \leq t \leq n\hat{\tau}$ and $n \geq n_0$:

$$\begin{aligned}
\left|D_n^-(t)/n - \delta^-(t/n)\right| &= |\sum_{j,k}\sum_{\theta\leq j} k(D_n^{j,k,\theta}(t)/n - \delta^{j,k,\theta}(t/n))| \\
&\leq \sum_{j,k}\sum_{\theta\leq j} k\left|D_n^{j,k,\theta}(t)/n - \delta^{j,k,\theta}(t/n)\right| \\
&\leq \sum_{j\wedge k\leq K_\varepsilon}\sum_{\theta\leq j} k\left|D_n^{j,k,\theta}(t)/n - \delta^{j,k,\theta}(t/n)\right| + 2\varepsilon, \qquad \text{(III.26)}
\end{aligned}$$

and

$$|D_n(t)/n - \delta(t/n)| \leq \sum_{j\wedge k\leq K_\varepsilon}\sum_{\theta\leq j}\left|D_n^{j,k,\theta}(t)/n - \delta^{j,k,\theta}(t/n)\right| + 2\varepsilon, \qquad \text{(III.27)}$$

We obtain by Corollary 6.8 that

$$\sup_{t\leq\hat{\tau}n}\left|D_n^-(t)/n - \delta^-(t/n)\right| \leq 2\varepsilon + o_p(1) \qquad \text{(III.28)}$$

$$\sup_{t\leq\hat{\tau}n}|D_n(t)/n - \delta(t/n)| \leq 2\varepsilon + o_p(1) \qquad \text{(III.29)}$$

We nw study the stopping time T_n and the size of the default cascade D_f defined in (III.16). First assume $I(\pi) > \pi$ for all $\pi \in [0, 1)$, i.e., $\pi^* = 1$. Then we have

$$\forall\tau < \hat{\tau}, \delta^-(\tau) = \sum_{j,k,\theta} k\delta^{j,k,\theta}(\tau) - \tau > 0.$$

We have then that $T_n/n = \hat{\tau} + O(\varepsilon) + o_p(1)$ and from convergence (III.29), since $\delta(\hat{\tau}) = 1 - O(\varepsilon)$, we obtain by tending ε to 0 that $|D_n(T_n)| = n - o_p(n)$. This proves the first part of the theorem.

Now consider the case $\pi^* < 1$, and furthermore π^* is a stable fixed point of $I(\pi)$. Then by definition of π^* and by using the fact that $I(1) \leq 1$, we have $I(\pi) < \pi$ for some interval $(\pi^*, \pi^* + \tilde{\pi})$. Then $\delta^-(\tau)$ is negative in an interval $(\tau^*, \tau^* + \tilde{\tau})$, with $\tau^* = \lambda\pi^*$.

Let ε such that $2\varepsilon < -\inf_{\tau\in(\tau^*,\tau^*+\tilde{\tau})}\delta^-(\tau)$ and denote $\hat{\sigma}$ the first iteration at which it reaches the minimum. Since $\delta^-(\hat{\sigma}) < -2\varepsilon$ it follows that with high probability $D^-(\hat{\sigma}n)/n < 0$, so $T_n/n = \tau^* + O(\varepsilon) + o_p(1)$. The conclusion follows by taking the limit $\varepsilon \to 0$.

6.5 Proof of Theorem 4.3

Strong connectivity sparse random directed graphs with prescribed degree sequence has been studied by Cooper and Frieze in [52]. Let λ_n represent the average degree (then by Condition 3.1, $\lambda_n \to \lambda$ as $n \to \infty$), and $\mu_n(j,k)$ represent the empirical distribution of the degrees, assumed to be proper (as defined below), then [52, Theorem 1.2] states that if

$$\sum_{j,k} jk \frac{\mu(j,k)}{\lambda} > 1, \tag{III.30}$$

then the graph contains w.h.p. a strongly connected giant component.

We remark that the theorem above is given in [52] under stronger assumptions on the degree sequence, adding to Assumption 3.1 the following three conditions, in which Δ_n denotes the maximum degree:

- Let $\rho_n = \max(\sum_{i,j} \frac{i^2 j \mu_n(i,j)}{\lambda_n}, \sum_{i,j} \frac{j^2 i \mu_n(i,j)}{\lambda_n})$. If $\Delta_n \to \infty$ with n then $\rho_n = o(\Delta_n)$.
- $\Delta_n \leq \frac{n^{1/12}}{\log n}$.
- As $n \to \infty$, $\nu_n \to \nu \in (0, \infty)$.

Following [52] we call a degree sequence proper if it satisfies Assumption 3.1 together with the above conditions.

A first reason for adding these conditions in [52] is to ensure that Equation (III.1) holds. However, following Janson [93], the restricted set of conditions 3.1 is sufficient. The second reason is that [52] gives a more precise results on the structure of the giant component. For our purpose, to find the sufficient condition for the existence of strongly connected giant component, we show that these supplementary conditions may be dropped.

It is easy to see that a bounded degree sequence (i.e., $\Delta_n = O(1)$) which satisfies Assumption 3.1 is proper. We use this fact in the following.

Lemma 6.9. *Consider the random directed graph $G_n^*(\mathbf{d}_\mathbf{n}^-, \mathbf{d}_\mathbf{n}^+, \mathbf{E}_\mathbf{n})$, where the degree sequence satisfies Assumption 3.1. If*

$$\sum_{j,k} jk \frac{\mu(j,k)}{\lambda} > 1, \tag{III.31}$$

then with high probability the graph contains a strongly connected giant component.

Proof. By the second moment property and Fatou's lemma, there exists a constant C such that

$$\begin{aligned} \sum_{j,k} jk\mu(j,k) &\leq \sum_{j,k} (j^2 + k^2)\mu(j,k) \\ &\leq \liminf_{n\to\infty} \sum_{j,k} (j^2 + k^2)\mu_n(j,k) \leq C. \end{aligned}$$

Then, it follows that for arbitrary $\varepsilon > 0$, there exists a constant Δ_ε such that

$$\sum_{j \wedge k > \Delta_\varepsilon} jk\mu(j,k) \leq \varepsilon.$$

Thus, by choosing ε small enough, there exists a constant Δ_ε such that

$$\sum_{j\wedge k\leq \Delta_\varepsilon} jk\frac{\mu(j,k)}{\lambda} > 1.$$

We now modify the graph such that the maximum degree is equal to Δ_ε: for every node i such that $d_n^+(i)\wedge d_n^-(i) > \Delta_\varepsilon$, all its in-coming (resp. out-going) half-edges are transferred to new nodes with degree $(0,1)$ (resp. with degree $(1,0)$). Since these newly created nodes cannot be part of any strongly connected component, it follows that, if the modified graph contains such a component, then necessarily the initial graph also does. It is then enough to evaluate Equation (III.30) for this modified graph, which by construction verifies the Assumption 3.1 for the new empirical distribution $\tilde{\mu}$ with the average degree $\tilde{\lambda}$. Also, since the degrees of the modified graph are bounded, the supplementary conditions above also hold, i.e., the degree sequence is proper, and we can apply Cooper & Frieze's result. It only remains to show that $\sum_{j,k} jk\frac{\tilde{\mu}(j,k)}{\tilde{\lambda}} > 1$. Indeed, we have

$$\begin{aligned}\sum_{j,k} jk\frac{\tilde{\mu}(j,k)}{\tilde{\lambda}} &= \sum_{j\wedge k\leq \Delta_\varepsilon} jk\frac{\tilde{\mu}(j,k)}{\tilde{\lambda}}\\ &= \sum_{0<j,k\leq \Delta_\varepsilon} jk\frac{\tilde{\mu}(j,k)}{\tilde{\lambda}}\\ &= \sum_{0<j,k\leq \Delta_\varepsilon} jk\frac{\mu(j,k)}{\lambda} > 1.\end{aligned}$$

The last equality follows from the fact that for $0 < j,k \leq \Delta_\varepsilon$, we have

$$\frac{\tilde{\mu}(j,k)}{\tilde{\lambda}} = \frac{\mu(j,k)}{\lambda}.$$

This is true since the total number of edges, and the number of nodes with degree j,k for $0 < j,k \leq \Delta_\varepsilon$, stays unmodified.

□

We now proceed to the proof of Theorem 4.3. Our proof is based on ideas applied in [74, 92] for site and bond percolation in configuration model. Our aim is to show that the skeleton of contagious links in the random financial network is still described by configuration model, with a degree sequence verifying Assumptions 3.1, and then apply Lemma 6.9.

For each node i, the set of contagious out-going edges is given by

$$C_n(i) := \{l \mid (1-R)e_n(i,l) > \gamma_n(i)\}.$$

Let us denote their number by

$$c_n^+(i) := \#C_n(i).$$

We denote by G_n^c the unweighted skeleton of contagious links in the random network $G_n^*(\mathbf{e_n})$, endowed with the capital ratios $\gamma_\mathbf{n}$.

In order to characterize the law of G_n^c, we adapt Janson's method [92] for the directed case.

Lemma 6.10. *The unweighted skeleton of contagious links G_n^c has the same law as the random graph constructed as follows:*

1. *Replace the degree sequence* $(\mathbf{d}_\mathbf{n}^+, \mathbf{d}_\mathbf{n}^-)$ *of size* n *by the degree sequence* $(\tilde{\mathbf{d}}_{\mathbf{n}'}^+, \tilde{\mathbf{d}}_{\mathbf{n}'}^-)$ *of size* n'*, with*

$$\begin{aligned} n' &= n + m_n - \sum_{i=1}^{n} c_n^+(i), \\ \forall\ 1 \le i \le n,\ \tilde{d}_{n'}^+(i) &= c_n^+(i),\ \tilde{d}_{n'}^-(i) = d_n^-(i), \\ \forall\ n+1 \le i \le n',\ \tilde{d}_{n'}^+(i) &= 1,\ \tilde{d}_{n'}^+(i) = 0. \end{aligned}$$

2. *Construct the random unweighted graph* $G_{n'}^*(\tilde{\mathbf{d}}_{\mathbf{n}'}^+, \tilde{\mathbf{d}}_{\mathbf{n}'}^-)$ *with* n' *nodes, and the degree sequence* $(\tilde{\mathbf{d}}_{\mathbf{n}'}^+, \tilde{\mathbf{d}}_{\mathbf{n}'}^-)$ *by configuration model.*

3. *Delete* $n^+ = n' - n$ *randomly chosen nodes with out-degree* 1 *and in-degree* 0*.*

Proof. The skeleton G_n^c can be obtained in a two-step procedure. First, disconnect all non-contagious links in $G_n^*(\mathbf{e}_\mathbf{n})$ from their end nodes and transfer them to newly created nodes of degree $(1,0)$. Then delete all new nodes and their incident edges. Looking at graphs as configurations, and since the first step changes the total number of nodes but not the number of half-edges, it is easy to see that there is a one to one correspondence between the configurations before and after the 'rewiring'. Thus, the graph after rewiring is still described by the configuration model, and has the same law as $G_{n'}^*(\tilde{\mathbf{d}}_{\mathbf{n}'}^+, \tilde{\mathbf{d}}_{\mathbf{n}'}^-)$. Finally, by symmetry, the nodes with out-degree 1 and in-degree 0 are equivalent, so one may remove randomly the appropriate number of them. □

Note that since the degree sequence before rewiring verifies Condition 3.1, so does the degree sequence after rewiring. Moreover, since we are interested in the strongly connected component and nodes of degrees $(1,0)$ will not be included, we can actually apply Lemma 6.9 to the random graph resulting by the above contagion process. Hence, we may study the strongly connected component in the intermediate graph $G_{n'}^*(\tilde{\mathbf{d}}_{\mathbf{n}'}^+, \tilde{\mathbf{d}}_{\mathbf{n}'}^-)$.

Let us denote by $l_{n'}(j,k)$, the number of nodes with out-degree j and in-degree k in the graph $G_{n'}^*(\tilde{\mathbf{d}}_{\mathbf{n}'}^+, \tilde{\mathbf{d}}_{\mathbf{n}'}^-)$, and by $\tilde{\lambda}_{n'}$, the average degree. Then the average directed degree in this random graph is given by $\nu_n := \sum_{j,k} jk l_{n'}(j,k)/(\tilde{\lambda}_{n'} n')$.

We first observe that $\tilde{\lambda}_{n'} n' = \lambda n$, since the number of edges is unchanged after rewiring of the links. For every $k > 0$, the quantity $\sum_j j l_{n'}(j,k)$ represents the number of out-going edges belonging to nodes with in-degree k in the graph after rewiring, which in turn represents the number of contagious out-going edges belonging to nodes with in-degree k in the graph before rewiring. But so does $\sum_j p_n(j,k,1) n \mu_n(j,k) j$. So, for all k

$$\begin{aligned} \sum_j j \frac{l_{n'}(j,k)}{\lambda_{n'} n'} &= \frac{1}{\lambda_{n'} n'} \sum_j p_n(j,k,1) n \mu_n(j,k) j \\ &= \sum_j j p_n(j,k,1) \frac{\mu_n(j,k)}{\lambda_n} \\ &\overset{n\to\infty}{\to} \sum_j j p(j,k,1) \frac{\mu(j,k)}{\lambda}, \end{aligned}$$

where convergence holds by the second moment property in Assumption 3.1. Applying Lemma 6.9 to the sequence of degrees in the graph after rewiring shows that when

$$\sum_k k \lim_n \sum_j j \frac{l_{n'}(j,k)}{\lambda_{n'} n'} = \sum_k \sum_j j p(j,k,1) \frac{\mu(j,k)}{\lambda} > 1,$$

then with high probability there exists a giant strongly connected component in the skeleton of contagious links.

Chapter IV

Stress Testing the Resilience of Financial Networks

We propose a framework for stress testing the resilience of a financial network to external shocks affecting balance sheets. Whereas previous studies of contagion effects in financial networks have relied on large scale simulations, our approach uses a simple analytical criterion for resilience to contagion, based on an asymptotic analysis of default cascades in heterogeneous networks. In particular, our methodology does not require to observe the whole network but focuses on the characteristics of the network which contribute to its resilience. Applying this framework to a sample network, we observe that the size of the default cascade generated by a macroeconomic shock across balance sheets may exhibit a sharp transition when the magnitude of the shock reaches a certain threshold: beyond this threshold, contagion spreads to a large fraction of the financial system. An upper bound is given for the threshold in terms of the characteristics of the network. ***Keywords: systemic risk; random graphs; stress test; default risk; macroprudential regulation.*** *This work has appeared as "Hamed Amini, Rama Cont and Andreea Minca, Stress testing the resilience of financial networks, International Journal of Theoretical and Applied Finance" (2011) [9].*

Contents

1 Introduction

In the Supervisory Capital Assessment Program, implemented by the Board of Governors of the Federal Reserve System in 2009 [121], the 19 largest US banks were asked to project their losses and resources under various macroeconomic shock scenarios. The program determined which of the large banks needed to augment its capital base in order to withstand the projected losses. Although underlying this stress test was the concern that the failure of these large banks might generate contagion in the US financial system, contagion effects were not directly taken

into account when designing the stress tests nor in evaluating the magnitude of losses in the stress scenarios.

Various models for default contagion in banking systems have been proposed in the recent literature, in the framework of *network* models. In this approach, a banking system is modeled as a weighted directed graph in which nodes represent the financial institutions and edges represent exposures between institutions [66, 68]. The fundamental default of certain banks propagates to their counterparties as these write down from their capital the exposures to the defaulted banks [8, 48].

The literature contains many simulation-based studies of contagion in banking networks conducted using central bank data – examples include Elsinger et al. [68] for Austria, Cont et al. [48] for Brazil, Upper [132] for Germany – as well as similar studies on simulated networks [47, 120]. The conclusions regarding the magnitude of contagion differ across studies, as network topology and regulatory limits, differ from one country to another, but the complexity of the models involved prevent simple insights into the influence of different network characteristics on the results. For the Austrian network, the authors find that among the sources of systemic risk, the direct effect of correlation in the external shocks is far more important than direct contagion effects, which are only secondary. In their case contagious defaults occur only in scenarios where a large number of fundamental defaults occur. In the German network, on the contrary, the default of a single bank can wipe out a significant fraction of the system, so contagion risk is by no means secondary [132].

These studies suggest that some networks are intrinsically fragile and the default of a single bank may trigger a large cascade, whereas other networks might be more resilient to contagion. This intuition is supported by theoretical results on the resilience of networks to contagion [8], and the aim of this work is to integrate such theoretical insights into the stress testing framework, thus shedding some light on the results of such stress tests.

We propose in this work a simple framework for stress-testing the resilience to contagion in a financial network under macroeconomic shocks. Instead of relying on computationally intensive simulations, our approach relies on analytical insights obtained from the asymptotic analysis of the magnitude of default contagion in large networks [8]. Based on the asymptotic analysis of [8], we propose a measure of resilience to contagion, which involves the connectivity of nodes and the proportion of 'contagious' links in the network and use it to assess the resilience of the network under macroeconomic shocks. In particular, our methodology does not require to observe the whole network but focuses on the characteristics of the network which contribute to its resilience. Applying this framework to a sample network, we observe that the size of the default cascade generated by a macroeconomic shock across balance sheets may exhibit a sharp transition when the magnitude of the shock reaches a certain threshold: beyond this threshold, contagion spreads to a large fraction of the financial system. An upper bound is given for the threshold in terms of the characteristics of the network. As the resilience measure is a decreasing function of each bank's connectivity and fraction of contagious links, it can be used for monitoring/regulating the financial institutions that pose the highest systemic risk.

The paper is organized as follows. Section 2 presents some new results on the size of the default cascade generated by a single node. Section 3 presents a stress testing framework for analyzing the resilience of a network to macroeconomic shocks and discusses two examples: a random infinite network (Subsection 3.2) and a scale-free network whose size is comparable to existing banking networks (Subsection 3.3).

2 Size of default cascade

We now consider the structure of the skeleton of contagious links. Define the *susceptibility* of a random financial network

$$\chi(\mathbf{E_n}, \gamma_\mathbf{n}) := \frac{1}{n} \sum_{v \in [1,\ldots,n]} |C(v)|, \tag{IV.1}$$

with $C(v)$ the default cluster of v containing all nodes from which v is reachable by a directed path of contagious links.

The skeleton of contagious links is the subgraph obtained by retaining only the contagious links in the initial network. Thus, if we consider the new degree sequence for this subgraph, it is still a random graph chosen uniformly from all graphs with this degree sequence [8], so we can still apply asymptotic results for the random configuration model [26, 94]. In particular, Janson [94] shows that the susceptibility of the random graph with given vertex degrees converges under mild conditions to the expected cluster size in the corresponding branching process, which may be defined as a Galton-Watson branching process with initial offspring ξ_0 and general offspring ξ. We define

$$\tilde{\lambda} := \sum_{j,k} j\mu(j,k)p(j,k,1),$$

the average number of contagious links and note that the fraction of contagious links is $T := \frac{\tilde{\lambda}}{\lambda}$. The generating function of the initial offspring ξ_0 is

$$G_0(y) = \sum_{k_0, j, k \geq k_0} \mu(j,k) \binom{k}{k_0} (1-T)^{k-k_0} T^{k_0} y^{k_0} = \sum_{j,k} \mu(j,k)(1-T+Ty)^k,$$

while the generating function of the general offspring is

$$G(y) = \sum_{j,k} \frac{j\mu(j,k)p(j,k,1)}{\tilde{\lambda}} (1-T+Ty)^k.$$

It is easy to see that G_0 represents the generating function of the number of links pointing into a randomly chosen node after bond percolation with probability T (each incoming edge is removed with probability $1-T$ independently of all other incoming edges). In terms of our network model, G represents the generating function of the number of contagious links ending in a node which is start of a randomly chosen contagious link. The probability that such a node has degree (j,k) is given by a weighted version of μ: $\frac{j\mu(j,k)p(j,k,1)}{\tilde{\lambda}}$. We have that

$$\mathbb{E}(\xi) = G'(1) = \sum_{j,k} \frac{j\mu(j,k)p(j,k,1)}{\tilde{\lambda}} kT = \sum_{j,k} \frac{jk\mu(j,k)}{\lambda} p(j,k,1),$$

and

$$\mathbb{E}(\xi_0) = G_0'(1) = \sum_{j,k} k\mu(j,k)T = \tilde{\lambda}$$

For a branching process with initial offspring ξ_0 and general offspring ξ, its susceptibility is given by $1 + \frac{\mathbb{E}\xi_0}{(1-\mathbb{E}\xi)_+}$ (see [94, Theorem 3.1], [119]). By virtue of [94, Theorem 3.3] applied to the skeleton of contagious links, under Conditions 3.1 and 3.4, the average cascade size converges in probability (and in fact in L^1, in the subcritical case when $\mathbb{E}(\xi) < 1$) to the susceptibility of the corresponding branching process. We have:

- If the resilience measure is strictly positive,

$$\chi(\mathbf{E_n}, \gamma_\mathbf{n}) \xrightarrow{L^1} \chi_\infty := 1 + \frac{\sum_{j,k} j\mu(j,k)p(j,k,1)}{1 - \sum_{j,k} \frac{jk}{\lambda}\mu(j,k)p(j,k,1)}.$$

- If the resilience measure is zero or negative,

$$\chi(\mathbf{E_n}, \gamma_\mathbf{n}) \xrightarrow{p} \infty.$$

We show thus by a different method that the positivity of the resilience measure is a necessary condition for the non-occurrence of global cascades: this condition is equivalent to the non-explosion of the branching process associated to the skeleton of contagious links

$$\mathbb{E}(\xi) < 1.$$

The full distribution of the size of the default cluster can be computed once the generating functions G_0 and G are known (see Bertoin and Sidoravicius [22, Theorem 1] which connects the structure of clusters in random graphs with prescribed degree distributions to branching processes and Newman et al. [119] for the derivation in case of branching processes). We define the generating function H of the size of the default cluster generated by a randomly chosen contagious edge, which verifies the condition $H(y) = yG(H(y))$. The generating function H_0 of the size of a default cluster is then given by $H_0(y) = yG_0(H(y))$. If the resilience measure is negative, then the probability of a large scale epidemic triggered by a single node is equal to the explosion probability of the branching process. If we let y^* be the smallest solution of

$$y = \sum_{j,k} \frac{j\mu(j,k)p(j,k,1)}{\tilde{\lambda}}(1 - T + Ty)^k,$$

then the probability of a global cascade is given by

$$1 - \sum_{j,k} \mu(j,k)(1 - T + Ty^*)^k.$$

This last formula confirms the observations in Gleeson [80] that the probability of occurrence of a global cascade strongly depends on the out-degree distribution even when the average cascade size does not, such as in cases where the degree distribution factorizes and the fraction of contagious links does not depend on the out-degrees.

3 Stress testing

The analytical results presented above may be used to investigate the resilience of a financial network in a stress scenario, without the need for large scale simulation of default cascades. The idea is simply to apply shocks to balance sheets and to compute the impact of these shocks on the resilience measure (Definition (4.1)). Interestingly, it is observed that the final fraction of defaults generated by a fraction ε of fundamental defaults undergoes a sharp transition when the size of the shocks exceed a certain threshold.

We explain how such a stress test may be done and apply the stress test to two example of networks: an infinite random network, and a finite scale-free network whose properties mimic the empirical properties of banking networks [28, 48].

3.1 Stress testing resilience to macroeconomic shocks

Consider a banking system in which the ratio $\gamma(i)$ of each bank's capital to its total assets is restricted to be greater than a minimal capital ratio: $\gamma(i) \geq \gamma_{\min}$. If the ratio of institution i's interbank assets to its total assets is denoted by LR_i, then

$$c_i = \gamma_i A_i \frac{1}{LR_i} > 0. \tag{IV.2}$$

In a stress testing framework, we consider scenarios in which a given shock is applied to balance sheets of banks, resulting in the loss of a fraction $0 \leq S \leq 1$ of their external assets. To assess how such a stress scenario affects the resilience of the network to contagion, we evaluate the impact on the network of the default of a (small) fraction ε of nodes under stress scenarios of variable severity.

Using the notations in Table 1, the remaining capital of bank i is then given by

$$c_i(S) = (A_i + x_i \cdot (1-S) - L_i) \cdot \varepsilon(i) = (A_i + A_i(\frac{1}{LR_i} - 1) \cdot (1-S) - \frac{A_i}{LR_i}(1-\gamma_i))\varepsilon(i),$$

where $\varepsilon(i)$ are independent variables with

$$\mathbb{P}(\varepsilon(i) = 1) = \varepsilon = 1 - \mathbb{P}(\varepsilon(i) = 0),$$

$\varepsilon(i) = 1$ indicating whether i is in default in the stress scenario under consideration.

This can be re-written so as to underline the effect of the shock S on the capital

$$c_i(S) = \gamma_i A_i \frac{1}{LR_i}(1 - \frac{S}{\gamma_i}(1 - LR_i))\varepsilon(i),$$

which means that a loss equal to a fraction S of the external assets translates into a loss equal to a fraction $Z_i := \frac{S}{\gamma_i}(1 - LR_i)$ of the capital buffer. Thus, in the stress scenario characterized by a macroeconomic shock (S, ε), the ratio of capital to interbank assets is given by

$$\gamma_i(S, \varepsilon) = \gamma_i(1 - \frac{S}{\gamma_i}(1 - LR_i))\varepsilon(i). \tag{IV.3}$$

Starting from this expression, one can use the results of Chapter III to evaluate the resilience of the network and the fraction of final defaults as a function of the size of the macroeconomic shock S, without resorting to large scale simulations. In particular, given that the conditions (III.7) and (III.8) will depend on the shock size S, we will see that there is a *threshold* for the magnitude of S above which it destabilizes the network and makes it vulnerable to contagion. This 'phase transition' indicates that a given network has a maximal tolerance for stress; we will see in fact that this threshold may be easily computed from the characteristics of the network.

This approach is applicable to any large network, with an arbitrary distribution of exposures and degrees. To provide some analytical insight into the impact of macroeconomic shocks on the resilience to contagion, we will consider in the next two examples the case where both LR_i and γ_i are constant and equal to LR and γ_{min} respectively. Figures for the lending ratio LR have been given by [76, 109, 132]. We will take $LR = 20\%$ and $\gamma_{min} = 10\%$.

Then the fraction of capital lost in the stress scenario is given by

$$Z = \frac{S}{\gamma_{min}}(1 - LR),$$

so we have

$$\gamma_i(Z) = \gamma_{min}(1 - Z)\varepsilon(i).$$

One can observe that in this model, if $Z = 1$, a trivial global cascade ensues, in which all nodes are fundamental defaults: $\forall i,\ \gamma_i(Z) = 0$. However, as we shall see in the examples in the next sections, a sharp transition in the magnitude of the cascade occur for a threshold value of Z well below 1, which depends on the network characteristics.

3.2 An example of infinite network

We first apply the results to an infinite random scale-free network. Such a network may be obtained as the limit when $n \to \infty$ in the random graph given by a static version of the preferential attachment model [24]. Conditional on the sequence of out-degrees, an arbitrary out-going edge will be assigned to an end-node with probability proportional to the node's out-degree. The empirical distribution of the out-degree is assumed to converge to a power law with tail coefficient γ^+

$$\mu_n(j) := \#\{i \mid d^+(i) = j\} \overset{n\to\infty}{\to} \mu(j) \sim j^{\gamma^+ + 1}.$$

From the graph's construction, it is easy to see that the limit conditional law of the in-degree is a Poisson distribution

$$P(d^- = k | d^+ = j) = e^{-\lambda(j)} \frac{\lambda(j)^k}{k!},$$

with $\lambda(j) = \frac{j^\alpha \mathbb{E}^{\mu^+}(d^+)}{\mathbb{E}^{\mu^+}((d^+)^\alpha)}$, and α a real parameter. The main theorem in [24] states that the marginal distribution of the in-degree has a Pareto tail with exponent $\gamma^- = \frac{\gamma^+}{\alpha}$, provided $1 \leq \alpha < \gamma^+$. For $\alpha > 0$, one obtains positive correlation between in and out-degrees.

The exposures of each bank with out-degree j are assumed to be independent, and follow a Pareto law. The average exposure is an increasing deterministic function of j. We denote this law F_j.

Note that in this case the limit function $p(j, k, \theta)$ does not depend on the in-degree k (we denote this simply by $p(j, \theta)$), and the function I, whose smallest zero determines the final fraction of defaults (see Theorem 3.8), simplifies to

$$\begin{aligned} I(\pi) &= \sum_j \mu^+(j) \frac{\lambda(j)}{\lambda} \sum_{\theta=0}^{j} p(j,\theta)\beta(j,\pi,\theta) \\ &= \sum_j \mu^+(j) \frac{j^\alpha}{\mathbb{E}^{\mu^+}((d^+)^\alpha)} \sum_{\theta=0}^{j} p(j,\theta)\beta(j,\pi,\theta) \\ &= \sum_j \hat{\mu}^+(j) \sum_{\theta=0}^{j} p(j,\theta)\beta(j,\pi,\theta), \end{aligned} \tag{IV.4}$$

with $\alpha = \gamma^+/\gamma^-$, and $\hat{\mu}^+$ the size-weighted out-degree distribution given by

$$\hat{\mu}^+(j) = \mu^+(j) \frac{j^\alpha}{\mathbb{E}^{\mu^+}((d^+)^\alpha)},$$

which is the probability that the end node of a randomly chosen edge has an out-degree equal to j. Since the out-degree distribution is a Pareto distribution, the size biased out-degree distribution is also Pareto, but with a heavier tail with exponent $\gamma^+ - \alpha$. The resilience condition III.7 then simplifies to

$$\sum_j \hat{\mu}^+(j) j p(j,1) < 1. \tag{IV.5}$$

Under the macroeconomic shock Z, the function $p(j,\theta)$ is given by

$$p(j,\theta) = \mathbb{P}(X(\theta) > \gamma(Z) \sum_{l=1}^{j} X(l) - \sum_{l=1}^{\theta-1} (1-R) X(l) \geq 0),$$

where $(X(l))_{l=1}^{j}$ are i.i.d. random variables with law F_j under $\mathbb{P}$ and $\gamma(Z)$ is given by (IV.3). The function $p(j,\theta)$ is plotted in Figure IV.1 for a given value of the macroeconomic shock Z. The steep increase with the number of counterparty defaults θ shows how much the system is prone to contagion, especially for the institutions whose assets are concentrated across a small number of counterparties (i.e nodes with small out-degrees).

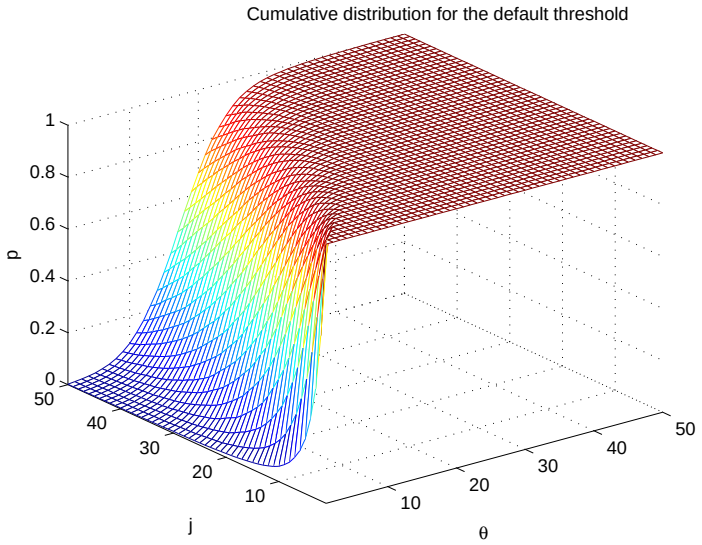

Figure IV.1: The conditional probability of default, Minimal capital ratio = 8%, Macroeconomic shock = 20%, Recovery rate = 0.

*

We consider that a node defaults in the first round with probability ε, such that $p(j,0) = \varepsilon$, for all j. We plot the function I given by (IV.4) for several values of the macroeconomic shock Z in Figure IV.2. We notice that the function I has three zeros for smaller values of Z, the smallest being close to zero, and as Z reaches a threshold value Z_c (in this case 42%) its only zero is close to one.

As stated in Theorem 3.8, if the resilience measure is positive, then with high probability, as the initial fraction of defaults tends to 0, no global cascades appear. On the other hand, if

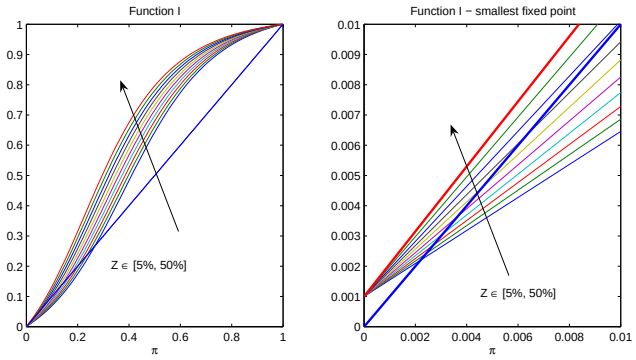

Figure IV.2: Function I for varying size of macroeconomic shock. Fraction of initial defaults = 0.1 %

the resilience measure is negative, the skeleton of 'contagious' links percolates, i.e. represents a positive fraction of the whole system, and we observe global cascades for any arbitrarily small fraction $\varepsilon > 0$ of initial defaults chosen uniformly among all nodes. The verification of Theorem 3.8 is shown in Figure IV.3. In the non-resilient regime global cascades may occur no

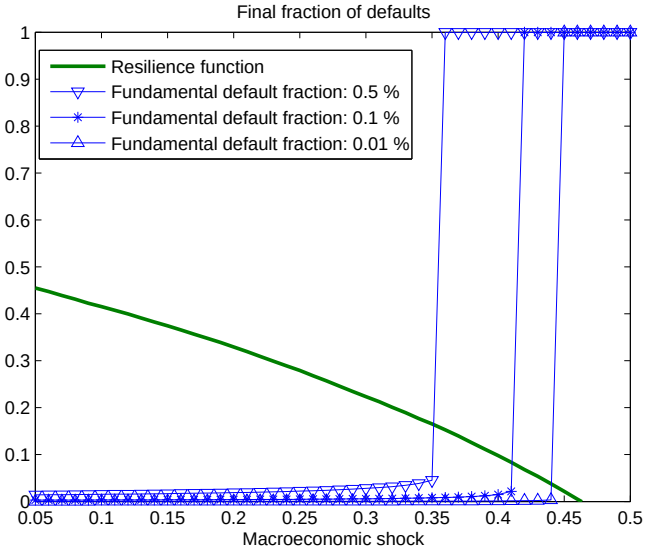

Figure IV.3: Final fraction of defaults: infinite network

matter how small the initial fraction of defaults is. On the contrary, in the resilient regime of the infinite network, if the initial fraction of defaults is small enough, global cascades are not possible. Therefore, the condition of positivity of the resilience measure is a necessary, but not sufficient condition for non occurrence of global cascades.

3.3 A finite scale-free network

We apply the results to a sample scale free network of 2000 nodes with heterogeneous degrees and exposures, generated from Blanchard's random graph model [24]. The empirical distribution of the sample network's degrees and exposures is shown in Figure IV.4, and its parameters were based on the analysis of the Brazilian [48] and Austrian [28] networks.

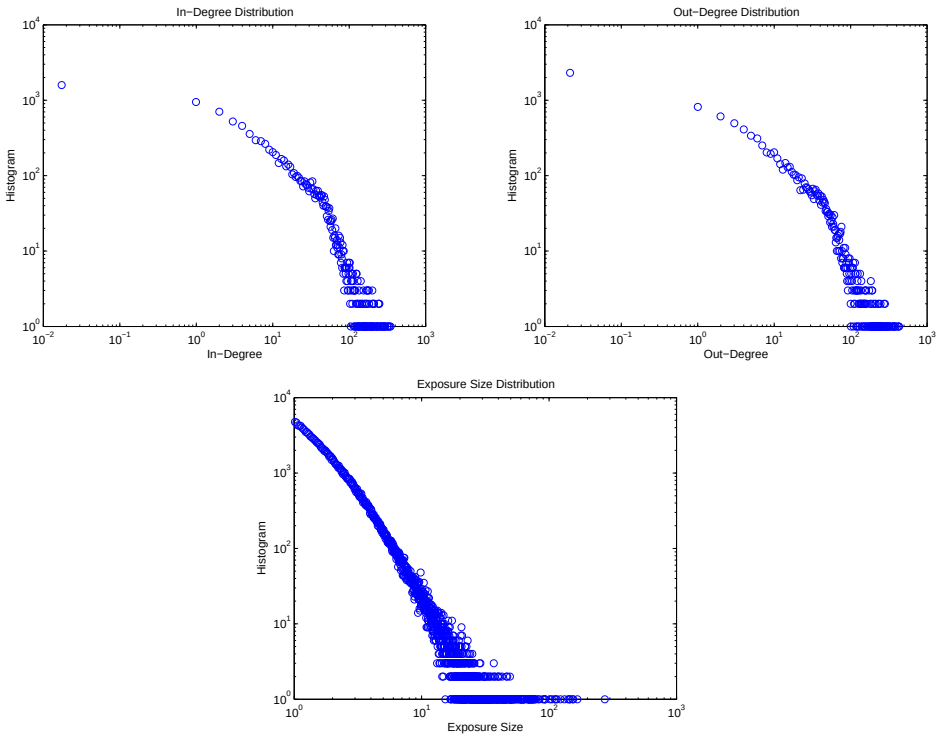

Figure IV.4: (a) The distribution of out-degree has a Pareto tail with exponent 3.5, (b) The distribution of the in-degree has a Pareto tail with exponent 2.5, (c) The distribution of the exposures has a Pareto tail with exponent 2.1.

As Figure IV.5 shows, we obtain highly correlated asset and liabilities sizes and the average exposure is increasing with the number of debtors for the more connected nodes. These properties are both observed in the empirical data.

In the finite sample, condition IV.5 translates to a condition on the average over all nodes of their number of 'contagious' links with a weight proportional to the out-degree to the power α:

$$\frac{1}{n}\sum_i w_i q_i < 1 \tag{IV.6}$$

with $q_i := \#\{j \in v \mid e_{i,j} > c_i\}$ and $w_i := \frac{(d^+(i))^\alpha}{\sum_l (d^+(l))^\alpha}$.

If α is positive, so the more correlated the in-degree and the out-degree are, the more weight is given to the most interconnected nodes. This confirms the intuition that the nodes posing

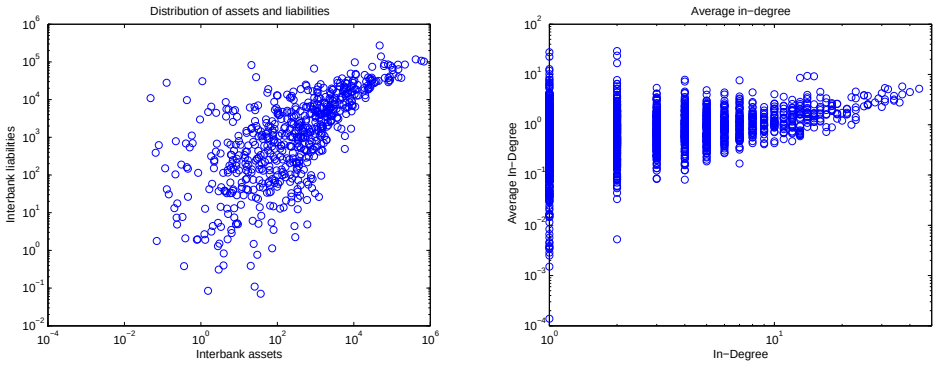

Figure IV.5: (a) Assets and liabilities, (b) Average exposures and connectivity

the highest systemic risk are those both overexposed and interconnected, but not necessarily the largest in terms of balance sheet size.

The value $p(j, 1)$ represents the limit fraction of contagious links entering nodes with out-degree j in the limit network. Figure IV.6 shows the good accordance between the theoretical values and the values computed in the sample network. This suggests that in practice, there

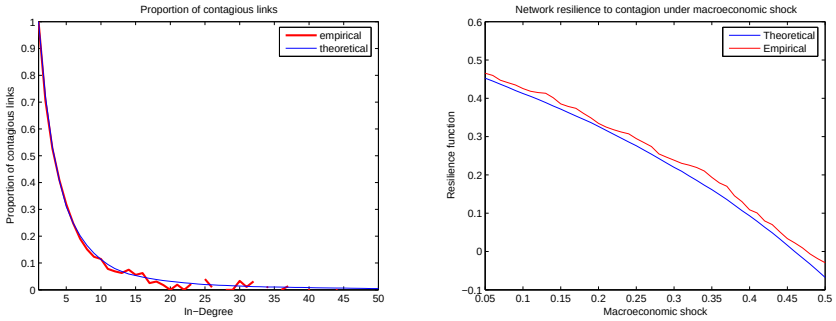

Figure IV.6: (a)Proportion of contagious links. (b)Resilience measure for varying size of macroeconomic shock in the sample and limit random network

is no need to estimate the parameters of the limit distribution, but instead work directly with the empirical data.

Definition 3.1 (Empirical resilience measure)**.** *In a network* $(\mathbf{e}, \gamma)$ *of size* n*, we define the empirical resilience measure*

$$1 - \frac{1}{m_n} \sum_i d^-(i) q_i, \tag{IV.7}$$

where m_n *is the total number of links in the network.*

We conduct the following simulation on the sample network: two nodes, uniformly selected among all nodes of the network initially default. Then for each value of the macroeconomic shock Z and the corresponding sizes of the capital buffers, we compute the final fraction of

defaults. In light of Figure IV.3, in the infinite network, for an initial fraction of defaults representing 0.1% of the network, the positivity of the resilience measure is also sufficient for global cascades not to occur.

The results are plotted in Figure IV.7 along with the 'empirical' resilience measure. We observe that for a given network and set of initial defaults, there exists a threshold value of the macroeconomic shock, beyond which the contagion spreads to essentially the whole network. If the initial fraction of defaults is small enough, the threshold value is given by the value of Z for which the empirical resilience measure becomes zero. This suggests the existence of a first order phase transition marked by the point where the resilience measure becomes negative. We thus verify Theorem 4.3 on the emergence of the giant vulnerable component, i.e. strongly connected skeleton of contagious links, when the resilience function becomes negative.

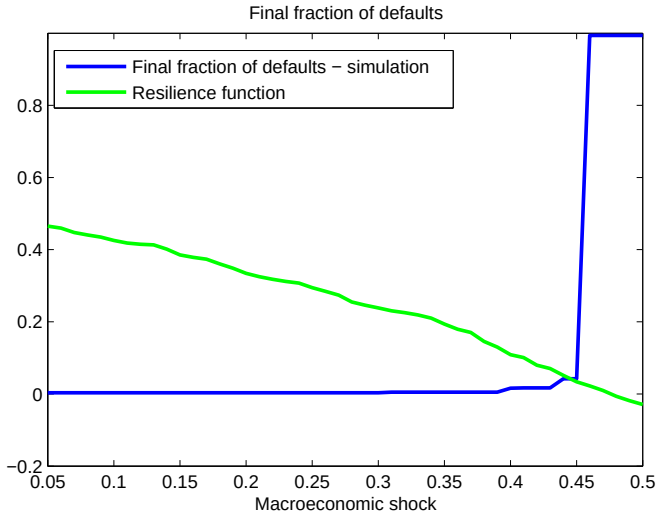

Figure IV.7: Final fraction of defaults triggered by an initial fraction of defaults representing 0.1% of the total network

4 Discussion

We have proposed a framework for evaluating the impact of a macroeconomic shock on the resilience of a banking network to contagion effects. Our approach complements existing stress tests used by regulators [121] and suggests to monitor the capital adequacy of each institution with regard to its *largest exposures*.

In practice, such a stress tests may be implemented in a decentralized fashion by requesting banks to project the effect of a macroeconomic stress scenario on their balance sheets, and report the quantities of interest – mainly the number of exposures exceeding capital in the stress scenario – to the regulator, who can then assess the resilience of the network using our proposed resilience measure. Our criterion for resilience suggests that one need not monitor/know the *entire* network of counterparty exposures, but simply the subgraph of "contagious" links, which

is much smaller. This intuition is indeed confirmed by simulation studies on a wide variety of networks [47, 48].

Chapter V

Credit Default Swaps and Systemic Risk

We propose a network model for OTC derivatives markets, that we calibrate to recent public data on the gross and net protection sold on the top reference entities as well as to the degree of concentration of the market on the top dealers. We introduce the concept of critical receivables, i.e. receivables that if not actually transferred would impede a bank to meet its payment obligations. We link the illiquidity transmission within the network to the percolation of the skeleton of such critical receivables, by introducing a measure of resilience to illiquidity contagion under a stress test scenario. We investigate the influence of central clearing on network stability. We find that, central clearing of CDS, in presence of a clearing facility of interest rate derivatives, reduces the probability of a systemic illiquidity spiral.

Contents

1 Introduction

The gross market value of OTC derivatives stands today at 24$tn, down from 35$tn in 2008 [18], but still a figure comparable to the total assets in the US financial system. This large size can be explained by the fact that, in most cases, financial firms hedge their exposures by entering offsetting contracts.

OTC market participants are part of "hedging chains", and, as such, their default may propagate not just to direct counterparties, but even further as those counterparties act as intermediaries in a hedging chain. This can be seen as a signature of systemic risk in OTC markets manifested through potential illiquidity cascades: when some firms in the hedging chain do not hold enough liquidity to cover their margin calls, counterparties for which those margin calls are critical in order to meet their own payment obligations become illiquid themselves.

What distinguishes credit default swaps from other OTC derivatives is the fact that these margin calls, equal to the variation of mark-to-market values, can be particularly large due to several reasons. Clearly, one important source of jumps in contract value is the actual default of the reference entity, since in this case, the payout equals the loss given default. An even more important source of large margin calls stems from large correlated jumps in the spreads of reference entities. Indeed, in the CDS market, a few protection sellers concentrate the large majority of the sold protection. These protection sellers will immediately face a liquidity shortage if reference entities across a given sector undergo at the same time large spread jumps. Illiquidity cascades driven by OTC derivatives in general, and CDS in particular, are a major part of systemic risk.

A recent literature was dedicated to OTC derivative markets. Avellaneda and Cont [14, 15] study transparency related issues. Duffie et al. introduce a model for information percolation in these markets [55].

The closest to our paper is Duffie and Zhu [63] who investigate in a simple gaussian framework the impact on financial stability of credit default swaps central clearing. The central insight in [63] is that the efficiency of a clearing house crucially depends on the tradeoff between bilateral netting across derivative classes and multi-netting via the clearing house. However, assessing this problem in absence of a model that mimics the heterogeneous and the hierarchical nature of OTC markets may be controversial.

Therefore, we explicitly introduce a network model for the most relevant classes of OTC derivatives, that we calibrate to recent data. Our network of CDS notionals is calibrated to the data on the gross and net protection sold on the top 1000 names recently published by The Depository Trust and Clearing Corporation (DTCC), as well as on the market share of the dealers defined by DTCC as 'any user that is, or is an affiliate of a user who is, in the business of making markets or dealing in credit derivative products' [130]. The structure of the network is hierarchical: we distinguish between market-makers / dealers and other market participants. In our model, a chain of intermediaries match a net protection buyer and a net protection seller of protection. We show how margin calls and derivative payables may lead to contagion via illiquidity cascades in such networks and we introduce a measure of resilience to illiquidity contagion under a stress test scenario. The point where this measure first become negative marks a phase transition in the behavior of contagion in the network: we pass from a regime where contagion stays contained to a few fundamentally illiquid institutions to a regime where illiquidity spreads system-wide.

In the second part of the chapter we apply these concepts to analyze the impact of central

clearing of credit default swaps on financial stability. A clearing facility modifies the structure of the network: every contract between two members of the clearing house is replaced by two contracts having the clearing house as a counterparty. Using a CDS network calibrated to DTCC data we explore the impact of introducing a CDS clearinghouse on the resilience of the network and the number of defaults. We determine the OTC derivative payables in a stress test scenario defined by the variation of the mark-to-market values of OTC derivatives. We argue that, while mark-to-market values of CDS are much lower than mark-to-market values of other OTC derivatives like interest rates swaps, in turbulent times, the absolute sizes of the variation of mark-to-market values are of the same order of magnitude.

Our analysis shows that, in a network where other major OTC derivatives (primarily IR swaps) are cleared, the addition of a CDS clearing facility enhances network stability and a significantly larger shock is necessary to trigger a phase transition. On the other hand, in absence of clearing of the other classes of OTC derivatives, central clearing of CDS may have little or no impact on financial stability. Moreover, the presence of a CDS clearing house increases the resilience of the network, provided all significant dealers are members of the clearing house.

This chapter is organized as follows. In Section 2, we introduce the subject of counterparty risk related to OTC derivatives. In Section 2.1 we make an empirical analysis of OTC markets. Then, in Section 3, we place the receivables related to OTC derivatives in a network context and we define an illiquidity cascade. In Section 4, we first propose a weighted random graph model for the OTC non-CDS exposure matrix. Then, in Subsection 4.2, we introduce a model of a CDS multi-network based on the construction, for each reference entity, of a network of notionals of CDS referencing that entity. In Section 5 we give a criterion for the resilience of an OTC network to illiquidity cascades under a stress test scenario. Last, in Section 6, we study numerically the impact of central clearing on the size of the illiquidity cascade. We complement by Appendix 8, which presents risk-neutral pricing of collateralized portfolios of OTC derivatives.

2 Over-the-counter markets

In an over the counter (OTC) transaction, two parties deal directly with one another, rather than passing through an exchange. As such, any of the parties bears counterparty risk, i.e. the risk of the other party's not fulfilling its obligations.

Let us consider a generic OTC transaction. At the inception date of the contract, say time 0, the two parties agree on some future cash flows between them. For one party, the mark-to-market (MtM) value of the contract at a time t is given by the difference between the discounted value of the future inflows and the future outflows. Since one party's inflow is the other party's outflow, the swap has opposite value for the two counterparties. Upon the default of one counterparty, the contract is terminated and a close-out payment equal to the mark-to-market value of the remaining cash flows is due. If the mark-to-market value is negative for the surviving party, then the latter will make the full close-out payment. On the other hand, if the mark-to-market value is positive for the surviving party, only a fraction of the due close-out payment will be received, so the surviving party suffers a loss.

Counterparty risk is mitigated in several ways. First, when two counterparties hold a portfolio of derivatives, these derivatives are usually placed under a netting agreement (called

the ISDA Master Agreement). In this case, upon default, a single terminating payment for all derivatives in the portfolio is due, determined by the mark-to-market net value of all derivatives in the portfolio. Second, the majority of the contracts are subject to collateral agreements: with a certain frequency -mostly daily-, the party with negative mark-to-market value of the portfolio posts collateral to its counterparty [90].

Consider, for example a portfolio between two parties a and b, consisting of two derivatives, one with a positive value of 200$\$mn$ for b and the other with positive value of 100$\$mn$ for a. The whole portfolio has thus a positive value of 100$\$mn$ for b. Assume that a defaults, and that the recovery rate is 0. Without netting and collateral, b would pay to a 100$\$mn$ and a would suffer a loss of 200$\$mn$ on the derivative with positive value. If netting is applied, a single terminating payment of 100$\$mn$ is due by a, and since a defaults and has zero recovery rate, this represents the loss of b. If a had previously posted collateral 50$\$mn$ to b, then b seizes this collateral and its loss will be the remaining 50$\$mn$.

We cite here ISDA Credit Support Documents [90] determining the amount of collateral to be posted:"(i) the [Collateral Taker]'s Exposure plus (ii) the aggregate of all Independent Amounts applicable to the [Collateral Provider], if any, minus (iii) the aggregate of all Independent Amounts applicable to the Collateral Taker, if any, minus (iv) the [Collateral Provider]'s Threshold. The term Exposure is defined in a technical manner that in common market usage essentially means the netted mid-market mark-to-market (MtM) value of the transactions that are subject to the relevant ISDA Master Agreement. If a Threshold is applicable to a party, the effect of the Credit Support Amount calculation is that Collateral is only required to be posted to the extent that the other party's Exposure (as adjusted by any Independent Amounts) exceeds that Threshold. An Independent Amount applicable to a party serves to increase the amount of collateral that is to be posted by that party. This is to provide a "cushion" of additional collateral to protect against certain risks, including the possible increase in Exposure that may occur between valuations of collateral (or between valuation and posting) due to the volatility of mark-to-market values of the transactions under the ISDA Master Agreement." Although not a technical term, "variation margin" is used to refer to the portion of required collateral that relates to the MtM of covered transactions (i.e. the "Exposure").

As OTC derivatives are passed to clearing houses, an "initial margin" is required, which has the same meaning as Independent Amount.

2.1 OTC derivatives: notional, mark-to-market and daily variations

The purpose of this section is to first make a comparative empirical study of mark-to-market values, notional sizes and daily variations of mark-to-market values of different types of derivatives and then, to have a closer look at concentration in the OTC market. Table V.1 gives an overview of the notional and gross market values of different types of OTC derivatives. An immediate observation is that interest rate and foreign exchange instruments account for 85% of the total notional size of the OTC market, while credit default swaps account for around 5%.

On the other hand, when looking at the daily return of the mark-to-market values of these instruments - that we approximate by the daily return of spreads (see Appendix 8) and respectively the swap fixed rate - the picture changes, as shown in Figure V.1. Turbulent times like the weeks following the failure of Lehman Brothers on the 15th Sept 2008, showed that the absolute value of the average 5-year CDS spread return for the high-grade names comprising

Table 19: Amounts outstanding of over-the-counter (OTC) derivatives
By risk category and instrument
In billions of US dollars

	Notional amounts outstanding					Gross market values				
Risk Category / Instrument	Jun 2008	Dec 2008	Jun 2009	Dec 2009	Jun 2010	Jun 2008	Dec 2008	Jun 2009	Dec 2009	Jun 2010
Total contracts	**672,558**	**598,147**	**594,495**	**603,900**	**582,655**	**20,340**	**35,281**	**25,314**	**21,542**	**24,673**
Foreign exchange contracts	**62,983**	**50,042**	**48,732**	**49,181**	**53,125**	**2,262**	**4,084**	**2,470**	**2,070**	**2,524**
Forwards and forex swaps	31,966	24,494	23,105	23,129	25,625	802	1,830	870	683	925
Currency swaps	16,307	14,941	15,072	16,509	16,347	1,071	1,633	1,211	1,043	1,187
Options	14,710	10,608	10,555	9,543	11,153	388	621	389	344	411
Interest rate contracts	**458,304**	**432,657**	**437,228**	**449,875**	**451,831**	**9,263**	**20,087**	**15,478**	**14,020**	**17,533**
Forward rate agreements	39,370	41,561	46,812	51,779	56,242	88	165	130	80	81
Interest rate swaps	356,772	341,128	341,903	349,288	347,508	8,056	18,158	13,934	12,576	15,951
Options	62,162	49,968	48,513	48,808	48,081	1,120	1,764	1,414	1,364	1,501
Equity-linked contracts	**10,177**	**6,471**	**6,584**	**5,937**	**6,260**	**1,146**	**1,112**	**879**	**708**	**706**
Forwards and swaps	2,657	1,627	1,678	1,652	1,754	283	335	225	176	189
Options	7,521	4,844	4,906	4,285	4,506	863	777	654	532	518
Commodity contracts	**13,229**	**4,427**	**3,619**	**2,944**	**2,852**	**2,213**	**955**	**682**	**545**	**457**
Gold	649	395	425	423	417	72	65	43	48	44
Other commodities	12,580	4,032	3,194	2,521	2,434	2,141	890	638	497	413
Forwards and swaps	7,561	2,471	1,715	1,675	1,551					
Options	5,019	1,561	1,479	846	883					
Credit default swaps	**57,403**	**41,883**	**36,046**	**32,693**	**30,261**	**3,192**	**5,116**	**2,987**	**1,801**	**1,666**
Single-name instruments	33,412	25,740	24,112	21,917	18,379	1,901	3,263	1,953	1,243	993
Multi-name instruments	23,991	16,143	11,934	10,776	11,882	1,291	1,854	1,034	559	673
of which index products	...	...	...	...	7,614					
Unallocated	**70,463**	**62,667**	**62,285**	**63,270**	**38,327**	**2,264**	**3,927**	**2,817**	**2,398**	**1,788**
Memorandum item:										
Gross Credit Exposure						3,859	5,005	3,744	3,521	3,578

Table V.1: Amounts outstanding of OTC derivatives. Source: BIS Quarterly Review, December 2010.

the CDX index can be several times larger than the absolute value of the return of the swap fixed rate. Moreover, spreads of institutions belonging to the same sector as a failed institution exhibit particularly large jumps due to cross-sector correlation. Such is the case of General Electric, which is a component of the CDX index within the sector 'financials', whose 5-year spread had a 70% jump following the default of Lehman Brothers. Institutions closer in their activity to that of the failed bank, like other dealer banks, suffered even larger jumps in spreads: the cost of protection for other dealers doubled over a few trading days in the aftermath of Lehman's default [33].

2.2 Concentration in OTC markets

Another important aspect drawn from empirical data is the concentration of the OTC market. Table V.2 extracted from [40] shows the notional positions of the top 5 US dealers on different types of OTC derivatives: forwards, swaps, options and credit.

According to this data, the top 5 US dealers alone hold an OTC derivative global market share of 46%. For credit derivatives in particular, their global market share is 71%. This is a piece of evidence that the credit derivatives market is significantly more concentrated than the other OTC markets. For CDS, a comprehensive analysis of concentration is made in [73]. According to DTCC data, the total notional amounts of outstanding CDSs sold by dealers worldwide, represent over 80% of total protection sold worldwide and a similar percentage is represented by protection bought by dealers. Also, the interdealer network accounts for 75% of total CDS notional. Remark that no precise number of dealers is given in DTCC data, they

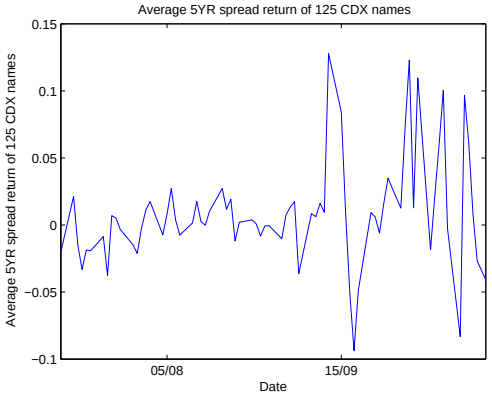

(a) Average 5-year CDS spread returns for the CDX.NA.IG index

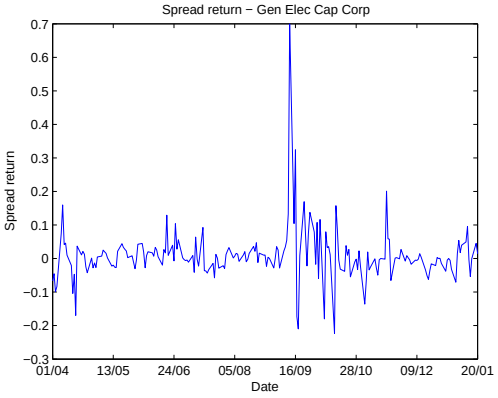

(b) GE 5-year CDS spread returns

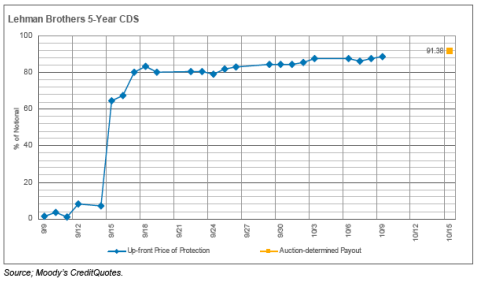

(c) Jump in cost of protection

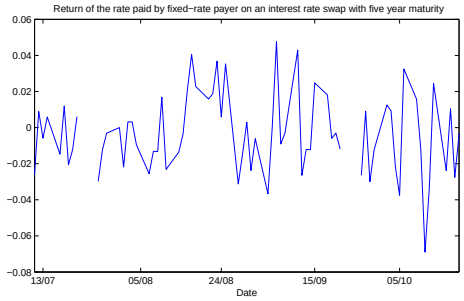

(d) Jump in the rate of fixed rate payer in IR Swap

Figure V.1: Jumps in OTC derivatives values.

are defined as "as any user that is, or is an affiliate of a user who is, in the business of making markets or dealing in credit derivative products".

When considering the distribution of the total notional among reference entities, we observe an important concentration on the top underlying names, as shown in Figure V.2.

In summary, we conclude from the data that non-credit OTC derivatives have a mark-to-market value one order of magnitude above credit derivatives. However, credit derivatives, in particular single name CDS may present much larger jumps in the mark-to-market values. Moreover, due to a much more important concentration of the market on top dealers and the fact that spreads exhibit large correlation across reference entities [44], we argue that the absolute value of jumps in a dealer's positions on CDS and non-CDS derivatives are comparable. Therefore, a realistic model for an OTC market should distinguish between two classes of OTC derivatives: non-CDS (primarily IR derivatives) and CDS.

Rank	Holding Company	Assets	Total OTC derivatives	Forwards	Swaps	Options	Credit
1	JPM	2117605	75510099	11806979	49331627	8899046	5472447
2	BAC	2268347	63983932	10287375	43481989	5847866	4366702
3	C	1913902	45151220	6895160	28638854	7071397	2545809
4	GS	911330	43998391	3805327	27391560	8568358	4233146
5	MS	807698	41124050	5458883	27161921	3854976	4648270

Table V.2: Notional Amount of Derivative Contracts Top 5 Holding Companies In OTC Derivatives December 31, 2010, $ millions. Source: OCC's Quarterly Report on Bank Trading and Derivatives Activities Second Quarter 2010.

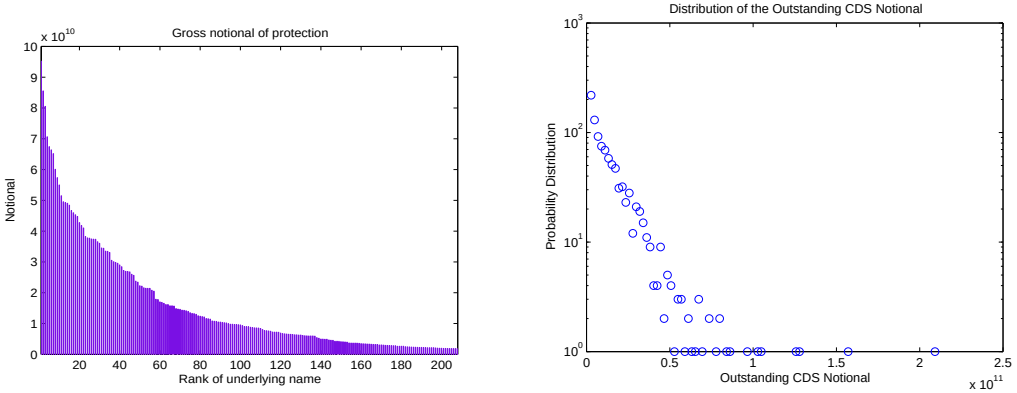

Figure V.2: Concentration on names: 47 % of the total CDS Notional is written of the top 5 names and 76 % on the top 10 names.

3 A network model for OTC derivatives receivables

At any time, a snapshot of the OTC market reveals a set of institutions ("banks") that are interlinked by their mutual claims.

Let us consider two successive time periods $t-1$ and t and consider that the snapshot is taken at the beginning of period t. For instance, we can think of "period" t as a trading day and at "time" t as the time when all positions are marked-to-market. As we have seen in Section 2, a party i has an obligation to pay a party j a cash flow equal to the variation of the mark-to-market value of all positions between i and j from the point of view of j. This variation is considered between the beginning of period $t-1$ (called time $t-1$) and the beginning of period t (called time t).

We denote this variation by $\xi_t(i,j)$. Thus, the payment flows due during period t may be modeled by a network with the vertex set $\mathbf{v} = \{1,\dots,n\}$ and the weighted directed edges $((\xi(i,j))_+)_{\{1\le i,j\le n\}}$.

We let $m_t(i)$ the liquidity position of bank i at time t. The liquidity position $m_t(i)$ is constituted by cash in main currencies or other highly liquid instruments like high-grade government securities. At time t, the liquidity position is affected by an exogenous liquidity shock $\delta_t(i)$.

Several observations should be made at this point regarding the interpretation of liquidity

Net payables $\Delta m_t(i)$	Liquidity shock $\delta_t(i)$
OTC derivatives inflows $\sum_j(\xi_t(i,j))_+$	OTC derivatives outflows $\sum_j(\xi_t(j,i))_+$

Table V.3: Payables at time 0.

and liquidity shocks. First, there is clear evidence that banks rehypothecate the collateral they receive against their exposures [89, 127], so the liquidity position $m_t(i)$ is obtained by adding to the bank's liquid assets the difference (positive or negative!) between the total (highly liquid) collateral received and the total collateral posted to other banks. In an hypothetical example, if all liquid assets of a bank are posted as collateral against its negative exposures, they cannot be used to make additional payments.

Second, the illiquid portfolio of the bank plays a crucial role, depending on the economic cycle[2]. During a boom, due to increases in the value of the illiquid portfolio and the consequent leverage reduction, it is easy for banks to obtain additional liquidity on the market by pledging illiquid assets as collateral. Empirical evidence shows that this is precisely what they do [3]. By the end of the boom cycle, banks will possess a large portfolio of illiquid assets funded by short term debt with small haircuts, where the haircut is defined as the difference between the book value of illiquid portfolio and its value as collateral. During a bust, prices start falling and not only that no supplementary liquidity enters the market, but liquidity starts to be withdrawn. Withdrawal of liquidity comes in the form of increases in haircuts. An increase of 100% is equivalent to total withdrawal of funding. With each increase in haircuts applied to the illiquid portfolio of a bank, there is an outflow of liquidity that is equal to the increase in haircuts times the book value of the funded illiquid portfolio. The situation where haircut increases to 100% is called a 'run by short term creditors' and this problem has been investigated in the economics literature by Morris and Shin [115] using global games theory.

Our focus in the current paper is different, so in our case we account for liquidity outflows due to changes in funding conditions only via the exogenous liquidity shock $\delta_t(i)$. In our paper we consider that the reference observation time of the OTC market is during a bust period, and without intervention from a lender of last resort. Thus, from now on we let

$$\delta_t(i) \geq 0.$$

We can write the net interbank liquidity outflow of bank i as the difference between the total liquidity outflow and the total liquidity inflow (see Table V.3):

$$\begin{aligned}\Delta m_t(i) &= \sum_j (\xi_t(i,j))_+ - \sum_j (\xi_t(j,i))_+ + \delta_t(i) \\ &= \sum_j \xi_t(i,j) + \delta_t(i), \end{aligned} \tag{V.1}$$

where the second equality holds due to the anti-symmetricity of the matrix ξ.

A bank is said to be **liquid** if it can withstand the net liquidity outflow, i.e.

$$m_t(i) - \sum_j \xi_t(i,j) - \delta_t(i) \geq 0, \tag{V.2}$$

and illiquid otherwise.

Remark 3.1. *For the sake of completeness, let us compare our liquidity Condition (V.2) with the liquidity condition given in [115], where illiquidity is due to withdrawal of short term funding alone. In absence of payables or collateral related to OTC derivatives, the liquidity condition would be*

$$m_t(i) - \delta_t(i) \geq 0, \tag{V.3}$$

with $m_t(i)$ the bank's liquid assets. We denote by $\phi(i)$ the book value of the illiquid portfolio, $H_{t-1}(i)$ the haircut applied to this illiquid portfolio at the previous period and by $H_t(i)$ the haircut at the beginning of the current period. Since the liquidity outflow $\delta_t(i)$ is equal to the increase in haircuts times the book value of the illiquid portfolio, Condition (V.3) becomes

$$\begin{aligned} &m_t(i) - (H_t(i) - H_{t-1}(i)) \cdot \phi(i) > 0, \text{ which can be written as} \\ &m_t(i) + (1 - H_t(i)) \cdot \phi(i) > (1 - H_{t-1}(i)) \cdot \phi(i). \end{aligned}$$

This condition is equivalent to the absence of a run of short term creditors in [115].

We can now give the definition of the network of OTC derivative payables, on the vertex set $\mathbf{v} = [1, \ldots, n]$.

Definition 3.2. *A **network of OTC payables** $(\xi_\mathbf{t}, \delta_\mathbf{t}, \mathbf{m_t})$ is defined by*

- *a sequence of liquidity positions $\{m_t(i)\}_{1 \leq i \leq n}$,*
- *a sequence of exogenous liquidity outflows $\{\delta_t(i)\}_{1 \leq i \leq n}$,*
- *a matrix of OTC payables $\{\xi_t(i,j)\}_{1 \leq i,j \leq n}$.*

Clearly, if the bank cannot withstand the net liquidity outflow it will default on its payment obligations during the time period t and an illiquidity cascade may emerge. If default would be immediately visible to the market, than defaults during the period t would instantaneously change the network of margin calls. We argue that there is a delay between the actual default and the time the market acknowledges it. We make thus the following assumption.

Assumption 3.3. *Defaults that occur during period t are revealed at the end of the period t. As such, during the period t the matrix ξ_t remains constant. Upon default, we consider that in the short run recovery rates are 0 [8].*

3.1 Illiquidity cascades

We say that a bank is fundamentally illiquid at time t if $m_t(i) - \sum_j \xi_t(i,j) - \delta_t(i) < 0$. Such a situation may arise from large jumps in mark-to-market values of net OTC derivatives payables, stemming for example from large correlated jumps in the spreads of reference entities of CDS. Institutions with large unilateral positions are particularly prone to this kind of illiquidity. Nonetheless, our model allows for a bank to become fundamentally illiquid via the exogenous shock $\delta_t(i)$. As explained in [61], the most likely coup de grâce to a distressed dealer bank is the withdrawal of overdraft facilities by its clearing bank. This situation can be modeled here via this exogenous shock.

A bank becomes illiquid due to contagion during the period t if its liquidity position is such that it depends on its derivative receivables to meet its payment obligations. Such a situation can arise for highly 'leveraged' banks, i.e. well hedged and holding little liquidity.

As illustrated in Figure V.3, consider the example of an institution A that buys protection from an institution B on a reference entity k for a total notional $N^{(k)}$. Institution B will hedge

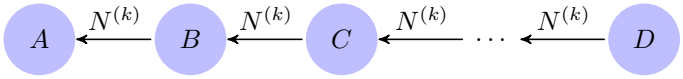

Figure V.3: Chains of intermediaries in OTC markets

its exposure to the default of the reference entity by buying protection from an institution C on the same notional amount as it sold protection on to A, and so on, until reaching an institution D which is a net seller of protection. All the intermediary institutions are well hedged and have little incentive to keep a high liquidity position, especially if counterparties have high ratings (i.e. are deemed as having small probability of default). On the other hand, margin calls may be particulary large following jumps in the spread of the reference entity. If the end net seller of protection defaults, then there is potential of domino effects along the above chain of intermediaries.

Definition 3.4 (Illiquidity cascade during a period t)**.** *Starting from the liquidity positions at time t, $\{m_t(i)\}_{1\leq i\leq n}$, the exogenous liquidity shocks $\{\delta_t(i)\}_{1\leq i\leq n}$ and the network of payables $\{\xi_t(i,j)\}_{1\leq i,j\leq n}$, the illiquidity cascade can be found by repeatedly adding to the net liquidity outflow Δm_t given by Eq. (V.1) the payables from illiquid banks.*

- *Set $\mathbb{D}_0$, the set of initial defaults, equal to the set fundamentally illiquid banks, i.e. $\{i \in \mathbf{v} \mid m_t(i) - \sum_j \xi_t(i,j) - \delta_t(i) < 0\}$.*
- *For $r \geq 1$, set $\mathbb{D}_r = \{i \in \mathbf{v} \mid m_t(i) - \sum_j \xi_t(i,j) - \delta_t(i) - \sum_{j\in\bigcup_{k<r}\mathbb{D}_k<0}(\xi_t(j,i))_+ < 0\}$, the set of banks becoming illiquid in round $r > 0$.*

We obtain an increasing sequence of default sets $\mathbb{D}_0 \subset \mathbb{D}_1, \ldots, \subset \mathbb{D}_{n-1}$. The set $\mathbb{D}_{n-1}$ represents the set of illiquid banks during the period t .

We make several remarks.

First, the liquidity position m_t and the network ξ_t of payables tend to be negatively correlated. Again, let us take the example of a CDS protection seller. In a first approximation, the jump in the negative position of the seller is given by the jump in the spread of the reference entity. Or, as [44] point out, the spread return exhibits positive autocorrelation, volatility clustering and heteroscedasticity. Their empirical distribution is heavy tailed. Moreover, empirical data shows that spread returns are correlated across certain classes of reference entities. It follows that, a large value for derivatives payables is very likely to occur after a period of increases in spreads, which had the effect of fragilizing the liquidity position of the seller. This is a typical example of wrong-way risk, particularly exacerbated if this seller concentrates positions on several correlated reference entities.

Second, one should not ignore that large downward jumps in absolute market values may also cause contagion. In case banks use rehypothecation, there is no guarantee that a party

with negative exposure will receive back its excess collateral in case the (absolute value) of the exposure diminishes. This may cause the party to become illiquid if it is part of a hedging chain. Whereas the danger of rehypothecation has been pointed out in relation to this kind of over-collateralization [127], one should keep in mind that the risk of over-collateralization incurred by one party is symmetrical to the risk of under-collateralization incurred by the other party (for the CDS example, returns of CDS spreads have symmetrical heavy tailed distributions [44]).

4 A random network model for OTC markets

In the previous section we have modeled a snapshot of the OTC market as a network of OTC payables due at time t and we have defined the illiquidity cascade on this network during the period t.

This section details the construction of the network of OTC payables, given by the variations of mark-to-market values of OTC derivatives. As argued in Section 2.1, in case of CDS, variations of their MtM value are more realistically defined as percentages of the outstanding notional. Therefore, a model for a network $\xi_{\mathbf{t}}$ of payables related to OTC deivatives contains the following elements:

1. A model of the network of mark-to-market values of non-CDS OTC derivatives. This network's features are observable at time $t-1$.
2. A model of n networks of outstanding notional of CDS. These networks' features are observable at time $t-1$.
3. A model for variations of mark-to-market values of OTC derivatives. These variations are unobservable at time $t-1$.

We consider that the liquidity position m_t is observable at time $t-1$.

Definition 4.1 (Payables network)**.** *Let $\mathbf{g_{t-1}}$ and $\{\mathbf{N^{(k)}_{t-1}}\}_{k=1}^n$ the networks of non-CDS exposures and CDS outstanding notionals for each reference entity at time $t-1$. Let $\{\Delta S_t(k)\}_{k=1}^n$ and ΔM_t be the spread variations and respectively the return of the MtM values of non-CDS derivatives. The network of payables at time t is given by*

$$\xi_t = \triangleright(g_{t-1}\Delta M_t + \sum_k N^{(k)}_{t-1}\Delta S_t(k)), \tag{V.4}$$

where the operator $\triangleright$ gives the net flows: $\triangleright a = (a - a^T)_+$.

The rest of this section details the construction of the networks $\mathbf{g_{t-1}}$ and $\{\mathbf{N^{(k)}_{t-1}}\}_{k=1}^n$. For simplicity we drop the subscript from these notations.

The construction of the OTC network with vertex set $\mathbf{v} = \{1, \ldots, n\}$ is centered around the fact that a small subset of $n_d \ll n$ of these institutions, among the largest and most interconnected, act as dealers in the OTC market, meaning that they act primarily as intermediaries between other institutions, so that generally they are counterparties to off-setting contracts. Without loss of generality, we consider that dealers are represented by nodes $\{1, 2, \ldots, n_d\}$ and that non-dealers are represented by nodes $\{n_d + 1, \ldots, n\}$.

The model is based on the following parameters:

- The aggregate gross value of the OTC market as given (source: BIS);
- The non-credit derivatives market share for the top 10 dealers (source: OCC);
- The credit derivatives market share for the top 10 dealers (source: DTCC);
- The gross CDS protection bought on the top 1000 reference entities (source: DTCC);
- The net CDS protection bought on the top 1000 reference entities (source: DTCC).

4.1 A random model for a (non CDS) exposure network

We detail the construction of the network $(\mathbf{v}, \mathbf{g})$ of non CDS exposures. We introduce a weighted version of Blanchard's random graph model [24].

Recall that in Blanchard's random graph model, conditionally on a prescribed sequence of out-degrees, an arbitrary out-going edge will be assigned to an end-node with probability proportional to the power α of the node's out-degree. For $\alpha > 0$, one obtains positive correlation between in and out-degrees.

In order to account for the heterogeneity of the degrees, the empirical distribution of the out-degree is assumed to converge to a power law with tail coefficient γ^+:

Condition 4.2.

$$\mu_n^+(j) := \#\{i \mid d_n^+(i) = j\} \overset{n\to\infty}{\to} \mu^+(j) \sim j^{\gamma^+ + 1}. \tag{V.5}$$

The main theorem in [24] states that the marginal distribution of the out-degree has a Pareto tail with exponent $\gamma^- = \frac{\gamma^+}{\alpha}$, provided $1 \leq \alpha < \gamma^+$:

$$\mu_n^-(j) := \#\{i \mid d_n^-(i) = j\} \overset{n\to\infty}{\to} \mu^-(j) \sim j^{\gamma^- + 1}.$$

We now extend this model to account for the heterogeneity of weights. The intuition behind our construction can be given by rephrasing the Pareto principle: 20% of the links carry 80% of the mark-to-market value of non CDS derivatives. Therefore, we will distinguish between two types of links. Links of type A represent a percentage a of the total number of links and carry a percentage a' of the total mark-to-market value. All other links are said to be of type B.

We can now define the random graph model that we use to model the non-CDS mark-to-market values.

Definition 4.3 (Weighted Blanchard Model)**.** *Let $(d_n^+(i))_{i=1}^n$ a prescribed sequence of out-degrees, assumed to verify Condition (4.2). For every node i, its $d_n^+(i)$ in-coming links are partitioned into $d_n^{+,A}(i)$ links of type A and $d_n^{+,B}(i)$ links of type B:*

$$d_n^+(i) = d_n^{+,A}(i) + d_n^{+,B}(i). \tag{V.6}$$

We denote $m^A := \sum_{i=1}^n d_n^{+,A}(i)$ and by $m^B := \sum_{i=1}^n d_n^{+,B}(i)$ their respective numbers. We let $F^A : \mathbb{R}_+^{m^A} \to [0,1]$ and $F^B : \mathbb{R}_+^{m^B} \to [0,1]$ the joint probability distributions functions for the weights carried by links of type A and B respectively. The probability distribution functions F^A and F^B are assumed to be invariant under permutation of their arguments.

The random graph is generated then as follows:

- *Generate the weighted subgraph of links of type A by Blanchard's algorithm with prescribed degree sequence* $\{d_n^{+,A}(i)\}_{i=1}^n$ *and parameter* $\alpha > 0$.
- *Draw* m^A *random variables from the joint distribution* F^A. *Assign these exchangeable variables in arbitrary order to the links of type A.*
- *Proceed similarly for the links of type B.*

The tail coefficient γ^+ is calibrated to the dealers' market share in OTC derivatives V.2. We take $\alpha = 1$.

The topology of the non-CDS exposure network is governed by the following parameters :
$$\gamma^+ = 2,\ \alpha = 1,\ a = 5\%.$$

Denoting by T the total gross mark-to-market value of non-CDS derivatives, the exposures are governed by the cumulative distribution functions F^A and F^B. We generate the weights of type A as the differences of the order statistics of m^A i.i.d. random variables, uniformly distributed in the interval $[0, a' \cdot T]$. We take F^B as the distribution of m^B i.i.d. random variables drawn from the Pareto distribution with tail coefficient γ_L.

The exposure sequence is governed by the following parameters : $T = 3.5\$tn$, $a' = 80\%$,
$$\gamma_L = 1.1.$$

4.2 A random CDS network model

We now condition on the network $(\mathbf{v}, \mathbf{g})$ of gross exposures after netting. The model for the CDS network on a name i is based on the following parameters

- For every reference entity k, the gross CDS notional, $gross(k)$, defined as the sum of the notionals of all CDS contracts referencing k.
- For every reference entity k, the net CDS notional $net(k)$, defined as the sum over all nodes of the notional of net protection bought (i.e. the positive part of the notional of protection bought minus notional of protection sold) on the reference entity k.
- An exponent $\beta > 1$, such that the probability of a bank i to be a counterparty of a randomly chosen CDS contract is given by its CDS market share $p(i)$.
- A number of buyers of 'speculative' protection n_b.

For any reference entity k, the gross CDS notional represents the total notional of protection bought on i (obviously, it is also equal to the total notional of protection sold on name i). At the same time, the net protection sold by a bank i on a reference entity k equals the positive part of the notional of total protection sold minus the notional of total protection bought on reference entity k.

So, our aim is to construct the network $N^{(k)}$ such that

$$\sum_{s,b} N^{(k)}(s,b) = gross(k),$$

and

$$\sum_s (\sum_b N^{(k)}(s,b) - \sum_b N^{(k)}(b,s))_+ = net(k).$$

The set of **buyers** and the respective **notionals** is given as follows:

- Hedging CDS. All nodes j having a positive exposure i.e. $g(j,k) > 0$ buy CDS protection on a notional equal to $C \cdot g(j,k)$, where C is $1 \wedge \frac{net(i)}{\sum_j g(j,k)}$.
- The remaining aggregate net notional is distributed uniformly among a number n_b of buyers, chosen independently according to the probability distribution p.

Given the protection buyers and respective notional amounts, we choose a set of sellers as shown in Figure V.4.

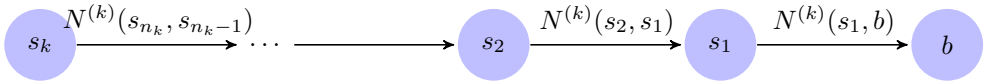

Figure V.4: Hedging chain

More precisely, for each contract:

- Choose a set of n_k sellers i.i.d. with probability distribution p,
- Set $N^{(k)}(s_1, b)$ the notional of protection bought by b from the seller s_1,
- Every node s_i is a seller of protection to s_{i-1} and a buyer of protection from s_{i+1},
- Node s_{n_k} is a net seller of protection.

The length of this hedging chain is set equal to $\lceil \frac{gross(k)}{net(k)} \rceil$ and we have for all i:

$$N^{(k)}(s_i, s_{i-1}) = N^{(k)}(s_1, b).$$

The random network given by our model is calibrated by construction to the sequence of net and gross CDS notional $(gross(i), net(i))_{1 \leq i \leq n}$ and to the market shares.

5 Resilience to illiquidity cascades under a stress test scenario

In this section we consider the following problem: an observer of the non credit exposure network and the CDS outstanding nationals and of all liquidity positions at time $t-1$ wants to asses whether the OTC network would be resilient to illiquidity contagion at time t, under a stress test scenario defined by:

- $\forall k$, $\Delta S_t(k) = \Delta \hat{S}(k)$,
- $\Delta M = \Delta \hat{M}_t$,

- $\forall k$, $\delta_t(k) = \hat{\delta}(k)$.

We denote by $(\hat{\xi}, \hat{\delta}, m_t)$ the network of payables at time t under this stress test scenario. Clearly this network is observable at time $t-1$. The illiquidity cascade can then be investigated on the network $\hat{\xi}$ using the asymptotic analysis given in [8]. By analogy with contagious exposures defined in [8], we can introduce the notion of:

Definition 5.1 (Critical receivables)**.** *Let i be a node that does not become fundamentally illiquid under the stress test, i.e. $m_t(i) - \sum_j \hat{\xi}(i,j) - \hat{\delta}(i) > 0$. We say that, under the stress test scenario, there is a critical cash flow between k and i if*

$$(\hat{\xi}(k,i))_+ > m_t(i) - \sum_j \hat{\xi}(i,j) - \hat{\delta}(i), \tag{V.7}$$

i.e. node i cannot meet its margin calls if node k is illiquid. We write in this case $k \hat{\rightsquigarrow} i$.

Moreover, we denote by

$$c_t^-(i) = \#\{j \in \mathbf{v} \ s.t. \ \hat{\xi}(i,j) > 0\},$$

the *in-degree* of a node i, given by the number of its in-flows, while its *out-degree* of a node i is the number of its out-flows

$$c_t^+(i) = \#\{j \in \mathbf{v} \ s.t. \ \hat{\xi}(i,j) < 0\}.$$

The empirical distribution of the degree is given by

$$\mu_n(j,k) := \frac{\#\{i : c^+(i) = j, c^-(i) = k\}}{n}. \tag{V.8}$$

We let the fraction of contagious links belonging to nodes with degree (j,k)

$$q_n(j,k) := \frac{\#\{i,l : c^+(i) = j, c^-(i) = k, l \hat{\rightsquigarrow} i\}}{j\mu_n(j,k)n} \tag{V.9}$$

Following [6], we make the following assumptions on these quantities:

Assumption 5.2. 1. *The degree distribution condition:* the proportion $\mu_n(j,k)$ of nodes with degree (j,k) tends to $\hat{\mu}(j,k)$, i.e.

$$\mu_n(j,k) \overset{n\to\infty}{\to} \hat{\mu}(j,k)$$

2. *Finite expectation property:* $\sum_{j,k} j\hat{\mu}(j,k) = \sum_{j,k} k\hat{\mu}(j,k) = \hat{\lambda} \in (0,\infty)$;

3. *Second moment property:* $\sum_{i=1}^n (c_n^+(i))^2 + (c_n^-(i))^2 = O(n)$.

4. There exists a function $q : \mathbb{N}^2 \to [0,1]$ such that for all $j,k,\theta \in \mathbb{N}$

$$q_n(j,k) \to \hat{q}(j,k),$$

as $n \to \infty$

Definition 5.3 (Resilience function under a stress test)**.** *We define the resilience function, depending on the stress test parameters and networks of exposures and CDS Notionals observed at time $t-1$.*

$$\hat{\nu} := 1 - \sum_{j,k} \frac{j\hat{\mu}(j,k)}{\hat{\lambda}} k\hat{q}(j,k). \tag{V.10}$$

We give the following result, proved in [8] :

Proposition 5.4. *Assume degrees $(\mathbf{c}^+, \mathbf{c}^-)$ verify Assumption 5.2. If $\hat{\nu} < 1$, then for any ε, there exists ρ_ε such that if the fraction fundamentally illiquid banks is less than ρ_ε, then with high probability, the fraction of illiquid banks is less than ε. In this case we say that the network is resilient at time t. If $\hat{\nu} > 1$ then the skeleton of contagious margin calls contains with high probability a strongly connected giant component, thus any default of a node in this component triggers the illiquidity of the whole component.*

6 Numerical results

The purpose of this section is to analyze the impact of central clearing on an OTC network. This network is constructed as a sample of the random network introduced in the previous section. When the complete network is observed at time $t-1$, we may use the resilience measure to asses the transmission of illiquidity under a stress test.

In the last part of this section we check whether our conclusions hold on 5000 networks drawn from our model.

6.1 The stress test scenario

Starting from the OTC networks, the network of flows $\hat{\xi}$ is determined in our example according to following stress test scenario:

- The gross market values of credit default swaps having as a reference entity one of the dealers have an absolute jump equal to 15% of the notional;
- The gross market values of credit default swaps having as a reference entities other financial institution aside dealers, has an absolute jump equal to 10% of the notional;
- The gross market value of credit default swaps having other reference entities has an absolute jump equal to 5% of the notional.
- The gross market value of the other OTC derivatives confounded has a relative jump equal 5%.

For any bank i, the liquidity position before any cash-flows $m_t(i)$, which recall is observable at time $t-1$, is assumed to be the minimal liquidity position such that, no bank has any contagious margin calls in the event of a jump equal to a percentage $\gamma OTC = 5\%$ of the MtM

value of non-CDS derivatives and respectively of the CDS notionals. Therefore, we have

$$\begin{aligned} m(i) :=& \gamma OTC \cdot (\sum_j g(j,i) - \sum_j g(i,j) + \max_j (g(i,j) - g(j,i))_+)_+ \\ &+ \gamma OTC \cdot (\sum_j \sum_k N^{(k)}(j,i) - \sum_j \sum_k N^{(k)}(i,j)) \\ &+ \gamma OTC \cdot \max_j (\sum_k N^{(k)}(i,j) - \sum_k N^{(k)}(j,i))_+. \end{aligned} \tag{V.11}$$

Clearly, since our stress test is more severe, contagious margin calls will appear in the system. We investigate the role of central clearing in mitigating the propagation of illiquidity via these (unprepared for) contagious margin calls, in several clearing configurations. Concerning the CDS, we consider three case studies:

1. The case where CDS are not centrally cleared;
2. The case where CDS are centrally cleared with a set of 20 dealers;
3. The case where CDS are centrally cleared but only a reduced set of 10 dealers have access to the clearing house.

Concerning the other derivatives, in their majority IR derivatives, we compare the following cases:

1. The case without central clearing;
2. The case of dedicated clearing house;
3. The case of joint clearing with CDS.

Note that the definition of the liquidity buffer given by Eq. (V.11) is independent of any cross derivative class netting. The reason for this is that different cases of clearing strongly affect the netting opportunities, whereas we need precisely a definition of the liquidity that would serve us as common base for comparing these cases.

On the other hand, the liquidity position of the clearing houses is defined by taking into account the possibilities of cross derivative class netting. Also, more precaution is taken: not only the clearing house is not allowed to have contagious margin calls, but it must withstand the default of the two members to which it has the largest exposure. Note also that the cash inflows of any clearing house equal its outflows. So, for a clearing house c, its liquidity position is given by

$$m(c) := 2 \cdot \gamma OTC \cdot \max_j (g(c,j) - g(j,c) + \sum_k N^{(k)}(i,c) - \sum_k N^{(k)}(c,i))_+ \tag{V.12}$$

6.2 A sample OTC network

The features of a sample of the random network $\mathbf{g}$ of non-CDS exposures are shown in Figure V.5.

Based on this sample, a CDS network generated from the model of Section 4.2, has, by construction, the same features as given by the empirical data: the top five CDS dealers sell

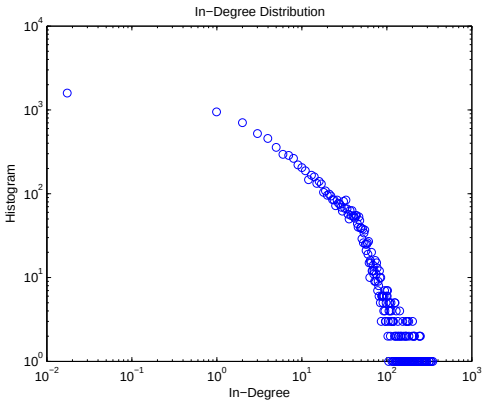

(a) The distribution of out-degree has a Pareto tail with exponent 2

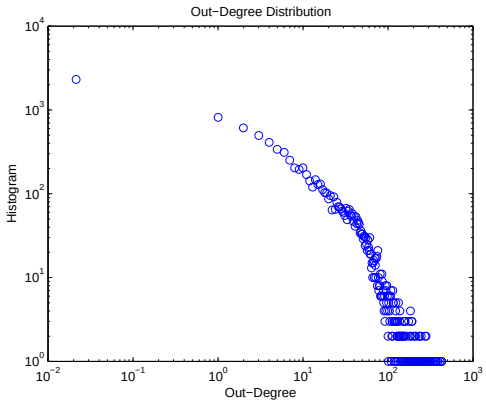

(b) The distribution of the in-degree has a Pareto tail with exponent 2

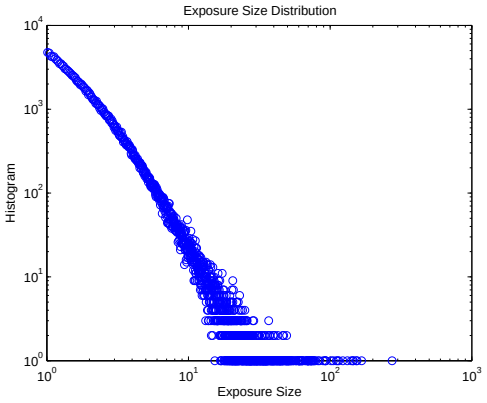

(c) The distribution of the exposures is heavy tailed

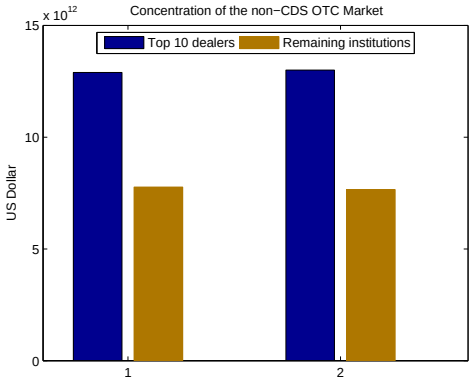

(d) Concentration on the top dealers

Figure V.5: Features of the OTC (non-CDS) exposure network

protection totaling 65% of the CDS outstanding notional, the top ten sell protection totaling 87 % of the outstanding notional. Also, as shown by Figure V.6, the subnet of CDS contracts sold by the top ten dealers to other top ten dealers is a complete network. This network represents in our calibrated sample 76 % of the total outstanding notional.

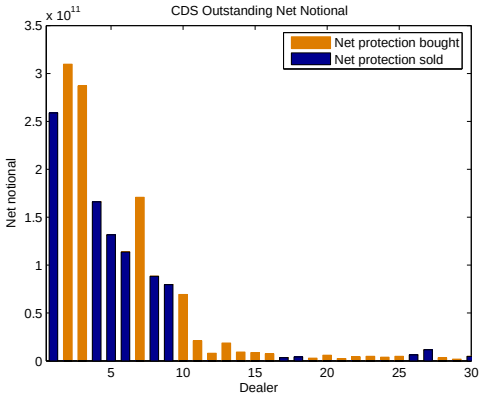

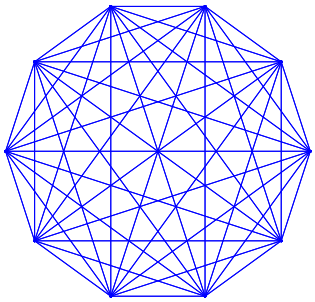

(a) The Dealer structure of the CDS Market : first 10(b) Dealer to dealer network: complete network repre-largest dealers sell/buy 87 % / 88 % of the total CDSsenting 76 % in terms of outstanding CDS notional Notional

Figure V.6

The results of the calibration to DTCC data on the net and gross notional sold on the top reference entities are show in Figure V.7. Since the top reference entities are not necessarily financial institutions, the total notionals of protection sold on nonfinancial names - the data also includes sovereigns - have been aggregated (in Figure V.7 the point with the highest notional corresponds in fact to all non-financial names).

6.3 To clear or not to clear?

Using the liquidity positions and stress test considered in the previous section, we now asses the impact of central clearing on the sample network presented in the previous section. Table V.4 gives the average cash flow under the stress tests scenario. We find, for our calibrated sample network, that the lowest average exposure corresponds to the case of joint clearing of CDS and IR derivatives. These results confirm the results shown in [63] in a gaussian and complete network setting.

	Without CDS CH	With CDS CH (top 20 dealers)	With CDS CH (top 10 dealers)
Without IR CH	5.92	5.40	5.68
Dedicated IR CH	5.25	4.27	4.67
IR/CDS CH	5.25	4.03	4.48

Table V.4: Average exposure (in mn $)

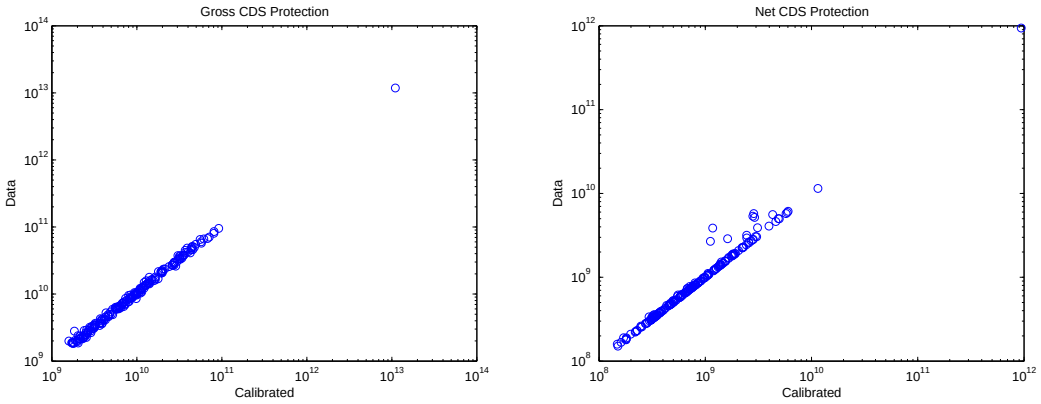

Figure V.7: Calibration to DTCC Data [130]

However, in a heterogenous network, the average size of the exposure is unlikely to adequately measure systemic risk. We will therefore compute the resilience measure given by Definition 5.3. Figure V.8 shows the size of the illiquidity cascade in the stress scenario as a function of a varying exogenous liquidity shock $\hat{\delta}$. For every bank i, the liquidity shock is taken as a fixed percentage of the liquidity position $m_t(i)$ given in Eq. (V.11) and this percentage is constant over all banks. In all cases, we relate the size of the illiquidity cascade to the resilience measure.

These results show that, similarly to [9], as the resilience measure becomes negative, the skeleton of contagious margin calls percolates: an illiquidity cascade occurs, affecting an important fraction of the financial system. Relating the appearance of these phase transitions to the resilience measure allows to asses the effect of central clearing in a way we deem more relevant to systemic risk than the average exposure.

The question is: what is the effect of central clearing on the resilience measure and the point at which phase transitions occur? The results show, that in absence of central clearing of the other classes of derivatives, clearing CDS does not impede the phase transition. It is the large size of the jump in IR swaps (recall the stress test considered a jump equal to 5 % of the MtM value of IR swaps) that plays its role here and the system cannot withstand even a small liquidity shock. However, when IR swaps are centrally cleared, CDS clearing has an important impact on impeding the phase transition. Both in the case where the IR swaps are cleared in a dedicated CH and the case of joint clearing, when a CH for CDS with the top 20 members is introduced, the phase transition occurs for a significantly larger liquidity shock. Without CDS clearing, a liquidity shock of 3% induces a phase transition. With CDS clearing with 20 members, a phase transition occurs when the liquidity shock reaches 12%. Nonetheless, we observe that the benefits of central clearing decrease when less members are allowed in the CH. We can explain this in the following way. Recall that the CDS network is constructed by introducing the so called hedging chains. The clearing house will compress the hedging chains consisting exclusively of members of the CH. For example if a hedging chain has length 10 and all intermediaries are members of the CH, then this chain will have length

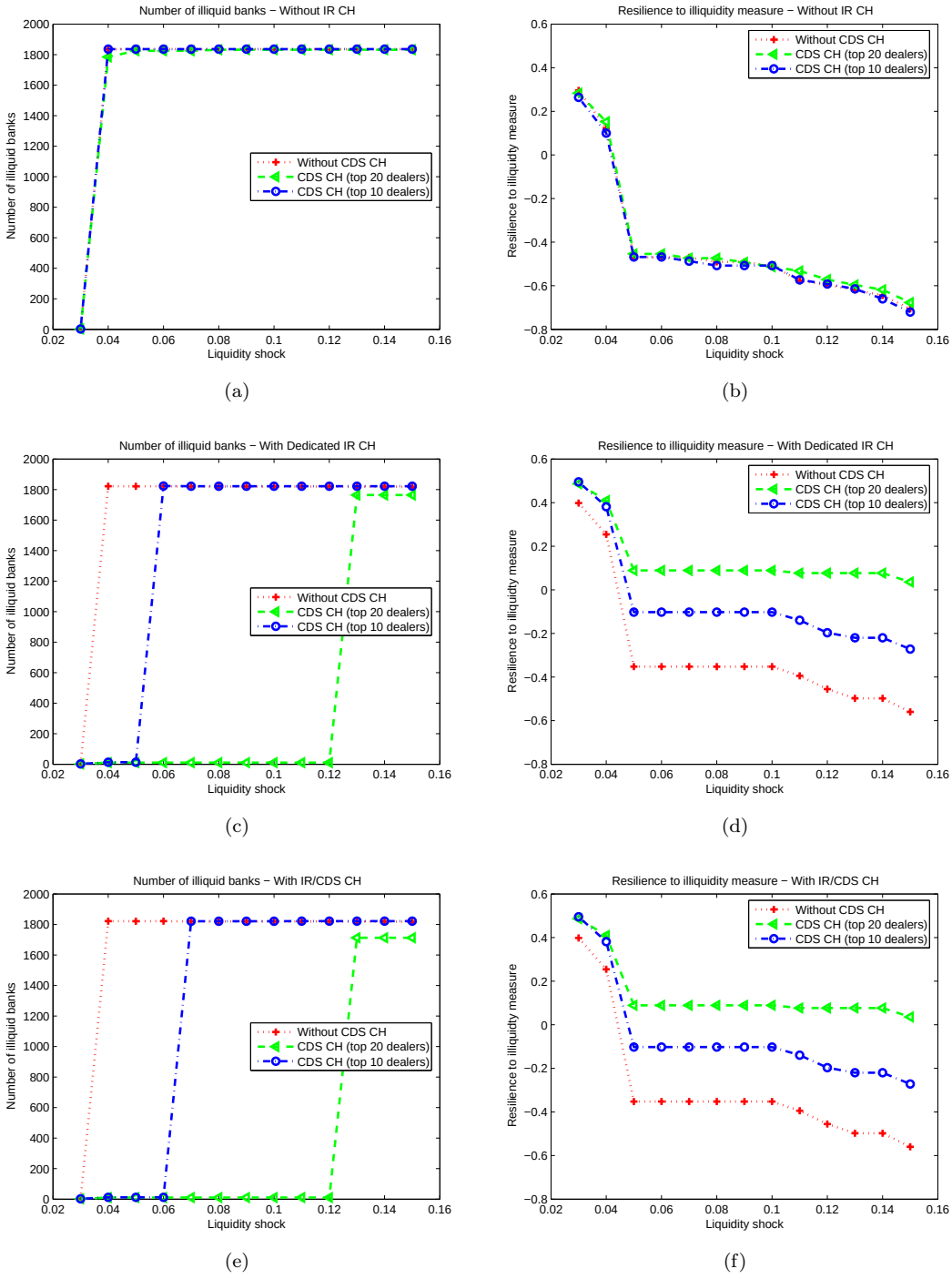

Figure V.8: Number of illiquid banks and resilience measure for different clearing cases

one after compression. On the other hand it suffices for only one of the intermediaries to be a non-member of the CH for the benefits to decrease and the desired compression to be reduced. It follows that not just the size of notional of protection sold/bought should be a criterion to allow a member in the clearing house, but it should also be accounted for the number of hedging chains passing through this node. A significant dealer is a node that has both an important market share but more importantly, is present as an intermediary is a large proportion of the hedging chains.

We have so far investigated the impact of central clearing on one sample of the random network of OTC derivatives.

We now draw 5000 samples and compute the number of defaults on each of the samples, in the same cases investigated previously. The results are shown in Figure V.9.

Figures V.9a and V.9b, concerning the case without a dedicated clearing house for IR derivatives, present a fair amount of simulations where, introducing central clearing for CDS has a negative impact on financial stability, and the CDS clearing house not only that does not impede phase transitions but it seems to induce them.

On the other hand, as shown in Figures V.9c and V.9d, when IR derivatives are centrally cleared in a dedicated house, clearing of CDS enhances the network stability, in particular in the case where more significant members were allowed in the clearing house.

The third group of results - Figure V.9e and V.9f - where IR and CDS are cleared in the same clearing facility point out one case among 5000 where the CDS clearing house decreases network stability. Whereas the probability of a negative impact of a CDS clearing house cannot be excluded in our model, we find that in the vast majority of simulations ($99,98\%$ of cases) the CDS clearing facility decreases the probability of a system wide illiquidity contagion.

7 Conclusions

We have introduced a hierarchical network model for studying illiquidity contagion in OTC derivatives markets, which takes into account public data on the gross and net notional exposures of dealers and their market share for credit default swaps and interest rate derivatives. In such a setting, liquidity shocks may generate contagion due to margin calls across counterparties in a hedging chain.

Our model provides a framework for studying the magnitude and dynamics of illiquidity cascades in OTC markets, in a stress test scenario formulated in terms of liquidity shocks. We obtain a criterion for resilience of the network to liquidity shocks; our criterion highlights the role of 'critical receivables' i.e. receivables on which an intermediary depends to meet its own short-term obligations.

This resilience criterion provides a measure of contagion risk which, unlike the average expected exposure used in previous studies [63], takes into account the structure of the network and the heterogeneity of exposures. We show that this risk measure is directly related to the size of the illiquidity cascade triggered by the initial default of a small number of market participants.

This framework allows to assess the (much-debated) impact, in terms of systemic risk, of introducing a CDS clearinghouse. Our simulations show that, in absence of a clearing facility for interest rate swaps, an additional clearing facility for CDS does not necessarily have a positive impact on financial stability. On the contrary, when interest rate derivatives (mainly swaps)

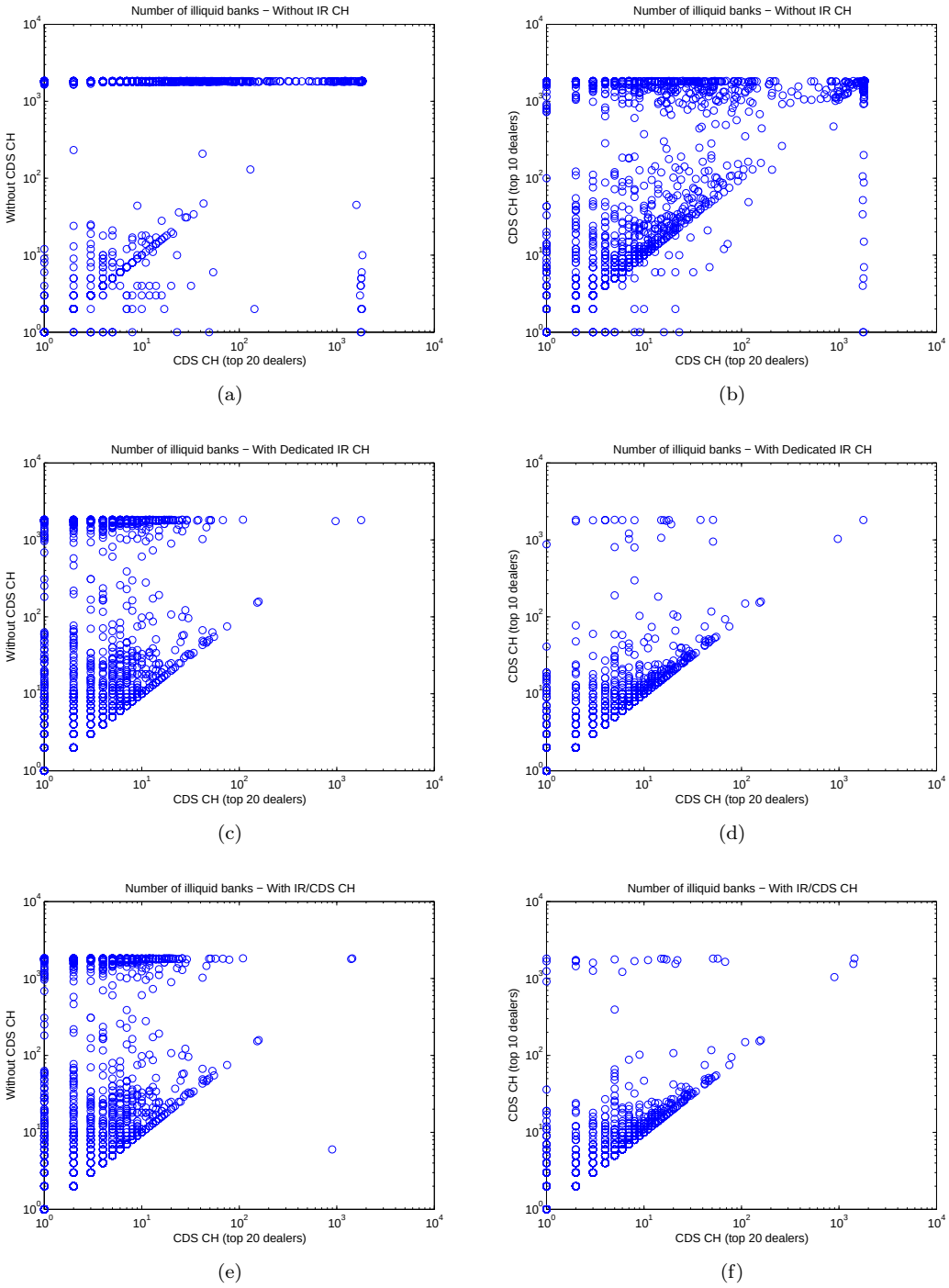

Figure V.9: Number of illiquid banks for different clearing cases. Liquidity shock: 9%

are centrally cleared –as is currently the case– a CDS clearinghouse can contribute significantly to financial stability by enhancing the resilience of the OTC network to large liquidity shocks, provided all significant dealers are members of the clearing house.

These results, which are somewhat different from Duffie & Zhu's [63] analysis based on expected average exposure in a complete network model with IID exposures, show the importance of taking into account the structure of the network and using a metric based on 'tail events', not just averages, when discussing the benefits of central clearing for systemic risk. Simulations of illiquidity cascades for a large number of networks confirm these conclusions and show that they hold with a high probability across a wide variety of network topologies.

8 Appendix: pricing portfolios with collateral and counterparty risk

8.1 Cash flows of collateralized CDS

We consider a CDS between a protection seller a and a protection buyer b referencing an entity k. The contract has the following characteristics: maturity T, notional $N^{(k)}(a,b)$, tenor $t_1,\ldots,t_J = T$ and contractual spread, S. For simplicity we consider that the spread S is a daily spread, i.e. $S := X\Delta$, where Δ is the fraction of a year represented by one day and X the annual spread. We assume that the CDS is subject to symmetric collateral agreement, with cash used as collateral and variation margin payments made daily, with haircut equal to zero. This type of collateral agreement has been previously referred to as extreme or full collateralization [11, 75], but this denomination might be misleading: the residual risk, in case of counterparty default, is essentially equal to the jump in the mark-to-market value of the contract if the reference entity does not default or, in case of simultaneous default of the reference entity, to the face value of the contract. Under no means can these be considered negligible as in the case of interest rate products [75], hence, the term *ex-ante full collateralization*, used in the sequel, is more appropriate.

Let us denote by $(\tau(i))_{i\in\{a,b,k\}}$ the respective default times of entities involved by the contract and let $\tau := \tau(a) \wedge \tau(b)$.

- At any date $u = 1,\ldots,T$, seller a pays the loss $(1-R(k))N^{(k)}(a,b)$ if $u-1 < \tau(k) \leq u$.
- At any date $t_l,\ l = 1,\ldots,J$, buyer b pays $(t_l - t_{l-1})SN^{(k)}(a,b)$ if $\tau(k) \geq t_l$.

The clean CDS cash flow received by the buyer at time t is given by

$$(1-R(k))N^{(k)}(a,b)\mathbb{1}_{t-1<\tau(k)\leq t\leq T} - SN^{(k)}(a,b)\mathbb{1}_{t\leq\tau(k)\wedge T}. \tag{V.13}$$

The CDS contract presented above is assumed to be a part of a larger portfolio of swaps between a and b, under the same collateral agreement, so that the total cash flow (negative of positive) between a and b is given by $D_t(a,b)$.

At valuation time t, we let the quantity $MtM_t(a,b)$ represent the (mid) mark-to-market value of the discounted future (i.e. from time $t+1$ on) total underlying cash flows of the portfolio.

According to the collateral agreement, party b holds collateral $MtM_{t-1}(a,b)$.

The additional collateral required from a is equal to $\Delta MtM_{t+1}(a,b)$ (note that if $\Delta MtM_t(a,b) < 0$ the protection seller receives back (resp. additional) collateral if $MtM_{t-1}(a,b) > 0$ (resp. $MtM_{t-1}(a,b) < 0$)).

At the same time, the collateral receiving party pays an over-night interest rate γ_t (which is determined in a pre-specified way) on the collateral received at time t, i.e. $\gamma_t MtM_t(a,b)$.

Now, we can give the cash flow at time t from a to b

$$\xi_t(a,b) := D_t(a,b) - (\gamma_{t-1}+1)MtM_{t-1}(a,b) + MtM_t(a,b). \tag{V.14}$$

More detail is given in Appendix 8 on the pricing of collateralized swap portfolios. For simplicity we will take from now on $\gamma_t = 0$. In this case the cash flow at time t between a and b is given by

Definition 8.1. *Cash flow at time t*

$$\xi_t(a,b) = \Delta MtM_t(a,b) + D_t(a,b). \tag{V.15}$$

8.2 Pricing of CDS

Due to its crucial importance when valuing credit instruments, counterparty risk is incorporated in the second generation credit models, either unilaterally [11, 107, 30, 31, 75]. For completeness, we detail here the valuation of portfolios of OTC swaps with counterparty risk. We consider a filtered probability space $(\Omega, \mathcal{F}, (\mathcal{F}_t)_{t\in[0,\dots,T]}, \mathbb{Q})$. The default times $(\tau(i))_{i\in\{s,b,k\}}$ are stopping times with respect to the filtration $(\mathcal{F}_t)_{t\in[0,\dots,T]}$. The process γ_t is adapted. We define the CDS discount factor

$$\Gamma_{t,u} = \frac{1}{\Pi_{s=t}^{u-1}(1+\gamma_s)}. \tag{V.16}$$

Eq. (V.14) gave the due cash flow from party a to party b. The loss of the surviving party is understood as its cost of replacing the original swap by another swap having the same future cash flows. When we account for counterparty risk, the value of this new swap is not necessarily the same as the value of the original swap (having the original counterparty survived) since the new counterparty will price it by regarding itself as risk free.

In case of an early default $\tau \le T$, according to the close-out netting agreement given by the ISDA documentation, the cash flow from a to b is

$$\xi_\tau^*(a,b) := D_t(a,b) - (\gamma_{\tau-1}+1)MtM_{\tau-1}(a,b) + MtM_\tau^*(a,b), \tag{V.17}$$

where $MtM_t^*(a,b)$ defines the mark-to-market value of the portfolio at time t when the defaulting party is replaced by a generic 'risk free' counterparty, denoted by x_a or x_b depending on the side it takes.

$$\begin{aligned} MtM_t^*(a,b) := MtM_t(x_a,b)\mathbb{1}_{t=\tau_a<\tau_b} + MtM_t(a,x_b)\mathbb{1}_{t=\tau_b<\tau_a} \\ + MtM_t(x_a,x_b)\mathbb{1}_{t=\tau_b=\tau_a}. \end{aligned} \tag{V.18}$$

If one of the parties is 'risk free' while the other is risky, we have

$$MtM_t^*(x_a, b) = MtM_t(x_a, x_b)\mathbb{1}_{t=\tau_b}. \tag{V.19}$$

When the recovery rates are given by $R(a)$ and $R(b)$ respectively, the cash flow received by the buyer at time τ is

$$\xi_\tau^*(a,b) - ((1-R(a))(\xi_\tau^*(a,b))^+\mathbb{1}_{\tau=\tau_a} - (1-R(b))(\xi_\tau^*(a,b))^-\mathbb{1}_{\tau=\tau_b}. \tag{V.20}$$

For the case of *ex-ante* full collateralization, and by the non-arbitrage theory [58], the following equality holds

$$\begin{aligned}\mathbb{E}^{\mathbb{Q}}[\xi_t(a,b)\mathbb{1}_{t<\tau} + \xi_\tau^*(a,b)\mathbb{1}_{t=\tau} + (1-R(b))(\xi_\tau^*(a,b))^-\mathbb{1}_{t=\tau_b} \\ - (1-R(a))(\xi_\tau^*(a,b))^+\mathbb{1}_{t=\tau_a}|\mathcal{F}_{t-1}] = 0.\end{aligned}$$

This can also be written

$$\begin{aligned}\mathbb{1}_{t-1<\tau}(\gamma_{t-1}+1)MtM_{t-1}(a,b) =& \mathbb{1}_{t-1<\tau}\mathbb{E}^{\mathbb{Q}}[\mathbb{1}_{t<\tau}MtM_t(a,b) + MtM_t^*(a,b)\mathbb{1}_{t=\tau} \\ &+ (1-R(b))(\xi_\tau^*(a,b))^-\mathbb{1}_{t=\tau_b} \\ &- (1-R(a))(\xi_\tau^*(a,b))^+\mathbb{1}_{t=\tau_a}|\mathcal{F}_{t-1}] = 0,\end{aligned} \tag{V.21}$$

or,

$$\begin{aligned}\mathbb{1}_{t<\tau}MtM_t(a,b) = \mathbb{1}_{t<\tau}(\mathbb{E}^{\mathbb{Q}}[\sum_{u=t+1}^{T\wedge\tau}\Gamma(t,u)D_u(a,b)|\mathcal{F}_t] + \mathbb{E}^{\mathbb{Q}}[\Gamma(t,\tau)(MtM_\tau^*(a,b) \\ + (1-R(b))(\xi_\tau^*(a,b))^-\mathbb{1}_{\tau=\tau_b} \\ - (1-R(a))(\xi_\tau^*(a,b))^+\mathbb{1}_{\tau=\tau_a})|\mathcal{F}_t]).\end{aligned} \tag{V.22}$$

In Eq. (V.22), if both a and b are 'risk free' entities, then $MtM_t(x_a, x_b)$ represents the clean mark-to-market process. It follows that

Lemma 8.2 (Clean mark-to-market)**.** *The clean mark-to-market value of a swap portfolio, is given by*

$$MtM_t(x_a, x_b) = \mathbb{E}^{\mathbb{Q}}[\sum_{u=t+1}^{T}\Gamma(t,u)D_u(a,b)|\mathcal{F}_t]. \tag{V.23}$$

One can thus see that the clean mark-to-market for collateralized swaps is obtained by discounting the future cash flows $(D_u(a,b))_{t<u\leq T}$ with the factors Γ. Since the portfolio clean mark-to-market value is the sum of the clean mark-to-market of the derivatives comprised in the portfolio, it follows in particular that

Lemma 8.3 (Clean CDS mark-to-market)**.** *The clean mark-to-market value of a credit default swap, is given by*

$$\begin{aligned}CDSMtM_t(x_a, x_b) =& \mathbb{E}^{\mathbb{Q}}[\sum_{u=t+1}^{T}\Gamma(t,u)((1-R(k))N^{(k)}(a,b)\mathbb{1}_{u-1<\tau(k)\leq u\leq T} \\ &- SN^{(k)}(a,b)\mathbb{1}_{u\leq\tau(k)\wedge T})|\mathcal{F}_t].\end{aligned} \tag{V.24}$$

If party a only is 'risk free' we obtain

$$\begin{aligned}\mathbb{1}_{t<\tau_b} MtM_t(x_a,b) =& \mathbb{1}_{t<\tau_b}(\mathbb{E}^{\mathbb{Q}}[\sum_{u=t+1}^{T\wedge\tau_b}\Gamma(t,u)D_u(a,b)|\mathcal{F}_t] \\ &+\mathbb{E}^{\mathbb{Q}}[\Gamma(t,\tau_b)(MtM^*_{\tau_b}(x_a,b)+(1-R(b))(\xi^*_{\tau_b}(x_a,b))^-|\mathcal{F}_t]).\end{aligned} \tag{V.25}$$

By Eq.(V.19), and by the law of iterated expectations and the value of the clean mark-to-market in Eq.(V.23), we have

$$\begin{aligned}\mathbb{1}_{t<\tau_b} MtM_t(x_a,b) =& \mathbb{1}_{t<\tau_b}(\mathbb{E}^{\mathbb{Q}}[\sum_{u=t+1}^{T}\Gamma(t,u)D_u(a,b)|\mathcal{F}_t] \\ &+\mathbb{E}^{\mathbb{Q}}[\Gamma(t,\tau_b)(1-R(b))(\xi^*_{\tau_b}(x_a,b))^-|\mathcal{F}_t]), \quad with \\ \xi^*_{\tau_b}(x_a,b) =& D_{\tau_b} - (\gamma_{\tau_b-1}+1)MtM_{\tau_b-1}(x_a,b)+\mathbb{E}^{\mathbb{Q}}[\sum_{u=\tau_b+1}^{T}\Gamma(\tau_b,u)D_u(a,b)|\mathcal{F}_{\tau_b}].\end{aligned} \tag{V.26}$$

If the buyer only is 'risk free' we obtain similarly

$$\begin{aligned}\mathbb{1}_{t<\tau_a} MtM_t(a,x_b) =& \mathbb{1}_{t<\tau_a}(\mathbb{E}^{\mathbb{Q}}[\sum_{u=t+1}^{T}\Gamma(t,u)D_u(a,b)|\mathcal{F}_t] \\ &-\mathbb{E}^{\mathbb{Q}}[\Gamma(t,\tau_a)(1-R(a))(\xi^*_{\tau_a}(a,x_b))^+|\mathcal{F}_t]), \quad with \\ \xi^*_{\tau_a}(a,x_b) =& D_{\tau_a} - (\gamma_{\tau_a-1}+1)MtM_{\tau_a-1}(a,x_b)+\mathbb{E}^{\mathbb{Q}}[\sum_{u=\tau_a+1}^{T}\Gamma(\tau_a,u)D_u(a,b)|\mathcal{F}_{\tau_a}].\end{aligned} \tag{V.27}$$

It then follows form Eq.(V.18) that

$$\begin{aligned}MtM^*_t(a,b) =& \mathbb{E}^{\mathbb{Q}}[\sum_{u=t+1}^{T}\Gamma(t,u)D_u(a,b)|\mathcal{F}_t] + \mathbb{E}^{\mathbb{Q}}[\Gamma(t,\tau_b)(1-R(b))(\xi^*_{\tau_b}(x_a,b))^-|\mathcal{F}_t]\mathbb{1}_{t=\tau_a<\tau_b} \\ &-\mathbb{E}^{\mathbb{Q}}[\Gamma(t,\tau_a)(1-R(a))(\xi^*_{\tau_a}(a,x_b))^+|\mathcal{F}_t]\mathbb{1}_{t=\tau_b<\tau_a},\end{aligned} \tag{V.28}$$

hence from Eq. (V.22),

$$\begin{aligned}\mathbb{1}_{t<\tau} MtM_t(a,b) =& \mathbb{1}_{t<\tau}(\mathbb{E}^{\mathbb{Q}}[\sum_{u=t+1}^{T}\Gamma(t,u)D_u(a,b)|\mathcal{F}_t] \\ &+\mathbb{E}^{\mathbb{Q}}[\Gamma(t,\tau_b)(1-R(b))(\xi^*_{\tau_b}(x_a,b))^-\mathbb{1}_{\tau_a<\tau_b} \\ &-\Gamma(t,\tau_a)(1-R(a))(\xi^*_{\tau_a}(a,x_b))^+\mathbb{1}_{\tau_b<\tau_a} \\ &+(1-R(b))(\xi^*_{\tau}(a,b))^-\mathbb{1}_{\tau=\tau_b}-(1-R(a))(\xi^*_{\tau}(a,b))^+\mathbb{1}_{\tau=\tau_a})|\mathcal{F}_t]).\end{aligned} \tag{V.29}$$

Definition 8.4 (CDS Spread)**.** *The CDS spread $S_0(k)$ is such that the clean mark-to-market of the CDS at inception is equal to zero:*

$$S_0(k) = \frac{\mathbb{E}^{\mathbb{Q}}[\Gamma(0,\tau(k))(1-R(k))\mathbb{1}_{\tau(k)\le T}]}{\sum_{t=1}^{T}\mathbb{E}^{\mathbb{Q}}[\Gamma(0,t)\mathbb{1}_{t\le\tau(k)\wedge T}]}. \tag{V.30}$$

Bibliography

[1] T. Adrian and H. S. Shin. Financial intermediary leverage and value-at-risk. *Federal Reserve Bank of New York Staff Reports*, (338), 2008.

[2] T. Adrian and H. S. Shin. The changing nature of financial intermediation and the financial crisis of 2007-2009. *Annual Review of Economics*, 2(1):603–618, 2010.

[3] T. Adrian and H. S. Shin. Liquidity and leverage. *Journal of Financial Intermediation*, 19(3), July 2010.

[4] F. Allen and A. Babus. Networks in finance. In P. Kleindorfer and J. Wind, editors, *The Network Challenge*, pages 367–382. Wharton, 2009.

[5] F. Allen and D. Gale. Financial contagion. *Journal of Political Economy*, 108(1):1–33, 2000.

[6] H. Amini. Bootstrap percolation and diffusion in random graphs with given vertex degrees. *Electronic Journal of Combinatorics, 17: R25*, 2010.

[7] H. Amini. Bootstrap percolation in living neural networks. *Journal of Statistcal Physics*, 141:459–475, 2010.

[8] H. Amini, R. Cont, and A. Minca. Resilience to Contagion in Financial Networks. *SSRN eLibrary*, 2010.

[9] H. Amini, R. Cont, and A. Minca. Stress testing the resilience of financial networks. *To appear in the International Journal of Theoretical and Applied Finance*, 2011.

[10] M. Arnsdorf and I. Halperin. BSLP: Markovian bivariate spread-loss model for portfolio credit derivatives. *J. Comput. Finance*, 12(2):77–107, 2008.

[11] S. Assefa, T. Bielecki, S. Crépey, and M. Jeanblanc. CVA computation for counterparty risk assessment in credit portfolios. In T. Bielecki, D. Brigo, and F. Patras, editors, *Credit Risk Frontiers: Subprime Crisis, Pricing and Hedging, CVA, MBS, Ratings, and Liquidity*. Wiley: Bloomberg Press, 2011.

[12] M. Avellaneda. The minimum-entropy algorithm and related methods for calibrating asset-pricing models. In *Proceedings of the International Congress of Mathematicians, Vol. III (Berlin, 1998)*, number Extra Vol. III, pages 545–563 (electronic), 1998.

[13] M. Avellaneda, R. Buff, C. Friedman, N. Grandechamp, L. Kruk, and J. Newman. Weighted Monte Carlo: a new technique for calibrating asset-pricing models. *Int. J. Theor. Appl. Finance*, 4(1):91–119, 2001.

[14] M. Avellaneda and R. Cont. Transparency in credit default swap markets. *Finance Concepts Report*, 2010.

[15] M. Avellaneda and R. Cont. Transparency in otc interest rate derivatives markets. *Finance Concepts Report*, 2010.

[16] M. Avellaneda, C. Friedman, R. Holmes, and D. Samperi. Calibrating the volatility surfaces via relative entropy minimization. *Applied Mathematical Finance*, 4:37–64, 1997.

[17] J. Balogh and B. G. Pittel. Bootstrap percolation on the random regular graph. *Random Structures Algorithms*, 30(1-2):257–286, 2007.

[18] Bank for International Settlements. International banking and financial market developments. *BIS Quarterly Review*, December 2010.

[19] S. Battiston, D. D. Gatti, M. Gallegati, B. Greenwald, and J. E. Stiglitz. Liaisons dangereuses: Increasing connectivity, risk sharing, and systemic risk. *NBER Working Papers*, February 2009.

[20] E. A. Bender and E. R. Canfield. The asymptotic number of labeled graphs with given degree sequences. *Journal of Combinatorial Theory, Series A*, 24:296–307, 1978.

[21] A. Bentata and R. Cont. Mimicking the marginal distributions of a semimartingale. *Working paper, arXiv:0910.3992v2 [math.PR]*, 2009.

[22] J. Bertoin and V. Sidoravicius. The structure of typical clusters in large sparse random configurations. *Journal of Statistical Physics*, 135(1):87–105, 2009.

[23] J.-M. Bismut. Contrôle des processus de sauts. *C. R. Acad. Sci. Paris Sér. A-B*, 281(18):Aii, A767–A770, 1975.

[24] P. Blanchard, C.-H. Chang, and T. Krüger. Epidemic thresholds on scale-free graphs: the interplay between exponent and preferential choice. *Ann. Henri Poincaré*, 4(suppl. 2):S957–S970, 2003.

[25] B. Bollobás. The asymptotic number of unlabelled regular graphs. *J. London Math. Soc. (2)*, 26(2):201–206, 1982.

[26] B. Bollobás. *Random graphs*, volume 73 of *Cambridge Studies in Advanced Mathematics*. Cambridge University Press, Cambridge, second edition, 2001.

[27] B. Bollobás and O. M. Riordan. Mathematical results on scale-free random graphs. In *Handbook of graphs and networks*, pages 1–34. Wiley-VCH, Weinheim, 2003.

[28] M. Boss, H. Elsinger, M. Summer, and S. Thurner. The network topology of the interbank market. *Quantitative Finance*, (4):677–684, 2004.

[29] P. Brémaud. *Point processes and queues*. Springer-Verlag, New York, 1981. Martingale dynamics, Springer Series in Statistics.

[30] D. Brigo and A. Capponi. Bilateral Counterparty Risk Valuation with Stochastic Dynamical Models and Application to Credit Default Swaps. *SSRN eLibrary*, 2009.

[31] D. Brigo and M. Morini. Dangers of bilateral counterparty risk: the fundamental impact of closeout conventions. *arXiv:1011.3355v1*, 2010.

[32] D. Brigo, A. Pallavicini, and R. Torresetti. Calibration of cdo tranches with the dynamic generalized poisson loss model. *Working paper*, 2007.

[33] M. K. Brunnermeier. Deciphering the liquidity and credit crunch 2007-2008. *Journal of Economic Perspectives*, 23(1):77–100, 2009.

[34] R. Bruyère, R. Cont, R. Copinot, L. Fery, C. Jaeck, and T. Spitz. *Credit derivatives and structured credit*. Chichester: Wiley, 2005.

[35] J. Cain and N. Wormald. Encores on cores. *Electronic Journal of Combinatorics 13 (2006), RP 81*, 2005.

[36] J. Cain and N. Wormald. Encores on cores. *Electronic Journal of Combinatorics 13 (2006), RP 81*, 2006.

[37] J. Chan-Lau, M. Espinosa-Vega, K. Giesecke, and J. Sole. Assessing the systemic implications of financial linkages. In *Global Financial Stability Report*. International Monetary Fund, 2009.

[38] R. Cifuentes, G. Ferrucci, and H. Shin. Liquidity risk and contagion. *Journal of the European Economic Association*, 3:556–566, 2005.

[39] P. Collin-Dufresne, R. Goldstein, and J. Hugonnier. A general formula for valuing defaultable securities. *Econometrica*, 72(5):1377–1407, 2004.

[40] Comptroller of the Currency Administrator of National Banks. Occ's quarterly report on bank trading and derivatives activities second quarter 2010.

[41] R. Cont. Measuring systemic risk. *Working Paper*, 2010.

[42] R. Cont, R. Deguest, and Y. H. Kan. Default intensities implied by CDO spreads: inversion formula and model calibration. *SIAM J. Financial Math.*, 1:555–585, 2010.

[43] R. Cont and Y. H. Kan. Dynamic hedging of portfolio credit derivatives. *SIAM Journal on Financial Mathematics*, 2:112–140, 2011.

[44] R. Cont and Y. H. Kan. Statistical modeling of credit default swap portfolios. *Working paper*, 2011.

[45] R. Cont and A. Minca. Credit default swaps and systemic risk. *Working paper*, 2011.

[46] R. Cont and A. Minca. Recovering portfolio default intensities implied by cdo quotes. *Mathematical Finance*, 2011.

[47] R. Cont and A. Moussa. Too interconnected to fail: contagion and systemic risk in financial networks. *Working Paper*, 2010.

[48] R. Cont, A. Moussa, and E. B. e Santos. The brazilian financial system: network structure and systemic risk analysis. *Working Paper*, 2010.

[49] R. Cont and I. Savescu. Forward equations for portfolio credit derivatives. In *Cont, R. (ed.) : Frontiers in quantitative finance: credit risk and volatility modeling*. Wiley, 2008.

[50] R. Cont and P. Tankov. *Financial modelling with jump processes*. Chapman & Hall/CRC Financial Mathematics Series. Chapman & Hall/CRC, Boca Raton, FL, 2004.

[51] R. Cont and L. Wagalath. Running for the exit: distressed selling and endogenous correlation in financial markets. *Mathematical Finance*, 2011.

[52] C. Cooper and A. M. Frieze. The size of the largest strongly connected component of a random digraph with a given degree sequence. *Combinatorics, Probability & Computing*, 13(3):319–337, 2004.

[53] I. Csiszár. I-divergence geometry of probability distributions and minimization problems. *Ann. Probability*, 3:146–158, 1975.

[54] I. Csiszár. Sanov property, generalized I-projection and a conditional limit theorem. *Ann. Probab.*, 12(3):768–793, 1984.

[55] G. G. Darrell Duffie and G. Manso. Information percolation. *American Economic Journal: Microeconomics*, 2, 2010.

[56] S. Das, D. Duffie, and N. Kapadia. Common failings: how corporate defaults are correlated. *Journal of Finance*, 62(1):93–117, February 2007.

[57] M. Davis and V. Lo. Infectious defaults. *Quantitative Finance*, 1(4):382 – 387, 2001.

[58] F. Delbaen and W. Schachermayer. *The mathematics of arbitrage*. Springer Finance. Springer-Verlag, Berlin, 2006.

[59] D. W. Diamond and R. G. Rajan. Fear of Fire Sales and the Credit Freeze. *SSRN eLibrary*, 2009.

[60] X. Ding, K. Giesecke, and P. I. Tomecek. Time-changed birth processes and multiname credit derivatives. *Oper. Res.*, 57(4):990–1005, 2009.

[61] D. Duffie. The failure mechanics of dealer banks. *Journal of Economic Perspectives*, 24(1):51–72, 2010.

[62] D. Duffie and N. Garleanu. Risk and valuation of collateralized debt obligations. *Financial Analysts Journal*, 57(1):41–59, January/February 2001.

[63] D. Duffie and H. Zhu. Does a central clearing counterparty reduce counterparty risk? *Working paper*, 2010.

[64] B. Dupire. Pricing with a smile. *RISK*, (7):18–20, 1994.

[65] B. Dupire. A unified theory of volatility. *Working Paper, Paribas*, 1996.

[66] L. Eisenberg and T. H. Noe. Systemic Risk in Financial Systems. *Management Science*, 47(2):236–249, 2001.

[67] I. Ekeland and R. Témam. *Convex analysis and variational problems*, volume 28 of *Classics in Applied Mathematics*. Society for Industrial and Applied Mathematics (SIAM), Philadelphia, PA, english edition, 1999. Translated from the French.

[68] H. Elsinger, A. Lehar, and M. Summer. Risk Assessment for Banking Systems. *Management Science*, 52(9):1301–1314, 2006.

[69] P. Erdős and A. Rényi. On random graphs. I. *Publ. Math. Debrecen*, 6:290–297, 1959.

[70] P. Erdös and A. Rényi. On the evolution of random graphs. *Publ. Math. Inst. Hung. Acad. Sci*, 5:17–61, 1960.

[71] E. Errais, K. Giesecke, and L. R. Goldberg. Affine point processes and portfolio credit risk. *SIAM J. Financial Math.*, 1:642–665, 2010.

[72] S. N. Ethier and T. G. Kurtz. *Markov processes*. Wiley Series in Probability and Mathematical Statistics: Probability and Mathematical Statistics. John Wiley & Sons Inc., New York, 1986. Characterization and convergence.

[73] European Central Bank. Credit default swaps and counterparty risk, August 2009.

[74] N. Fountoulakis. Percolation on sparse random graphs with given degree sequence. *Internet Math.*, 4(4):329–356, 2007.

[75] M. Fujii and A. Takahashi. Derivative pricing under asymmetric and imperfect collateralization and CVA. *arXiv:1101.5849v2*, 2011.

[76] P. Gai and S. Kapadia. Contagion in Financial Networks. *Proceedings of the Royal Society A*, 466(2120):2401–2423, 2010.

[77] K. Giesecke. Portfolio credit risk: top-down vs bottom-u. In *Cont, R. (ed.) : Frontiers in quantitative finance: credit risk and volatility modeling*. Wiley, 2008.

[78] K. Giesecke. Portfolio credit risk: top down vs. bottom up approaches. In *Cont, R. (ed.) : Frontiers in quantitative finance: credit risk and volatility modeling*. Wiley, 2008.

[79] K. Giesecke and B. Kim. Estimating tranche spreads by loss process simulation. In *Hendersen et al. (eds.): Proceedings of the 2007 Winter Simulation Conference*, 2007.

[80] J. P. Gleeson. Mean size of avalanches on directed random networks with arbitrary degree distributions. *Phys. Rev. E*, 77(5):057101, May 2008.

[81] T. Goll and L. Rüschendorf. Minimal distance martingale measures and optimal portfolios consistent with observed market prices. In *Stochastic processes and related topics (Siegmundsburg, 2000)*, volume 12 of *Stochastics Monogr.*, pages 141–154. Taylor & Francis, London, 2002.

[82] C. Graham. Chaoticity for multiclass systems and exchangeability within classes. *J. Appl. Probab.*, 45(4):1196–1203, 2008.

[83] I. Gyöngy. Mimicking the one-dimensional marginal distributions of processes having an Itô differential. *Probab. Theory Relat. Fields*, 71(4):501–516, 1986.

[84] A. G. Haldane. Rethinking the financial networks. 2009.

[85] A. G. Haldane and R. M. May. Systemic risk in banking ecosystems. *Nature*, 469:351–355, 2011.

[86] M. Hellwig. Systemic aspects of risk management in banking and finance. *Swiss Journal of Economics and Statistics*, 131:723–737, 1995.

[87] M. Hellwig. Systemic risk in the financial sector: An analysis of the subprime-mortgage financial crisis. *De Economist*, 157(2):129–207, 2009.

[88] W. Hurewicz. *Lectures on ordinary differential equations*. The Technology Press of the Massachusetts Institute of Technology, Cambridge, Mass., 1958.

[89] ISDA. ISDA margin survey 2010. `http://www.isda.org/c_and_a/pdf/ISDA-Margin-Survey-2010.pdf`, 2010.

[90] ISDA. Market review of OTC derivative bilateral collateralization practices. `http://www.isda.org/c_and_a/pdf/ISDA-Margin-Survey-2010.pdf`, March 2010.

[91] J. Jacod. Multivariate point processes: predictable projection, Radon-Nikodým derivatives, representation of martingales. *Z. Wahrscheinlichkeitstheorie und Verw. Gebiete*, 31:235–253, 1974/75.

[92] S. Janson. On percolation in random graphs with given vertex degrees. *Electronic Journal of Probability*, 14:86–118, 2009.

[93] S. Janson. The probability that a random multigraph is simple. *Combinatorics, Probability and Computing*, 18(1-2):205–225, 2009.

[94] S. Janson. Susceptibility of random graphs with given vertex degrees. *http://arxiv.org/abs/0911.2636v1*, 2009.

[95] S. Janson. Probability asymptotics:notes on notation. *Institut Mittag-Leffler preprint 31*, 2009 spring.

[96] S. Janson, T. Łuczak, and A. Rucinski. *Random graphs*. Wiley-Interscience Series in Discrete Mathematics and Optimization. Wiley-Interscience, New York, 2000.

[97] R. Jarrow and P. Protter. Structural versus reduced form models: a new information based perspective. *Journal of Investment Management*, 2(2):34–43, 2004.

[98] R. A. Jarrow and F. Yu. Counterparty risk and the pricing of defaultable securities. *The Journal of Finance*, (56):1765–1799, 2001.

[99] N. Kiyotaki and J. Moore. Credit chains. *Mimeo, Walras-Bowley Lecture to the North American Meeting of the Econometric Society, Iowa City, IA*, 1996.

[100] N. Kiyotaki and J. Moore. Balance-sheet contagion. *American Economic Review*, 92(2):46–50, 2002.

[101] J. Kleinberg. Cascading behavior in networks: algorithmic and economic issues. In *Algorithmic game theory*, pages 613–632. Cambridge Univ. Press, Cambridge, 2007.

[102] S. Kusuoka. A remark on default risk models. In *Advances in mathematical economics, Vol. 1 (Tokyo, 1997)*, volume 1 of *Adv. Math. Econ.*, pages 69–82. Springer, Tokyo, 1999.

[103] R. Lagunoff and S. Schreft. A model of financial fragility. *Journal of Economic Theory*, 99:220–264, 2001.

[104] D. Lando. On cox processes and credit risky securities. *Review of Derivatives Research*, 2(2/3):99–120, 1998.

[105] Y. Leitner. Financial networks: Contagion, commitment and private sector bailouts. *Journal of Finance*, 60:2925–2953, 2005.

[106] A. Lipton and A. Rennie, editors. *Credit correlation: life after copulas*. World Scientific, 2008.

[107] A. Lipton and A. Sepp. Credit value adjustment for credit default swaps via the structural default model. *The Journal of Credit Risk*, 5(2):123–146, Summer 2009.

[108] F. Longstaff and A. Rajan. An empirical analysis of the pricing of collateralized debt obligations. *Journal of Finance*, 63:509–563, 2008.

[109] R. M. May and N. Arinaminpathy. Systemic risk: the dynamics of model banking systems. *Journal of The Royal Society Interface*, 7(46):823–838, 2010.

[110] A. Minca and H. Amini. Mathematical modeling of systemic risk. In *Financial Networks*, Springer Series in Mathematics. Springer, 2011.

[111] T. Misirpashayev and A. Lopatin. Two-dimensional markovian model for dynamics of aggregate credit loss. 2007.

[112] M. Molloy and B. Reed. A critical point for random graphs with a given degree sequence. In *Proceedings of the Sixth International Seminar on Random Graphs and Probabilistic Methods in Combinatorics and Computer Science, "Random Graphs '93" (Poznań, 1993)*, volume 6, pages 161–179, 1995.

[113] M. Molloy and B. Reed. The size of the giant component of a random graph with a given degree sequence. *Combinatorics, Probability and Computing*, 7:295–305, 1998.

[114] S. Morris. Contagion. *Review of Economic Studies*, 67(1):57–78, January 2000.

[115] S. Morris and H. S. Shin. Illiquidity component of credit risk. *Working paper*, 2009.

[116] J. Muller. Interbank credit lines as a channel of contagion. *Journal of Financial Services Research*, 29(1):37–60, 2006.

[117] M. Newman, Albert-László Barabási, and D. J. Watts. *The Structure and Dynamics of Networks*. Princeton University Press, 2006.

[118] M. E. J. Newman. Spread of epidemic disease on networks. *Phys. Rev. E*, 66(1):016128, Jul 2002.

[119] M. E. J. Newman, S. H. Strogatz, and D. J. Watts. Random graphs with arbitrary degree distributions and their applications. *Physical Review E*, 64:026118, 2001.

[120] E. Nier, J. Yang, T. Yorulmazer, and A. Alentorn. Network models and finacial stability. *Journal of Economic Dynamics and Control*, (31):2033–60, 2007.

[121] B. of Governors of the Federal Reserve System. The supervisory capital assessment program: Design and implementation. April 24, 2009.

[122] J.-C. Rochet and J. Tirole. Interbank lending and systemic risk. *Journal of Money, Credit and Banking*, 28(4):733–762, Nov. 1996. Part 2: Payment Systems Research and Public Policy Risk, Efficiency, and Innovation.

[123] R. Rouge and N. El Karoui. Pricing via utility maximization and entropy. *Math. Finance*, 10(2):259–276, 2000. INFORMS Applied Probability Conference (Ulm, 1999).

[124] P. Schönbucher. Portfolio losses and the term structure of loss transition rates: a new methodology for the pricing of portfolio credit derivatives. *Working paper*, 2005.

[125] P. J. Schonbucher. Information-driven default contagion. *Preprint ETH*, 2003.

[126] J. Sidenius, V. Piterbarg, and L. Andersen. A new framework for dynamic credit portfolio loss modelling. *Int. J. Theor. Appl. Finance*, 11(2):163–197, 2008.

[127] M. Singh and J. Aitken. Deleveraging after Lehman – Evidence from Reduced Rehypothecation. *SSRN eLibrary*, 2009.

[128] K. Soramaki, M. L. Bech, J. Arnold, R. J. Glass, and W. E. Beyeler. The topology of interbank payment flows. *Physica A: Statistical Mechanics and its Applications*, 379(1):317 – 333, 2007.

[129] M. Stutzer. A simple nonparametric approach to derivative security valuation. *Journal of Finance*, 51:1633–1652, 1996.

[130] The Depository Trust and Clearing Corporation. Trade information warehouse data. `http://www.dtcc.com/products/derivserv/data/index.php`.

[131] C. Upper. Simulation methods to assess the danger of contagion in interbank markets. *Journal of Financial Stability*, 2010.

[132] C. Upper and A. Worms. Estimating bilateral exposures in the german interbank market: Is there a danger of contagion? *Deutsche Bundesbank Discussion Paper No 09/02*, February 2002.

[133] D. J. Watts. A simple model of global cascades on random networks. *Proc. Natl. Acad. Sci. USA*, 99(9):5766–5771, 2002.

[134] N. Wormald. Differential equations for random processes and random graphs. *Annals of Applied Probability*, 5(4):1217–1235, 1995.

[135] N. Wormald. The differential equation method for random graph processes and greedy algorithms. In *Lectures on Approximation and Randomized Algorithms*, 1999.

[136] T. Zariphopoulou. A solution approach to valuation with unhedgeable risks. *Finance Stoch.*, 5(1):61–82, 2001.